Master's Thesis of Engineering

Structural Analysis and Design of Coupled Wall Considering Slab-Wall Interaction

슬래브-벽체 상호작용을 고려한 병렬벽의

구조해석 및 설계

August 2021

Graduate School of Engineering

Seoul National University

Architecture and Architectural Engineering

Myung Ho Jeon

Structural Analysis and Design of Coupled Wall Considering Slab-Wall Interaction

Advisor: Hong Gun Park

Submitting a Master's thesis of
Architecture and Architectural Engineering

August 2021

Graduate School of Engineering
Seoul National University
Architecture and Architectural Engineering

Myung Ho Jeon

Confirming the Master's thesis written by
Myung Ho Jeon

July 2021

Chair	Sung Gul Hong
Vice Chair	Hong Gun Park
Examiner	Cheol Ho Lee

Abstract

Structural Analysis and Design of Coupled Wall Considering Slab-Wall Interaction

Jeon, Myung Ho
Department of Architecture and Architectural Engineering
College of Engineering
Seoul National University

Gyeongju earthquake (’ 16.09.12) and Pohang earthquake (’ 17.11.15), the largest earthquake since the 1978 earthquake observation in Korea, have occurred, and the frequency of earthquakes has continued to increase. Therefore, public interest in the safety of structures in earthquakes is increasing. As interest in structural safety increased, a total of four revisions have been made since the introduction of seismic design standards in Korea in March 1988. Therefore, seismic design laws and applications have been changed accordingly. Recently, nonlinear analysis and seismic design of wall-type structure have been actively conducted in Korea by utilizing performance-based seismic design method. Typically, structural analysis of wall type structure for seismic design uses modeling method to constrain floor slabs with diaphragm method for ease of modeling and reduction of analysis time.

However, with the introduction of the Standard Floating Floor Insitution, the slab thickness of the wall-type strucuture must satisfy 210mm or more, regardless of the structural performance requirements, in order to cope with the floor impact sound. Due to the above regulations, it has been greatly increased compared to the past (120mm ~ 180mm). Therefore, it is expected that the lateral resistance capacity of the structure can be improved by the influence of the slab thickness.

Recently, in the case of wall-type structure, the wall section area per floor is decreasing. In addition, since the shape of the wall is diverse, such as T-type, L-type, and H-type, it will be difficult to simulate the interaction between the slab and the wall with only the diaphragm.

Therefore, this study focused on proposing a design method that considers the slab-wall interaction. Two-story RC frame of slab-coupled wall specimens were constructed among various wall shapes in which the slab-wall interaction occurs. And structural performance tests were performed through cyclic lateral loading. Based on the test results, a structural design method was proposed that considers the slab-wall interaction in the linear elastic analysis of the wall-type structure. In order to prove the proposed design method, the mechanism of the slab-wall structure was identified through the nonlinear finite element analysis and test. In addition, the effective stiffness of slabs and walls used in the elastic design was verified.

This study proposes a structural design method that considers the slab-wall interaction to simulate the behavior of the actual structure and to reduce the cost by decreasing the reinforcement quantity. Since the study was performed on the in-plane wall-slab structure, it is expected that it can be provided as a basis for future design methods considering various wall planes in which the slab-wall interaction occurs.

Keywords : Slab thickness, Diaphragm, Slab-wall interaction, Structural performance tests, Nonlinear finite element analysis, Elastic design method

Student Number : 2019-26856

Contents

List of Tables

List of Figures

Chapter 1. Introduction

1.1 Background

Gyeongju earthquake (’ 16.09.12) and Pohang earthquake (’ 17.11.15), the largest earthquake since the 1978 earthquake observation in Korea, have occurred, and the frequency of earthquakes has continued to increase. Therefore, public interest in the safety of structures in earthquakes is increasing. As interest in structural safety increased, a total of four revisions have been made since the introduction of Seismic Design Standards in Korea in March 1988, and seismic design laws and applications have been changed accordingly. Recently, nonlinear analysis and seismic design of wall-type structure have been actively conducted in Korea by utilizing Performance-Based Seismic Design methods. Typically, structural analysis of wall-type structure for seismic design uses modeling method to constrain floor slabs with diaphragm method for ease of modeling and reduction of analysis time. However, the thickness of the slab is applied more than 210mm, which is significantly increased compared to the previous 120mm to 180mm, in order to respond to the floor impact sound of wall-type structure. According to the Standard Floating Floor Institution, it is suggested that the slab thickness of wall-type structure should be at least 210mm. As a result, it can be inferred that the influence of the slab on the stiffness and strength of the wall-type structure increased.

1.2 Scope and Objectives

The purpose of this study is to propose a structural design method for the procedure and method to consider the slab-wall interaction effect in the structural analysis of wall-type structure. Among the various wall shapes in which the slab-wall interaction occurs, structural performance tests and analysis studies are conducted for the most typical form which is coupled wall. Figure 1-1 (a) is the rigid diaphragm model and (b) is a model considering the slab using a shell element.

First, a study was conducted to determine the effect that occurs when the structural analysis considering the slab-wall interaction is carried out. By referring to the method that the engineer considered the slab, the tendency is identified when considering the slab-wall interaction. Also, the load resistance mechanism of method that considering slab-wall interaction will be explained in this process.

Next, a structural performance test is performed on the coupled wall. The effect that occurs when the slab is considered is comparatively analyzed through structural performance tests and nonlinear finite element analysis. In addition, numerical analysis is performed on the specimen in which the structural performance test was conducted. In this process, the analysis results that are the basis for the proposed design method are provided through comparative analysis of test and numerical analysis.

Finally, the proposed design method and the current design method are applied to the prototype model. Through the following design methods, it is possible to compare the relative economical data between considering slab-wall interaction design.

This thesis contains the subject of the in-plane wall-slab system, but does not provide information on the out-of-plane slab-wall system. There have been only studies related to the analysis method considering the slab, but there have been no results of comparative analysis between the specimen and the analysis considering the slab. Therefore, the design method proposed in this thesis is expected to give a convincing answer for the in-plane wall-slab system. However, additional research is needed for the out-of-plane wall-slab system. As a result, the design method proposed in this study is expected to provide the basis for the development of a structural design method that considers the slab-wall interaction.

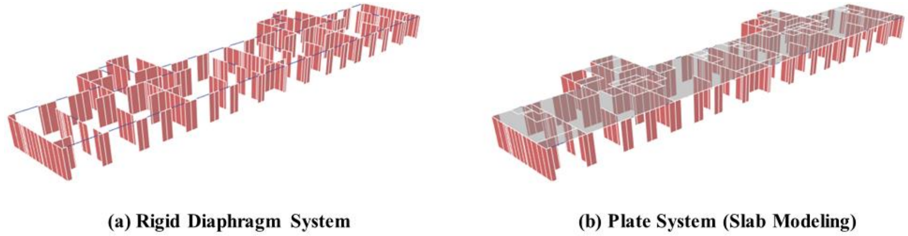

Figure 1-1 Case of Modeling

1.3 Outline of the Master's Thesis

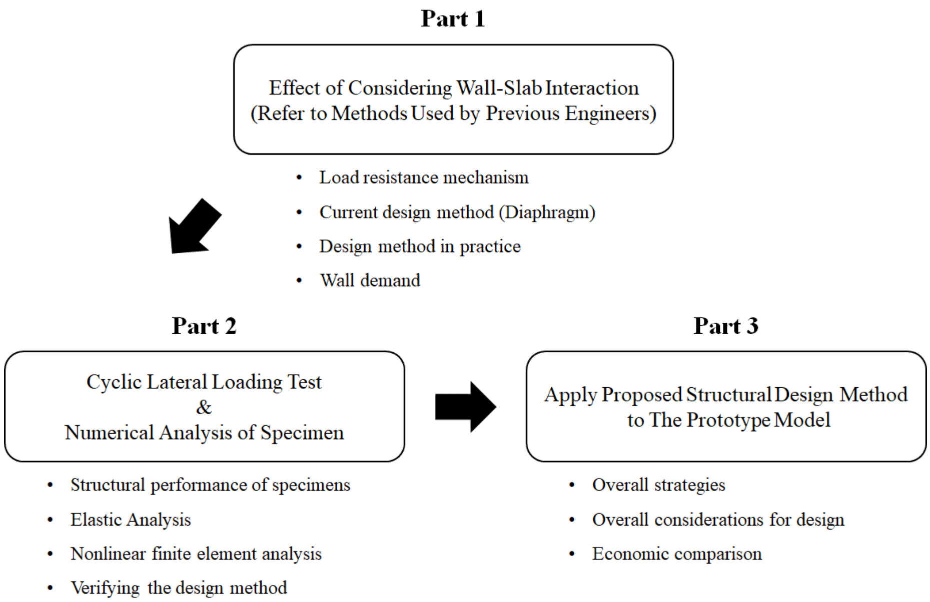

Figure 1-2 Outline of the master's thesis

Part 1

In chapter 3, A preliminary structural analysis is performed on a wall-type structure that does not consider the slab-wall interaction, which is diaphragm method, and a wall-type structure that considers the slab-wall interaction. By comparing two different condition, the case in which the load resistance mechanism occurs is defined and figure out the location in which the slab-wall interaction occurs. In addition, the tendancy of effects occurring in the slab model is confirmed by comparing the analysis results of two different models.

Part 2

In chapter 3 and 4, A structural performance test is performed on a coupled wall, which is a typical wall shape where the slab-wall interaction occurs. In addition, the design method to be proposed is verified by conducting a comparative analysis of structural performance tests, elastic analysis and nonlinear finite element analysis for the specimen.

Part 3

In chapter 5, design strategies and overall considerations for the structure design method considering the slab-wall interaction are announced. In addition, the proposed design method and the current design method are applied to the prototype model and compared in terms of economics.

Chapter 2. Literature Review

2.1 Code Review

2.1.1 Standard Floating Floor Insitution

With the introduction of the Standard Floating Floor Institution, the slab thickness of the wall-type structure must satisfy 210mm or more regardless of the structural performance requirements. In order to prevent the problem caused by the floor impact sound of the wall-type structure, the slab thickness is applied with a thickness of 210mm or more, which is significantly increased compared to the past 120 ~ 180mm. Through this, it is expected that the lateral resistance capability of the structure is improved by the influence of the slab.

Table 2-1 to Table 2-3 shows each code for standard floating floor system, and Figure 2-1 to Figure 2-3 shows each section of standard floating floor system.

Table 2-1 Code for Standard Floating Floor System 1 (Refer to Figure 2-1)

Type	Structure System	①Concrete Slab	②Resilient Material	③Lightweight Foam Concrete	④Finishing Mortar
1	Wall or Combined Rigid Frame Flate Plate Floor	210mm 150mm 180mm	20mm	40mm	40mm
2	Wall or Combined Rigid Frame Flate Plate Floor	210mm 150mm 180mm	-	20mm	40mm

∴ Must have at least the following thickness value

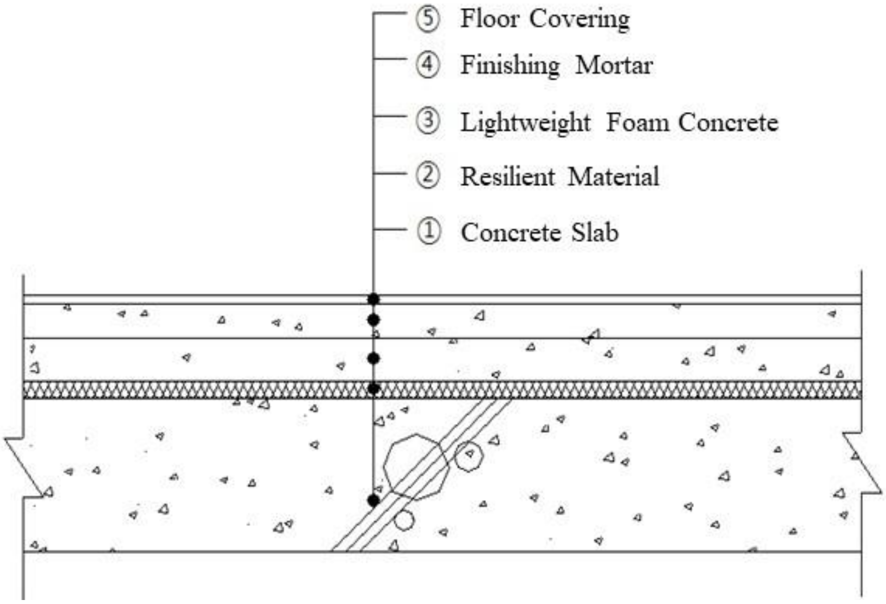

Figure 2-1 Section of Standard Floating Floor System 1

Table 2-2 Code for Standard Floating Floor system 2 (Refer to Figure 2-2)

Type	Structure System	①Concrete Slab	② Lightweight Foam Concrete	③ Resilient Material	④Finishing Mortar
1	Wall or Combined	210mm	40mm	20mm	40mm
	Rigid Frame	150mm			
	Flate Plate Floor	180mm			
2	Wall or Combined	210mm	-	20mm	40mm
	Rigid Frame	150mm			
	Flate Plate Floor	180mm			

∴ Must have at least the following thickness value

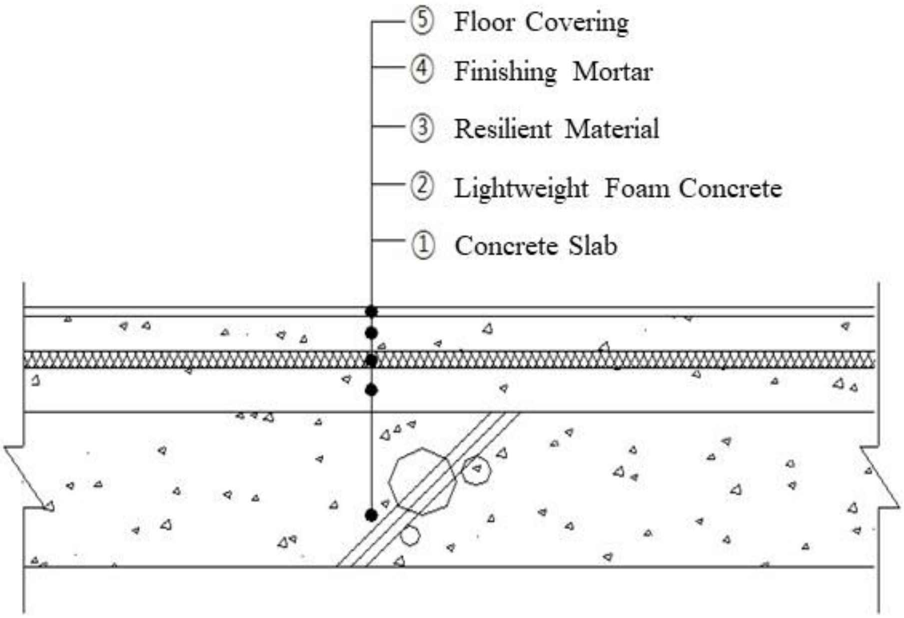

Figure 2-2 Section of Standard Floating Floor System 2

Table 2-3 Code for Standard Floating Floor system 3 (Refer to Figure 2-3)

Type	Structure System	①Concrete Slab	② Resilient Material	③ Finishing Mortar
1	Wall or Combined	210mm	40mm	50mm
	Rigid Frame	150mm		
	Flate Plate Floor	180mm		

∴ Must have at least the following thickness value

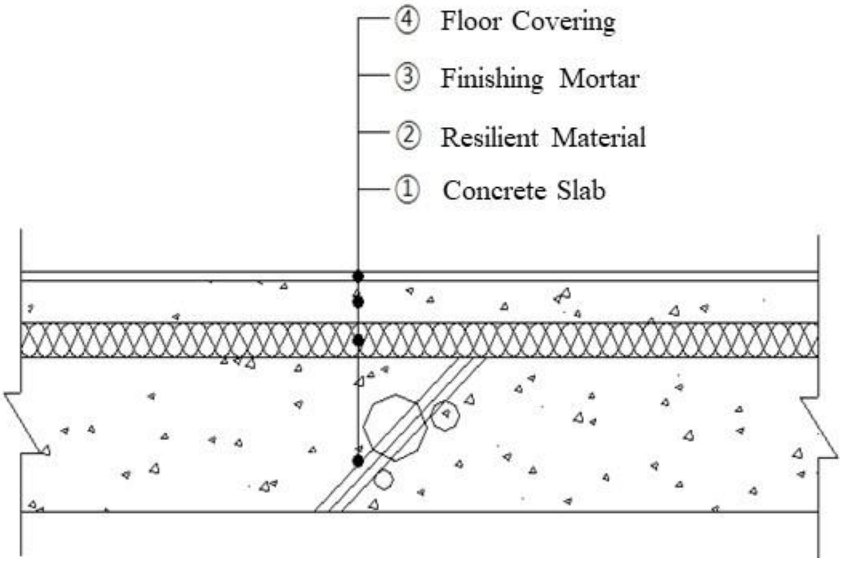

Figure 2-3 Section of Standard Floating Floor System 3

2.1.2 Korean Building Code 2016 (KBC 2016)

(a) 0306.7.2 Modeling

A mathematical model of building shall be able to describe the spatial distribution of mass and stiffness throughout the structure. For regular structures with independent orthogonal seismic-force-resisting systems, independent two-dimensional models are permitted to represent each system. For irregular structures without independent orthogonal systems, a three-dimensional model incorporating a minimum of three degrees of freedom consisting of translation in two orthogonal plan directions and torsional rotation about the vertical axis at each level of the structure shall be used. Where the diaphragms are flexible compared to the vertical elements of the seismic-force-resisting system, the model shall include the diaphragm's flexibility and additional degrees of freedom required to account for the influences of the diaphragm on the structure's dynamic response. For concrete and masonry structures, the effects of cracked sections shall be included. For steel moment frame systems, the contribution of panel zone deformations to overall story drift shall be included.

In case $\mathrm{P} - \Delta$ effects are considered to be significant, the effects shall be included in the analysis modeling or reflected on the analysis result.

When the area of the basement is significantly larger than that of the super-structure, the super-structure can be analyzed separately from the basement structure. Otherwise, the basement shall be modeled in conjunction with the super-structure. For the structure with basement, the lateral stiffness of the soil adjacent to the basement shall be neglected if the base level for site classification given in Section 0306.3.2.2 is defined as the bottom of the basement structure.

(b) 0306.12.2.3 Structural System

(1) The horizontal diaphragm or other structural elements shall provide continuity above the isolation interface and shall have adequate strength and ductility to transmit forces due to ground motion from one part of the structure to another.

(c) 0306.5.3 Determination of Fundamental Period

The fundamental period of the building in the direction under consideration shall be calculated as the fundamental period, T_a, determined from simplified methods in Section 0306.5.4 or shall be calculated by other theoretical methods considering the structural properties and deformational characteristics of the resisting elements. When T_a is calculated by theoretical methods, the calculated fundamental period, T_a, shall not exceed the product of the upper limit coefficient, C_u, from Table 0306.5.1 and the approximate fundamental period, T_a.

(d) 0306.7.3.5 Estimation of Design Values

(1) Design values such as the total base shear, V_t, story shear, story drift, story displacement, and member forces shall be determined by taking square root of the sum of the squares, SRSS, or complete quadratic combination, CQC, of the modal values.

(2) When the total base shear, V_t, obtained using the response spectrum analysis procedure is less than 85% of the base shear, V, obtained by the equivalent static procedure presented in Section 0306.5.3, the design values obtained from Section 0306.7.3.5(1) shall be multiplied by the modification factor, C_m, defined as follows:

$$C_m = 0.85\frac{V_T}{V} \geq 1.0$$

2.1.3 KDS 41 17 00, 2019 (Building Seismic Design Code)

(a) 7.2.3 Determination of Fundamental Period

The fundamental period of the building in the direction under consideration shall be calculated as the approximate fundamental period, T_a, determined from simplified methods in Section 7.2.4 or shall be calculated by the numerical analysis considering the structural properties and deformational characteristics of the resisting elements. However, the fundamental period calculated by the numerical analysis shall not exeed the product of coefficient of upper limit, C_u, from Table 7.2.1 and the approximate fundamental period, T_a.

(b) 7.3.2 Modeling

(4) For concrete and masonry structures, the effects of cracked sections shall be included. For steel moment frame systems, the contribution of panel zone deformations to overall story drift shall be included.

(c) 9.8.1 Structural Analysis

(1) Cracked stiffness of concrete members shall not be underestimated when the structural analysis is used to estimate seismic loads

(2) Cracked stiffness of concrete members shall not be overestimated when the structural analysis is used to estimate inelastic deformation

(3) Cracked stiffness of concrete members for the structural analysis shall be permitted to be determined according to 41 30 00 Building Concrete Design Code.

2.1.4 ASCE 7-16 (Seismic Design Requirements for Building Structures)

(a) 12.7.3 Structural Modeling

A mathematical model of the structure shall be constructed for the purpose of determining member forces and structure displacements resulting from applied loads and any imposed displacements or P-Delta effects. The model shall include the stiffness and strength of elements that are significant to the distribution of forces and deformations in the structure and represent the spatial distribution of mass and stiffness throughout the structure.

Structures that have horizontal structural irregularity Type 1a, 1b, 4, or 5 of Table 12.3-1 shall be analyzed using a 3-D representation. Where a 3-D model is used, a minimum of three dynamic degrees of freedom consisting of translation in two orthogonal plan directions and torsional rotation about the vertical axis shall be included at each level of the structure. Where the diaphragms have not been classified as rigid or flexible in accordance with Section 12.3.1, the model shall include representation of the diaphragm's stiffness characteristics and such additional dynamic degrees of freedom as are required to account for the participation of the diaphragm in the structure's dynamic response. In addition, the model shall comply with the following:

a. Stiffness properties of concrete and masonry elements shall consider the effects of cracked sections.

b. For steel moment frame systems, the contribution of panel zone deformations to overall story drift shall be included.

2.1.5 KDS 41 20 20, 20 (Bending Moment and Compression Design Criteria of Concrete Structure)

(1) The elastic secondary analysis is to use the cross-sectional characteristics of the member calculated in consideration of the effect of the axial force, the crack area over the length of the member, and the load sustaining effect.

(2) The following values can be used as the cross-sectional characteristics of structural members for the elastic secondary analysis.

① Modulus of elasticity (KDS 14 20 10 (refer to 4.3(1)))

② Sectional second moment:

- Column	:	$0.70I_g$
- Uncracked Wall	:	$0.70I_g$
- Cracked Wall	:	$0.35I_g$
- Beam	:	$0.35I_g$
- Flat-Plate or Flat-Slab	:	$0.25I_g$

③ Cross-sectional area : $1.00A_g$

(3) When a transverse continuous load is applied, area moment of inertia of the compression member obtained in (2) above is to be divided by $(1+\beta_{ds})$. β_{ds} is the ratio of the maximum continuous shear force factor to the maximum shear force factor of the entire layer, and a value of 1.0 or less should be used.

2.2 Practice Studies Review

2.2.1 Dongsung Structural Engineering (2005)

The elastic secondary analysis is to use the cross-sectional characteristics of the member calculated in consideration

(a) Target : Reinforced concrete wall-type apartment

(b) Purpose : 1) Comparative analysis of elastic analysis results when considering slab flexural stiffness, and 2) Development of adequate design method and economic evaluation when setting slab flexural stiffness.

(c) Result : When the slab effect was partially considered in partial story, the effect was not significant.

Table 2-4 Overview of Analysis Model

Parameter	Scope of parameter
Type of Apartment Plan	$84m^2$
Floor of Structure	15F, 20F, 25F
Analysis Model	Type 1 : Diaphragm Type 2 : Plate element for Slab Type 3 : Plate for the adequate floor slab (1/3 of the total) slab Type 4 : Plate for the every multiple of 3 story slab
Slab thickness	180mm

Table 2-5 Result of Analysis

Structural Behavior	Effect of Parameter (Compare to the diaphragm method)			
	Type 1	Type 2	Type 3	Type 4
Fundametal Period	100 %	82~88 %	90~94 %	93~95 %
Drift of Structure	100 %	70~77 %	84~86 %	87~89 %
Displacement of Structure	100 %	80~88 %	89~92 %	91~94 %
Wall Reinforcement	100 %	88~94 %	96~97 %	96~97 %
Slab Reinforcement	100 %	100~103 %	100~101 %	100~101 %
Foundation Reinforcement	100 %	100 %	100 %	100 %
Total Reinforcement	100 %	96~97 %	98~99 %	99~99 %

2.2.2 Gun Structural Engineering (2005)

The elastic secondary analysis is to use the cross-sectional characteristics of the member calculated in consideration

(a) Target : Reinforced concrete wall-type apartment

(b) Purpose : As the slab thickness increases due to the revision of the design standard, when considering the bending stiffness of the slab in a wall-type apartment, the behavior of structure and reinforcement quantity of the walls are compared.

(c) Result : 1) As the slab flexural stiffness was considered in addition to the diaphragm, the building stiffness increased significantly and the story drift decreased. 2) The reinforcement quantity of walls decreases as the slab effect is considered, but the effective stiffness must be properly considered because the reinforcement quantity of the slab increases.

Table 2-6 Overview of Analysis Model

Parameter	Scope of parameter
Type of Apartment Plan	148.5m^2
Floor of Structure	15F, 20F, 25F
Analysis Model	Type 1 : Diaphragm Type 2 : Diaphragm + Plate Slab (Effective Stiffness 15%) Type 3 : Diaphragm + Plate Slab (Effective Stiffness 25%)
Slab thickness	210mm

Table 2-7 Result of Analysis

Structural Behavior	Effect of Parameter (Compare to the diaphragm method)		
	Type 1	Type 2	Type 3
Fundametal Period	100 %	62~73 %	55~67 %
Shear Force of Strucuture	100 %	100 %	100~104 %
Story Drift	100 %	45~53 %	38~45 %
Wall Reinforcement	100 %	76~81 %	74~79 %
Slab Reinforcement	-	100 %	138~177 %

2.3 Liturature Review

2.3.1 Analysis Model 1 (Lee et al.)

A modeling method that can reduce the number of degrees of freedom while simulating the actual behavior of the slab is proposed. Plate element + pseudo beam was used, and the behavior of the structure was very similar compared to the case of modeling the slab using only the plate element.

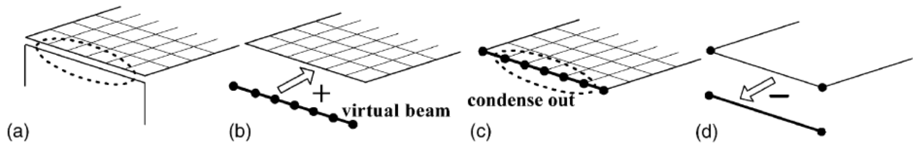

Figure 2-4 Case of Analysis Model 1

2.3.2 Analysis Model 2 (Pinho et al.)

Pseudo dynamic test was performed on the 3D frame structure, and based on this, a model was proposed to consider the slab effect. Diagonal truss model is used as a slab modeling technique. The analysis time can be shortened by greatly reducing the number of degrees of freedom, but it is difficult to simulate the actual behavior.

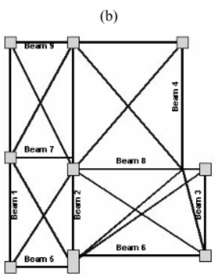

Figure 2-5 Case of Analysis Model 2

Chapter 3. Cyclic Lateral Loading Test

3.1 Introduction

Recently, nonlinear analysis and seismic design of wall type structure have been actively conducted in Korea by utilizing performance-based seismic design methods. Typically, structural analysis of wall type structure for seismic design uses modeling method to constrain floor slabs with diaphragm method for ease of modeling and reduction of analysis time. When performing the seismic design through the diaphragm, the wall acts as the main lateral load resistance system. In the case of a slab model, it does not apply as a lateral load resistance system at all.

However, the slab thickness of the wall-type structure must satisfy 210mm or more regardless of the structural performance requirements. It is because, in order to prevent the problem caused by floor impact sound, the slab thickness is regulated by law to have a value of 210mm or more, which is a greater value than the previous 120mm~180mm. For this reason, it can be inferred that the lateral load resistance capacity of the structure by the slab is increased than before.

In addition, in the case of recent wall-type structure apartment, the wall section area per floor has decreased and the shape of the walls is diverse, such as T-type, L-type, and H-type, etc. When the structural analysis is performed with a diaphragm without considering the influence of the slab and the slab-wall interaction that can occur in various walls, it will be difficult to simulate the behavior of actual structure.

In Chapter 3, Among the various wall shapes in which the slab-wall interaction occurs, a structural performance test is conducted for a coupled wall. Before carrying out structural performance tests, elastic analysis is performed considering the slab-wall interaction for general wall-type structure. Based on the results of elastic analysis, Structural performance tests were performed on two-story RC frame of slab-coupled wall structure. Through the test results, the effect of the slab on the structure is determined through the behavior, the failure mode, etc of specimens. In addition, nonlinear finite element analysis is performed for diaphragm specimens that cannot be tested in reality. The results of diaphragm analysis are compared and analyzed with the actual test to prove the lateral load resistance capacity of specimen increased by the slab.

3.2 Preliminary Elastic Analysis

3.2.1 Load Resistance Mechanism

The load resistance mechanism of the slab model is shown in Figure 3-1. V_1 shows the mechanism for resisting the shear force applied to the structure when the wall acts like a cantilever. This resists with the bending moment of the wall and is the same as the principle of the diaphragm. However, when the slab is modeled, the lateral resistance capacity is increased by the slab. In addition, the wall can obtain the effect of being partially integrated. Similar to the framing effect, axial force is generated on the wall by the slab, and the wall demand is reduced compared to the diaphragm model. Through this, in the case of the slab model, a mechanism is obtained that can resist the force of V_1 and the force of V_2.

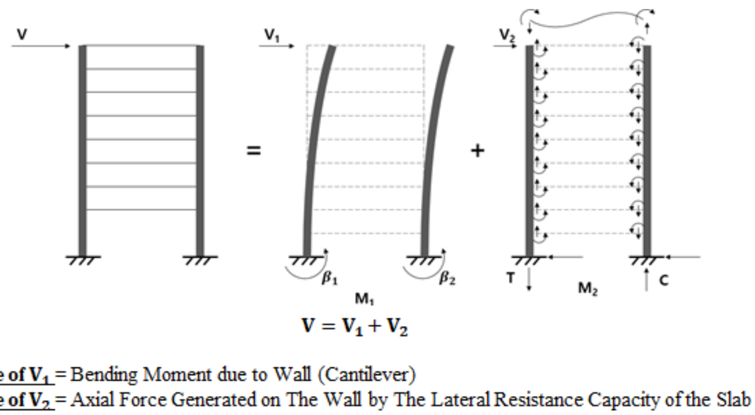

Figure 3-1 Load Resistance Mechanism

So far, slabs are thin and wide members, so there has been no problem even using the diaphragm. However, as the slab thickness increases, the influence of the slab on the structure increases. Therefore, when considering the slab, it is expected that there will be a significant effect on the increase in the stiffness and strength of the structure as well as the effect of reducing the quantity of wall reinforcing bars.

3.2.2 Location of Slab Effect

The location where the slab effect occurs can be known through the linear elastic analysis. As mentioned in the load resistance mechanism, when the slab is considered, the same effect as the framing effect occurs. Therefore, the stress in the slab generates shear force and bending moment, and axial force is generated in the wall. Therefore, if the location where the stress of the slab is concentrated is confirmed through linear elastic analysis, the shape of the wall where the slab-wall interaction occurs most can be known. Figure 3-2 shows the location where the slab effect occurs.

As can be seen in the Figure 3-2, coupled wall is the most typical wall shape, and it is the wall shape where the slab effect occurs a lot. Therefore, in this study, structural performance tests are performed in relation to the coupled wall-slab structure among walls of various shapes.

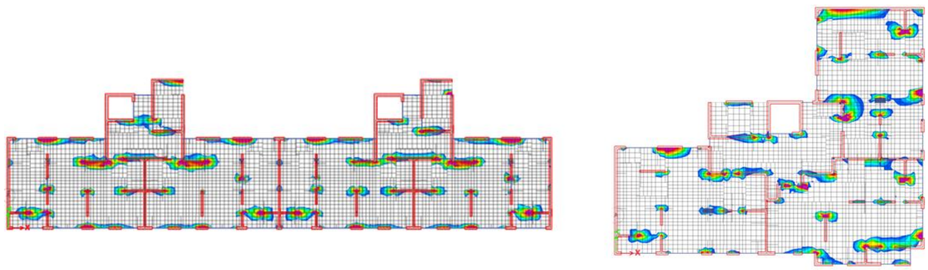

(a) – Shaped Plan Structure (b) L Shaped Plan Structure

Figure 3-2 Location of Slab Effect in Wall-Type Structure

3.2.3 Wall Demand

In the case of the model considering the slab, it was previously expected that the wall demand would decrease. Therefore, the demand of the 1st floor wall for one wall-type strucuture was compared with the diaphragm model and a total of four models. In the case of the diaphragm model, the wall used a membrane element and the slab was constrained by the diaphragm.

The four models are as follows, and the demands of the wall are compared with the diaphragm model in terms of axial force, shear force, and bending moment. 1) Wall (Shell 100%) + Slab (Diaphragm), 2) Wall (Shell 100%) + Slab (Shell 100%), 3) Wall (Shell 100%) + Slab (Shell 50%), 4) Wall (Shell 100%) + Slab (Shell 15%). When diaphragm is used for the slab and the shell element is used for the wall, there appears to be no difference from the case when the wall uses a membrane element. However, when considering the slab, it can be confirmed that the demands of wall is greatly reduced. Also, it can be seen from Figure 3-3 that the bending moment of the wall increases as the stiffness of the slab decreases. Using 100% stiffness of the slab is great for reducing the quantity of wall reinforcing bars, but it is inappropriate because the effect of early yielding of the slab cannot be considered. Therefore, it is important to find the appropriate stiffness of slab and wall.

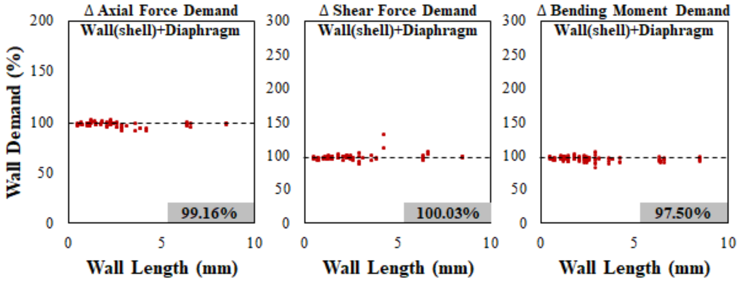

(a) Wall (Shell 100%) + Slab (Diaphragm)

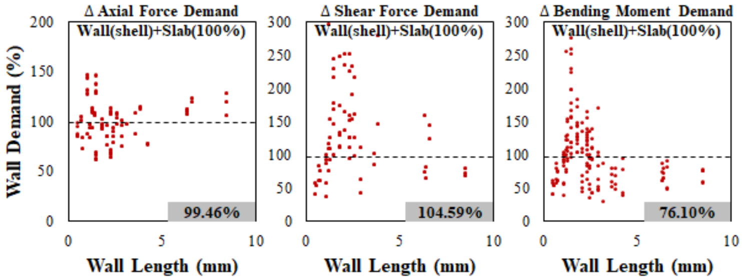

(b) Wall (Shell 100%) + Slab (Shell 100%)

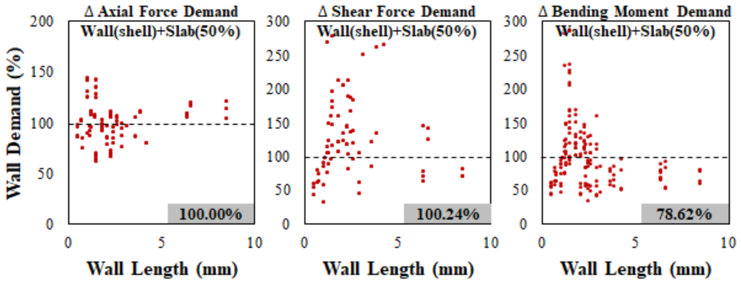

(c) Wall (Shell 100%) + Slab (Shell 50%)

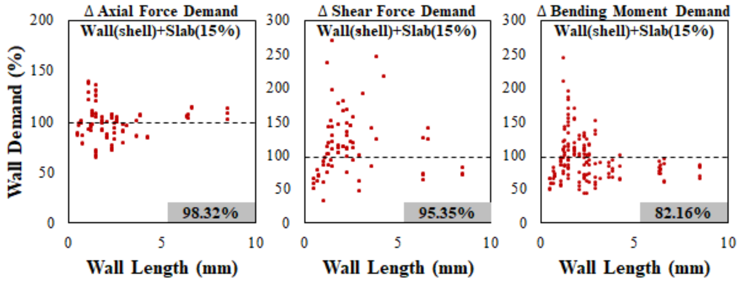

(d) Wall (Shell 100%) + Slab (Shell 15%)

Figure 3-3 Comparison of Wall Demands

3.3 Test Plan

3.3.1 Test Parameters

Table 3-1 is a table of variables for a total of 4 specimens. Lateral cyclic loading test were performed on specimens. A total of three were selected as variables for the specimen and are as follows. 1) slab thickness, 2) spacing between walls, 3) lattice-shaped shear reinforcement reinforcement at slab-wall joint. SWB1 specimen has a slab thickness of 80mm, which is less than 120mm, and contains 1) variables. SWB3 specimen contains 2) parameters as the spacing between walls is 600mm wider than 400mm. SWB4 specimen contains 3) variables as the lattice-shaped shear reinforcement reinforcement is reinforced at slab-wall joint. The following specimens were constructed and the structural performance tests were conducted.

Table 3-1 Parameters of Test specimens

Specimens	Slab Dimension (t_w) [mm]	Design Failure Mode	Concrete Strength f_c' [Mpa]	Reinforcement							Strength Prediction			
				Wall (Web & Flange)					Slab		Wall Shear Strength V_n [kN]	Flexural Strength V_f [kN]	Wall Friction Strength V_{sf} [kN]	$\frac{V_n}{V_f}$
				Horizonal			Vertical		Horizonal					
				f_{ywh} [Mpa]	ρ_{wh} [%]	$f_{ywh}\rho_{wh}$ [Mpa]	f_{ywv} [Mpa]	ρ_{wv} [%]	f_{yslab} [Mpa]	ρ_{hslab} [%]				
SWB1	80	Flexural	30	500	1.13	5.63	500	0.66	500	0.82%	1,351	229	1,398	5.9
SWB2	120	Flexural	30	500	1.13	5.63	500	0.66	500	0.55%	1,351	262	1,398	5.16
SWB3	120	Flexural	30	500	1.13	5.63	500	0.66	500	0.55%	1,351	262	1,398	5.16
SWB4	120	Flexural	30	500	1.13	5.63	500	0.66	500	0.55%	1,351	301	1,398	4.49

3.3.2 Detail of Test Specimens

Figure 3-4, Figure 3-6, Figure 3-8 and Figure 3-10 show the wall reinforcement details of each specimen. All the specimens have two-story RC frame of slab-coupled wall structure, and consist of specimens that are 1/2 scale of the actual structure. Therefore, the height of all walls is 1500mm. In addition, the cross section of all walls is 1000mm x 150mm, and the following two walls are arranged in a structure that is coupled by a slab for each story. The vertical reinforcing bars of the wall are D10 and are arranged at 155mm intervals. The horizontal reinforcing bars of the wall are D13 and are arranged at 150mm intervals. In addition, U tie bars of D10 were inserted on both sides of each wall to reinforce the side of the wall. The dowel bars are inserted into the wall connection so that the upper and lower walls can behave integrally when a cyclic lateral load is applied.

Figure 3-5, Figure 3-7, Figure 3-9 and Figure 3-11 show the slab reinforcement details of each specimen. The slab thickness of the specimen is composed of 80mm or 120mm, and the width of slab is 1300mm. In the case of slab, even if it is 1/2 scale, D10 was used because deformed reinforcement smaller than D10 was not available, and 246mm (about 250mm) was used for the rebar spacing. Since it has a thinner thickness compared to the actual structure, two layers of reinforcing bars were placed at the slab near the slab-wall joint to prevent failure mode like tearing in the horizontal direction of the specimen during the test. The following reinforcement bars are placed in the vertical direction of the specimen's loading direction. It was confirmed through a nonlinear finite element analysis program that there was no difference in the behavior of the specimen due to the reinforcement placement.

Figure 3-4 and Figure 3-5 are details of the slab and wall reinforcement of specimen SWB1. The variable of SWB1 is the slab thickness, and unlike other specimens, it has a slab thickness of 80mm.

Figure 3-6 and Figure 3-7 are details of the slab and wall reinforcement of specimen SWB2. Unlike SWB1, it is designed with a slab thickness of 120mm. Compared with SWB1, the influence of the structure due to the change in the slab thickness can be identified. Through the following test results, it is possible to figure out the tendency of the structural behavior due to the slab-wall interaction.

Figure 3-8 and Figure 3-9 are details of the slab and wall reinforcement of specimen SWB3. The variable of SWB3 is the spacing between walls. In the case of the other specimens, the spacing between the walls is 400mm, while the SWB3 has 600mm opening. The following test results will figure out how the behavior of the actual structure changes due to the slab-wall interaction when the gap between the walls is widened.

Figure 3-10 and Figure 3-11 are details of the slab and wall reinforcement of specimen SWB4. The variable of SWB4 is lattice-shaped shear reinforcement. For specimens except SWB4, two layers of reinforcing bars were placed at the slab near the slab-wall joint to prevent failure mode like tearing in the horizontal direction of the specimen during the test. As mentioned earlier, it was confirmed through a nonlinear finite element analysis program that the effect of reinforcement did not occur. In the case of the slab, since it is an element that is thinner and more widely distributed than other elements, it has great in-plane shear capacity and bending moment capacity, but out-of-plane shear capacity and bending moment capacity are very weak. Therefore, it is considered that the lateral load resistance capacity of the structure will be improved when the lattice-shaped shear reinforcement is located on the slab-wall joint. Through comparison with SWB2, it is possible to identify the behavior of the structure and the lateral load resistance capacity when the shear reinforcement is placed.

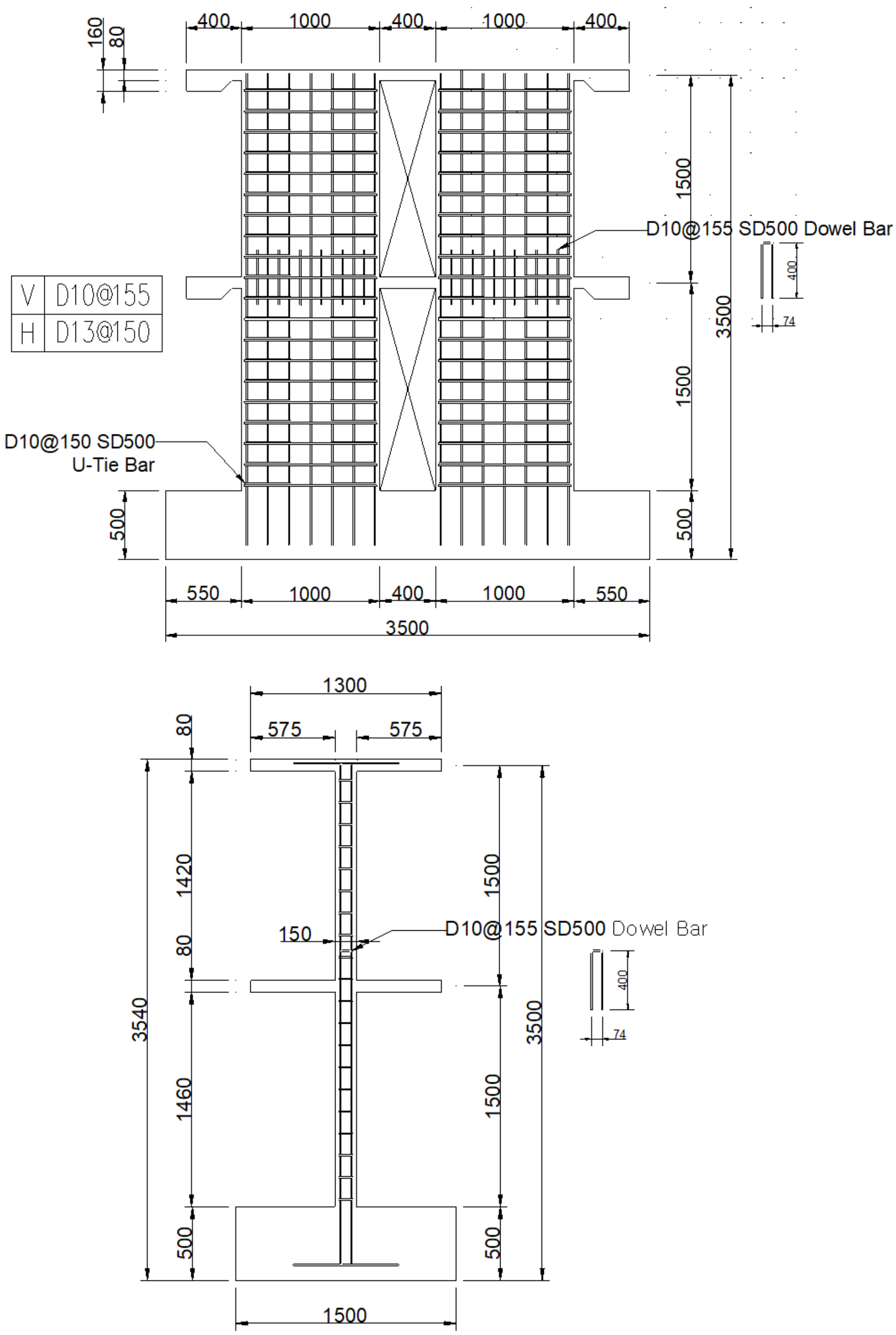

Figure 3-4 Wall Detail of Specimen SWB1

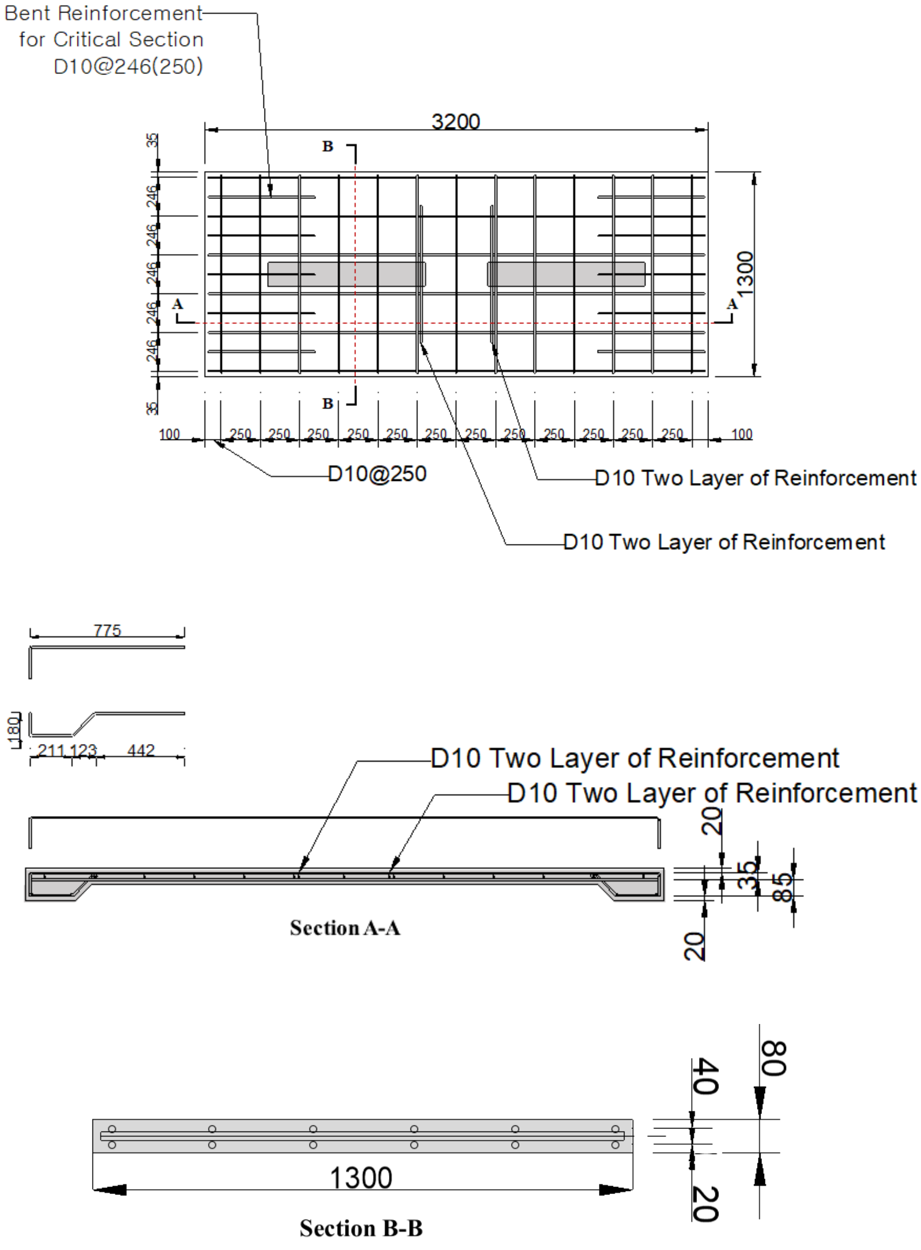

Figure 3-5 Slab Reinforcement Detail of Specimen SWB1

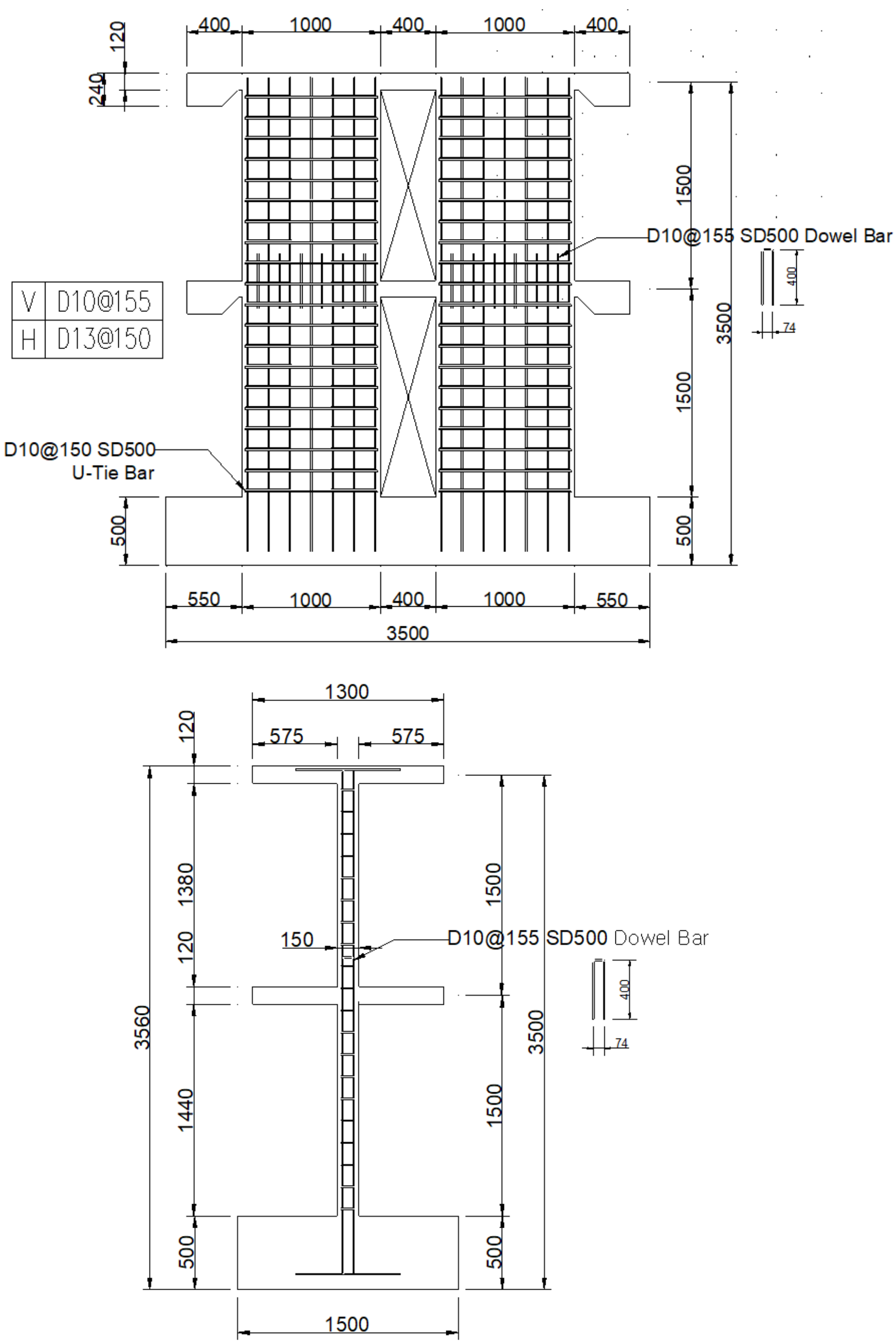

Figure 3-6 Wall Reinforcement Detail of Specimen SWB2

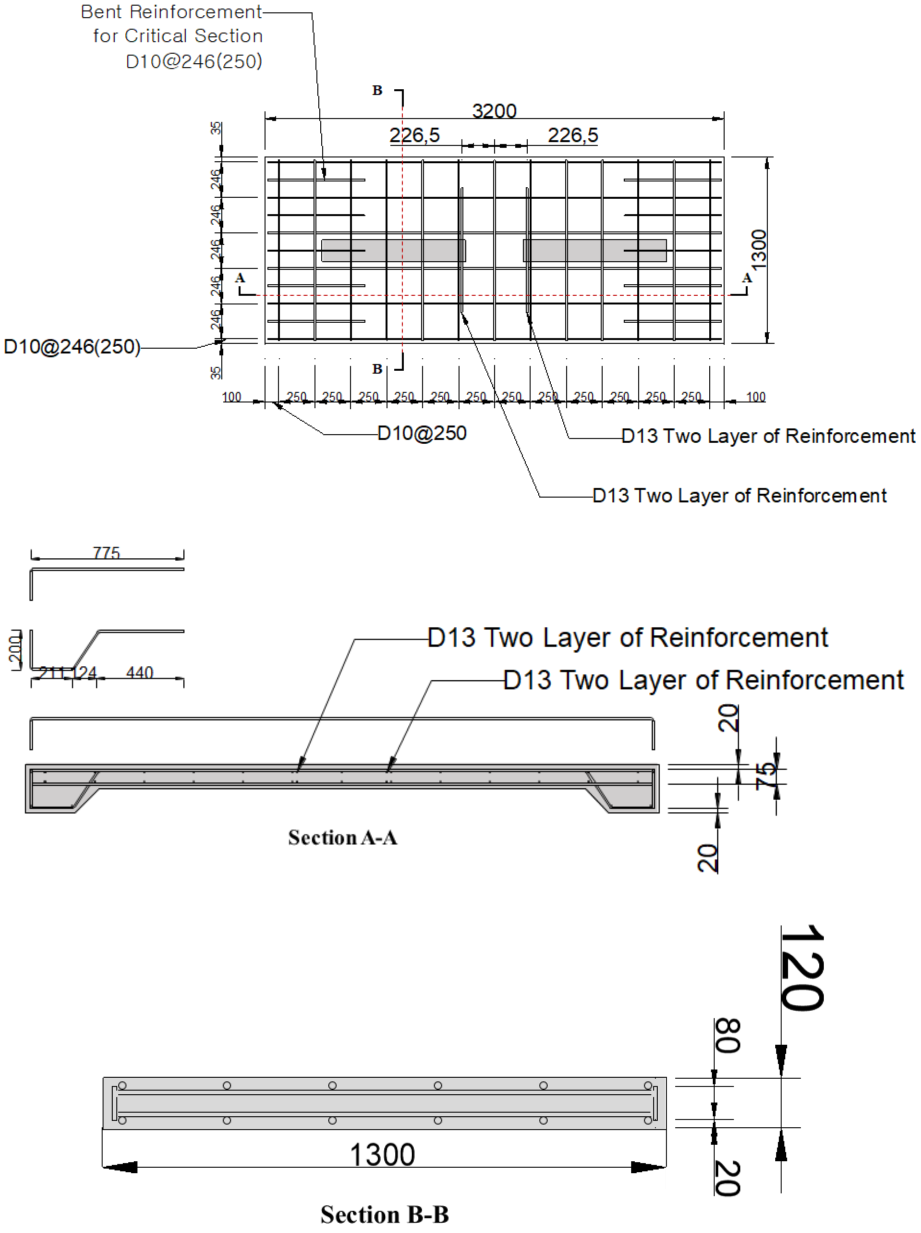

Figure 3-7 Slab Reinforcement Detail of SWB2

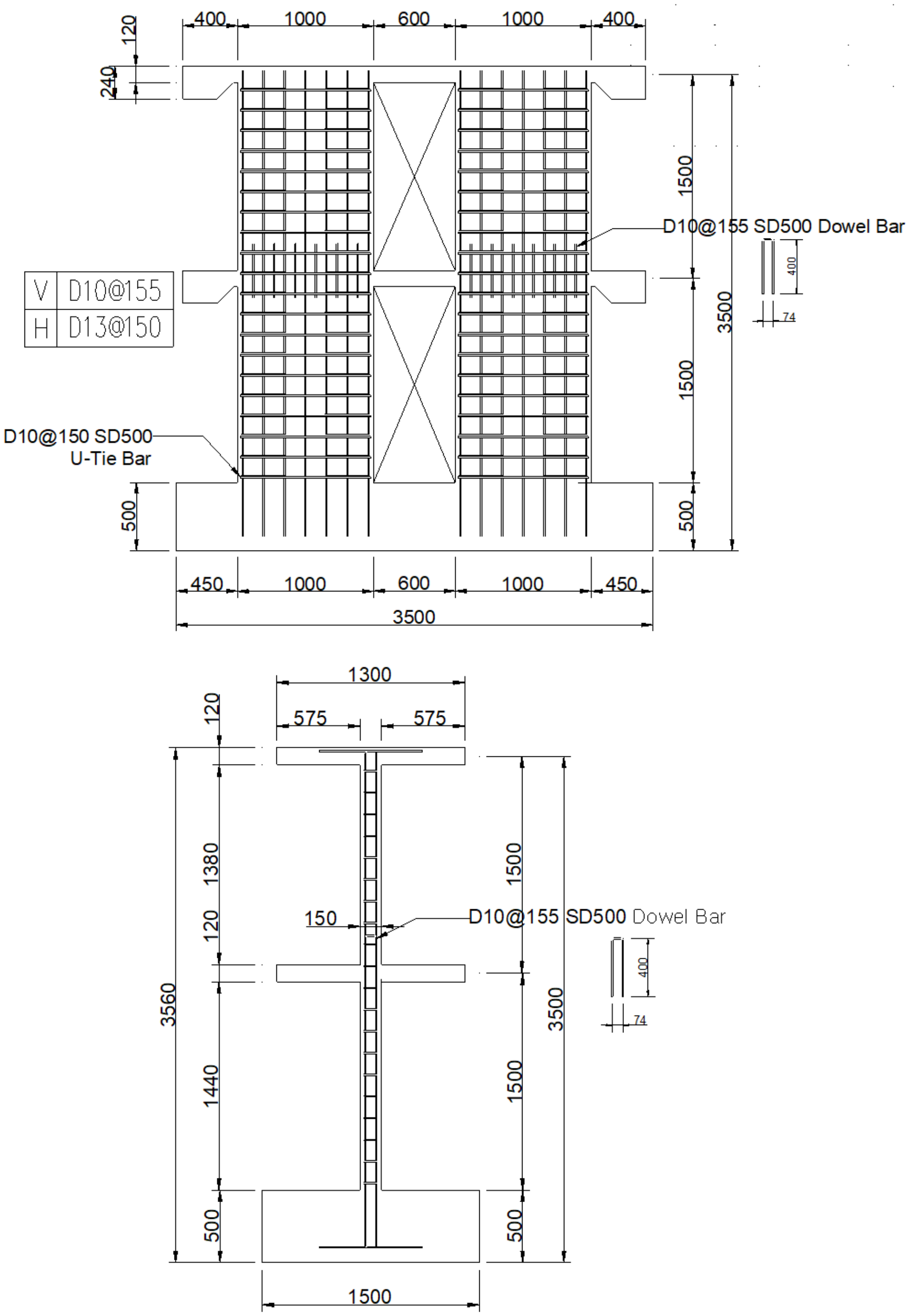

Figure 3-8 Wall Reinforcement Detail of Specimen SWB3

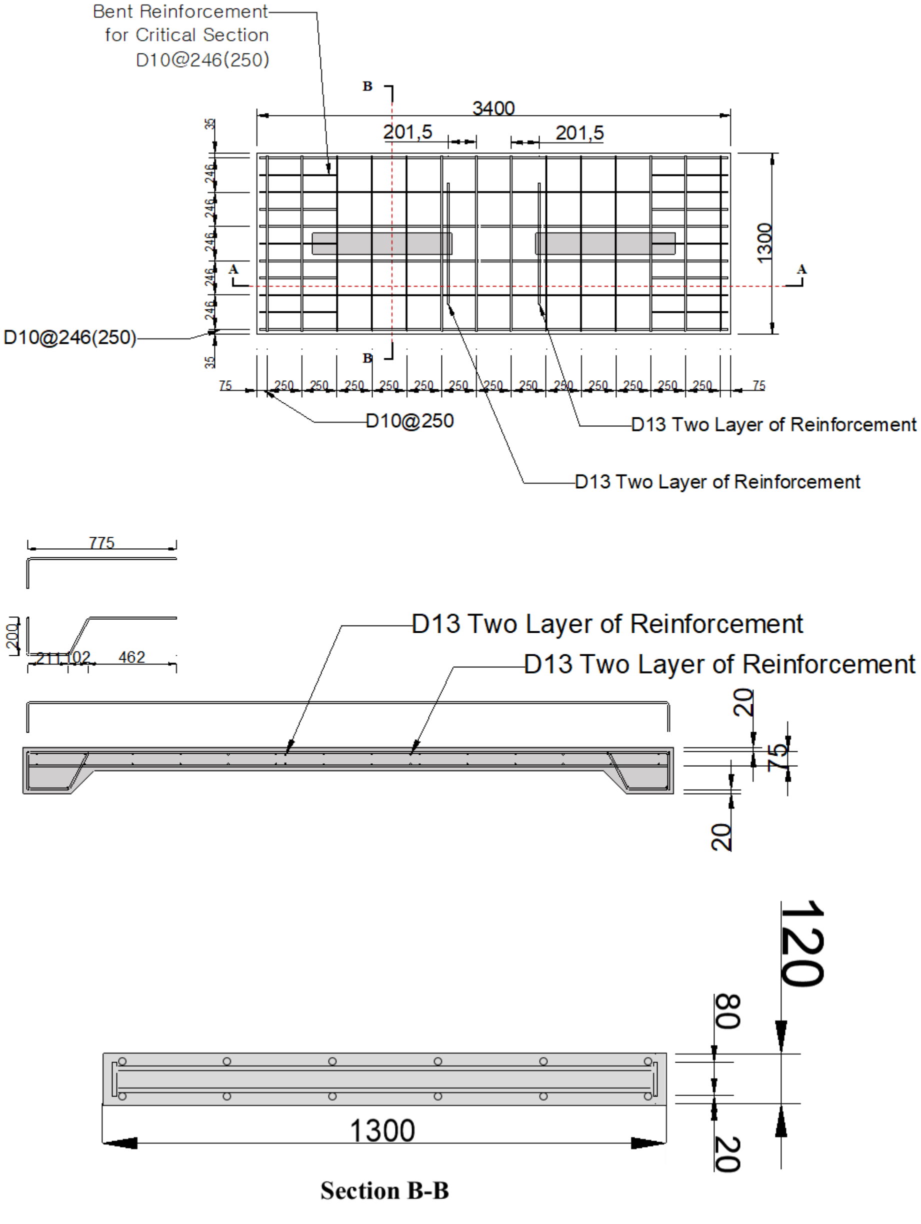

Figure 3-9 Slab Reinforcement Detail of SWB3

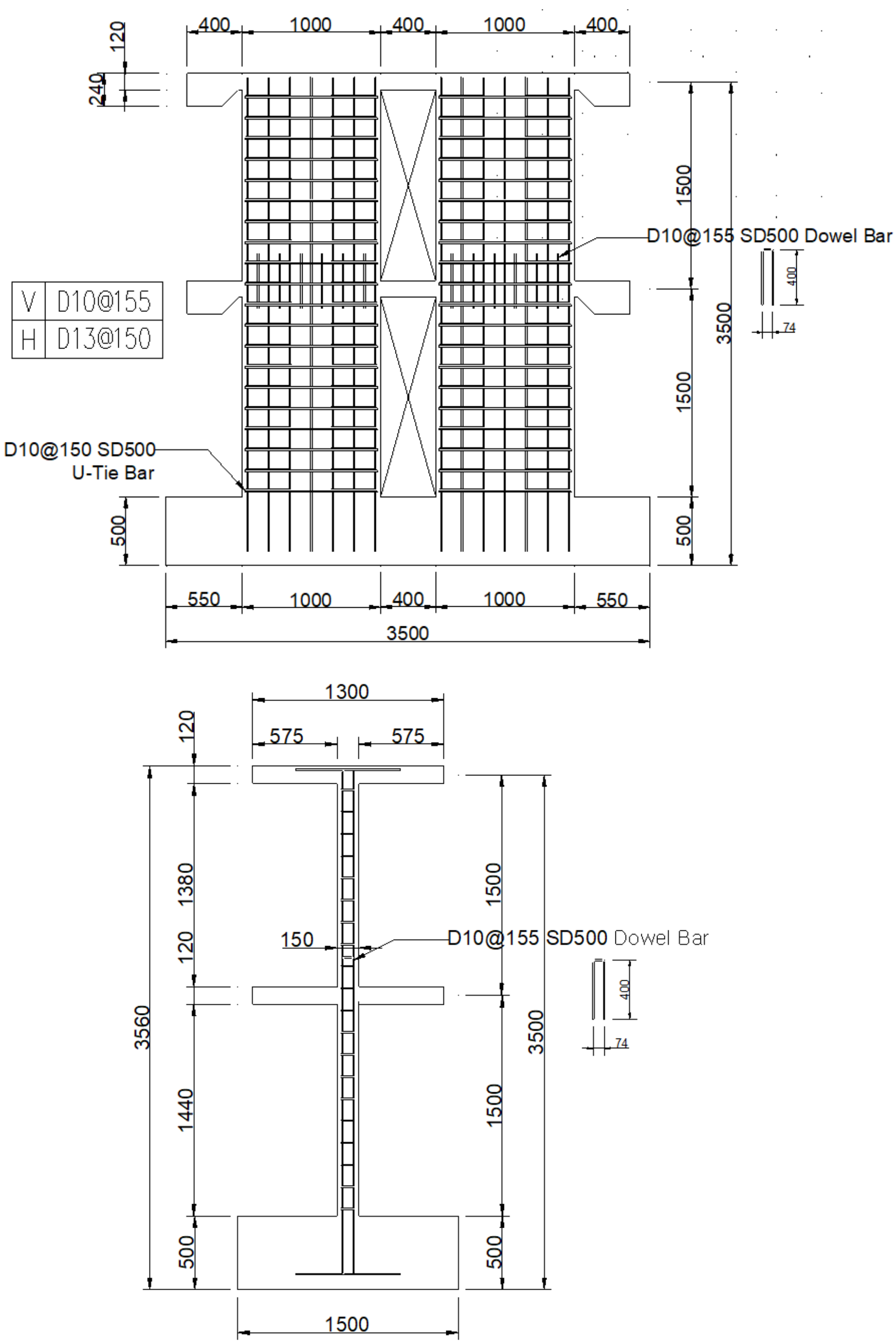

Figure 3-10 Wall Reinforcement Detail of Specimen SWB4

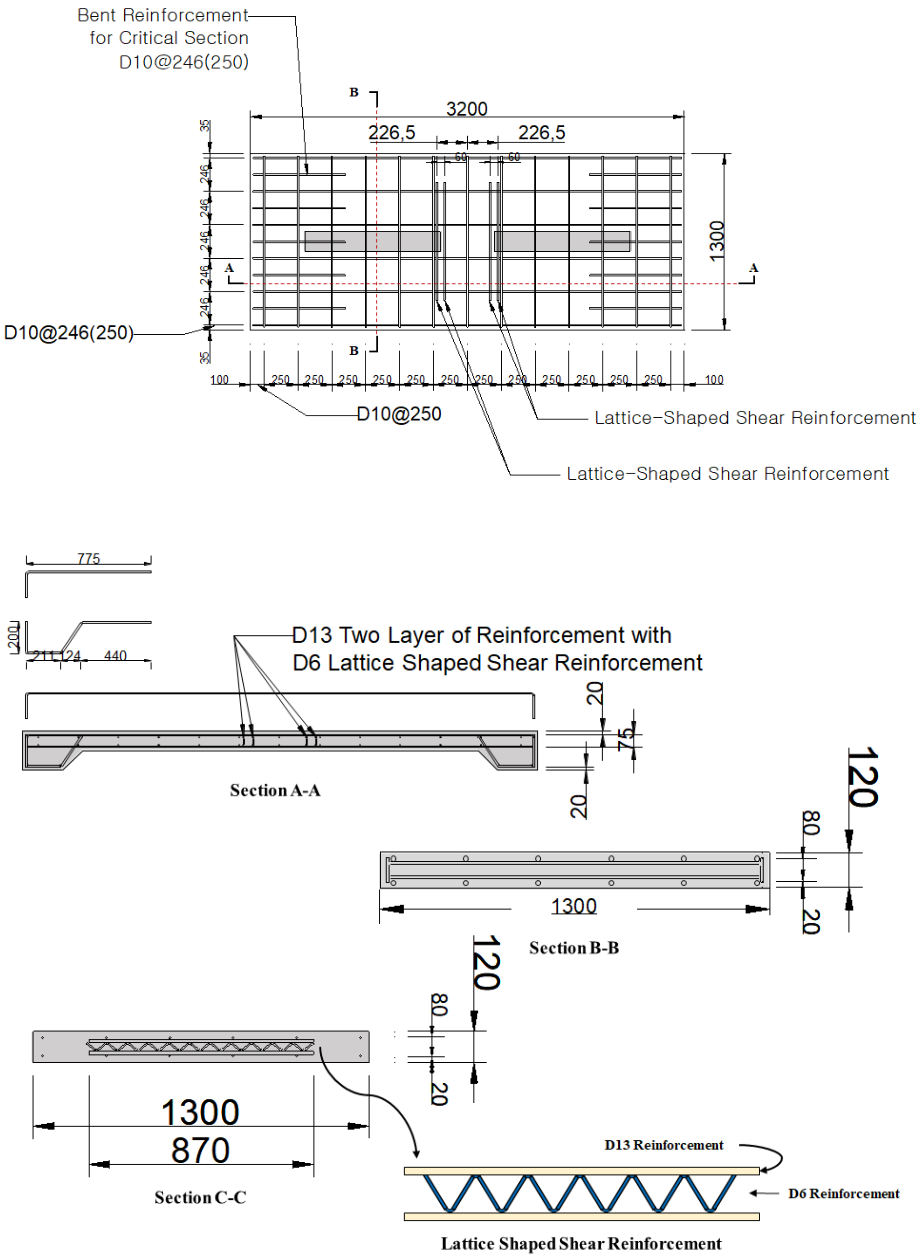

Figure 3-11 Slab Reinforcement of Specimen SWB4

3.3.3 Lifting Plan of Specimen

In the case of a specimen having a slab-wall structure, a problem occurs when the specimen is lifted by a method of lifting in general. Since the slab may crack due to the rope used for lifting, a lifting jig was manufactured and lifted as shown in Figure 3-12. As shown in Figure 3-12, it can be seen that no effect is applied to the slab when the specimen is lifted. When lifting, it was confirmed that the base of the specimen should be able to withstand the weight of the specimen and that no cracks occurred. In addition, it was designed in consideration of the load generated on the lifting jig.

Figure 3-12 Lifting specimen by lifting jig

3.3.4 Test Setup

Figure 3-13 and Figure 3-14 show the cyclic lateral loading test setup for ntwo-story RC frame of slab-coupled wall structure. In order to simulate the slab-wall interaction, the loading jig is directly connected to the slab using bolts embedded in the slab, and the jig is fixed with steel bars tensioned at both ends of the slab to enable both tension and compression. It is planned to transmit the load from the outside of the test specimen so that the out-of-plane deformation of the slab is not limited by the influence of the loading jig. The load is transmitted to the wall through the slab, and the load is transmitted according to the stiffness ratio of the wall. This maximizes the interaction between the wall and the slab. The horizontal load applied to the specimen is assumed to be an inverted triangular load distribution. Therefore, the actuator loading point is set so that the ratio of the lateral load acting on the upper and lower slabs is 2:1 ($F_T : F_B = 2 : 1$). The load of the jig and the actuator is supported by the support jig, and the degree of freedom in the horizontal direction is secured by installing a roller under the actuator connecting jig. Lateral support jig is installed on the left and right sides of the specimen to prevent out-of-plane conduction of the specimen.

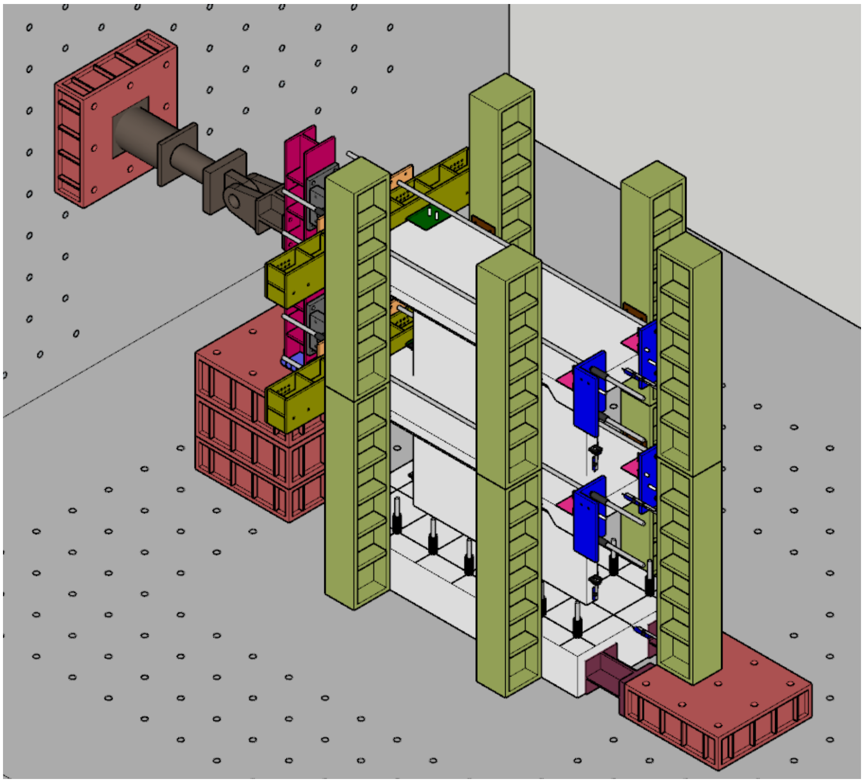

Figure 3-13 Cyclic Lateral Loading Test 1

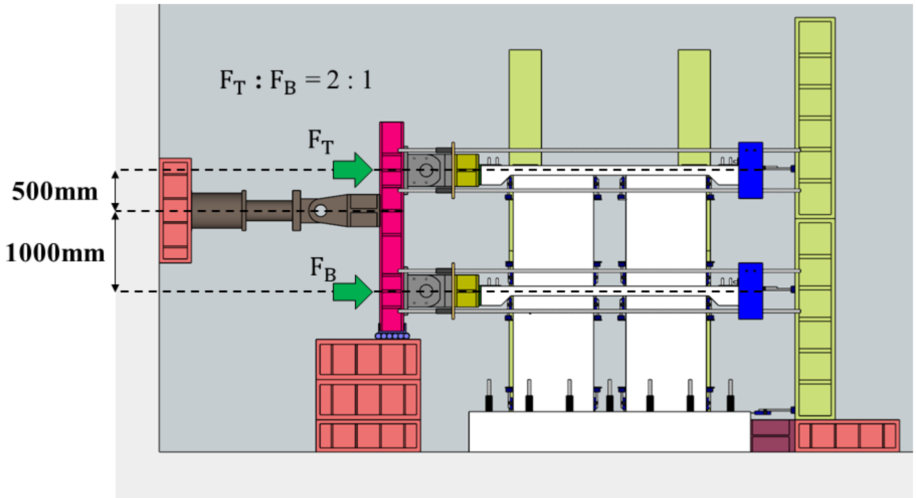

(a) Side View of Cyclic Lateral Loading Test Setup

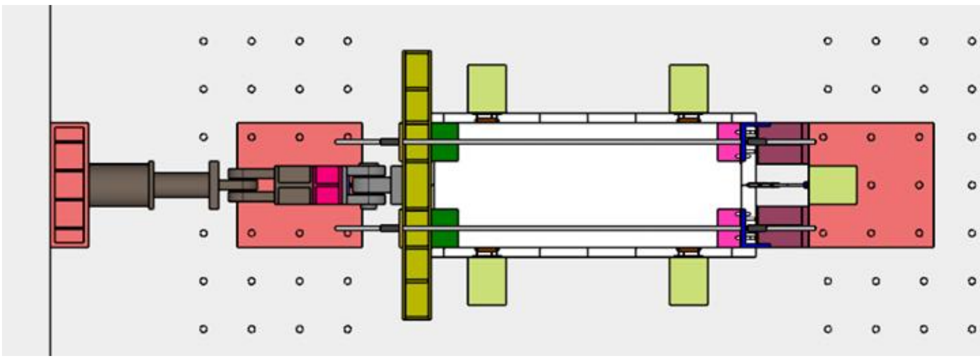

(b) Upper View of Cyclic Lateral Loading Test Setup

Figure 3-14 Cyclic Lateral Loading Test Setup 2

3.3.5 Loading Plan

Figure 3-15 shows loading pattern of the cyclic loading. Table 3-2 shows numerical value of lateral displacement and drift ratio of each step.

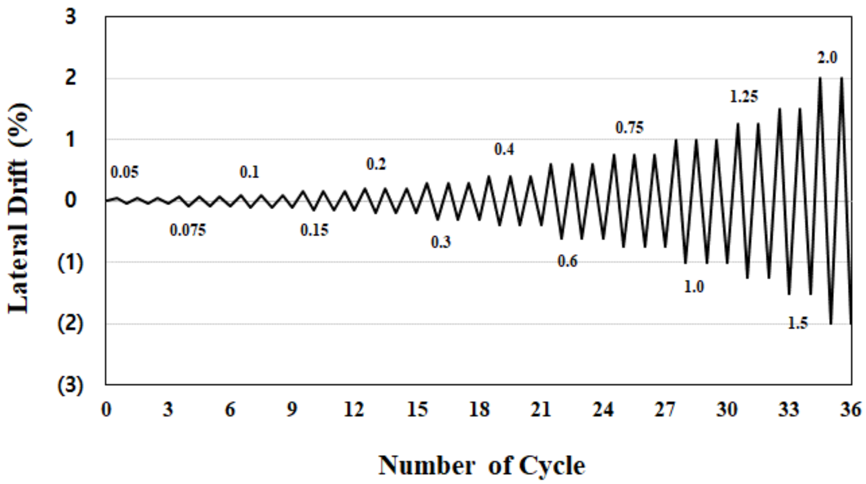

Figure 3-15 Lateral Loading Protocol

Table 3-2 Displacement or Drift of Loading Protocol

Step Number	Lateral Displacement [mm]	Lateral Drift [%]
Step 1	± 1.50	± 0.05
Step 2	± 2.25	± 0.075
Step 3	± 3.00	± 0.10
Step 4	± 4.50	± 0.15
Step 5	± 6.00	± 0.20
Step 6	± 9.00	± 0.30
Step 7	± 12.0	± 0.40
Step 8	± 18.0	± 0.60
Step 9	± 22.5	± 0.75
Step 10	± 30.0	± 1.00
Step 11	± 37.5	± 1.25
Step 12	± 45.0	± 1.50
Step 13	± 60.0	± 2.00

3.3.6 LVDT and Strain Gauge Plan

All the specimens were tested through the LVDT plan as shown in Figure 3-16. For each wall, two shear deformations and four flexural deformations were measured using LVDTs. In the case of the slab, the out-of-plane deformation was measured using LVDT at a distance of 50 mm from both sides of the wall. In addition, to measure the slip and rocking of the foundation, two measurements were made on each side, and the main displacement LVDT was measured using one at the center of the lower story slab and one at the center of the upper story slab. Therefore, a total of 42 LVDTs were measured using 24 LVDTs in the wall, 12 in the slab, 4 in the foundation, and 2 in the main displacement of specimens.

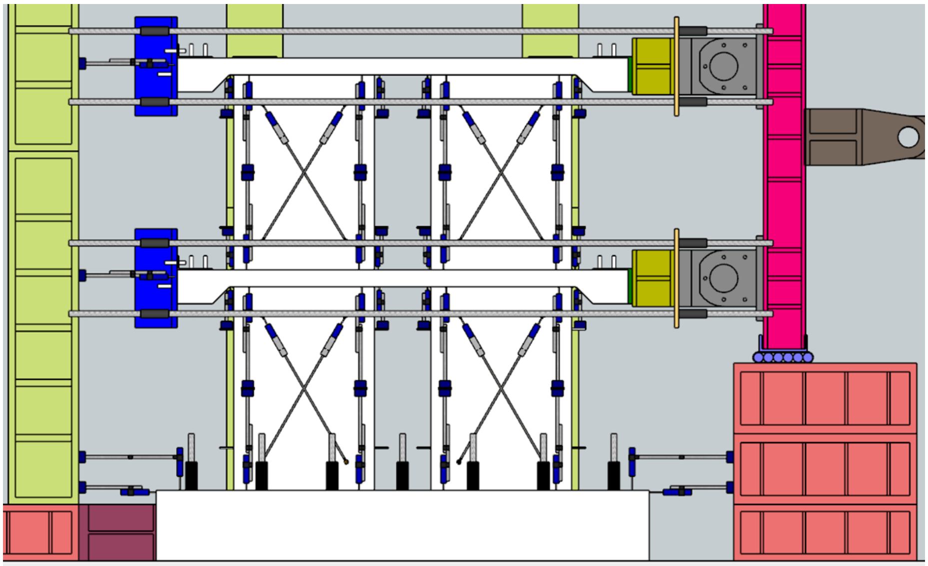

Figure 3-16 Plan of LVDT

In the case of the wall strain gauge plan, a strain gauge was attached to the vertical reinforcing bars of the upper story wall and lower story walls in order to check whether the wall behaves integrally. In addition, by attaching a strain gauge near the wall adjacent to the slab, it was confirmed whether there was an interaction between the wall and the slab. In addition, in the case of the horizontal rebar strain gauge on the wall, it was installed to check the effect of shear force, and the strain gauge plan for the wall is shown in Figure 3-17.

In the case of the slab strain gauge plan, an out-of-plane moment of the slab occurs near the slab-wall joint. In addition, in order to confirm the effect of load redistribution in the slab-wall specimen, a strain gauge was designed for the main and minor direction of flexural reinforcement of the slab between the walls as shown in Figure 3-18 and Figure 3-19.

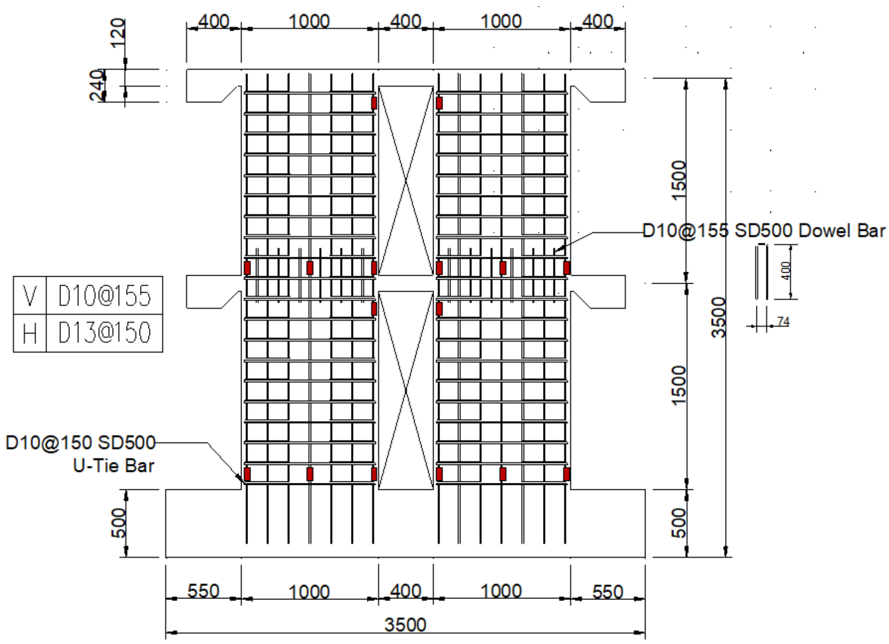

Figure 3-17 Strain Gauge Plan of Wall

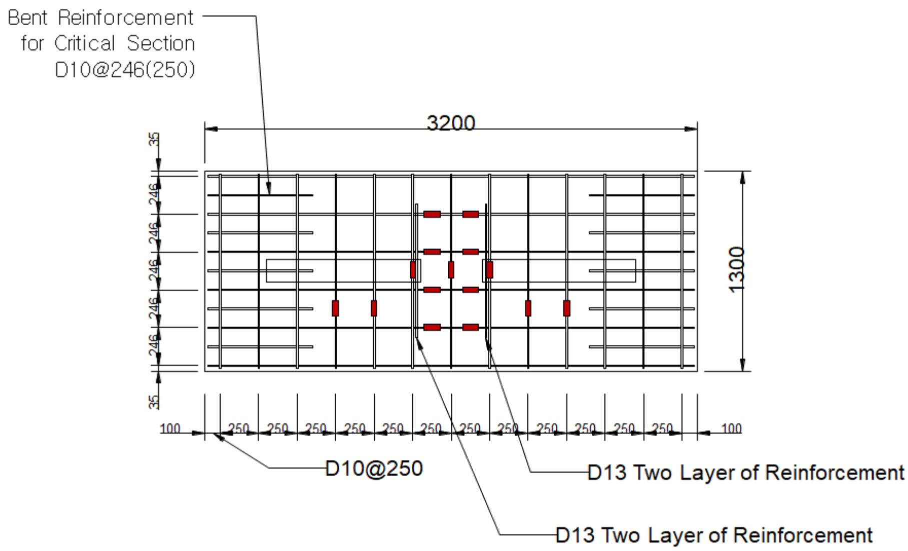

Figure 3-18 Strain Gauge Plan of Slab (SWB1, SWB2, SWB4)

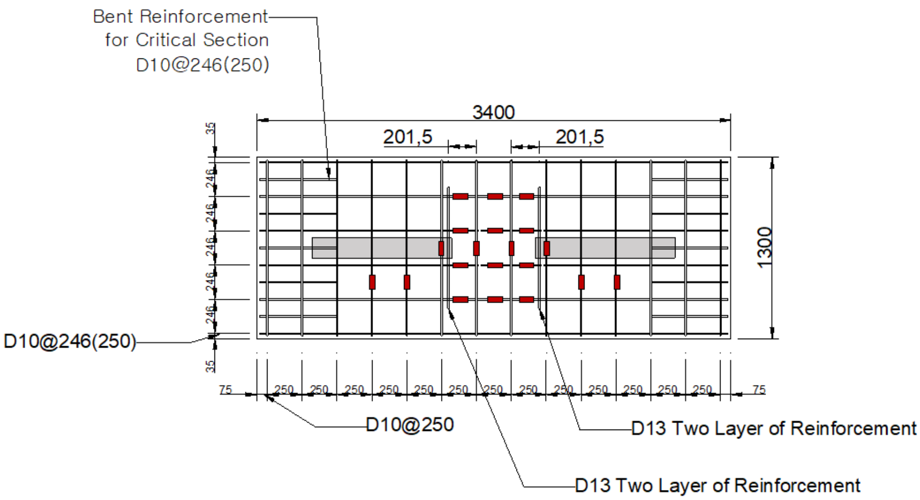

Figure 3-19 Strain Gauge Plan of Slab (SWB3)

3.3.7 Construction Process of Specimens

Figure 3-20 Construction Process of Foundation

Figure 3-21 Construction Process of Lower Story

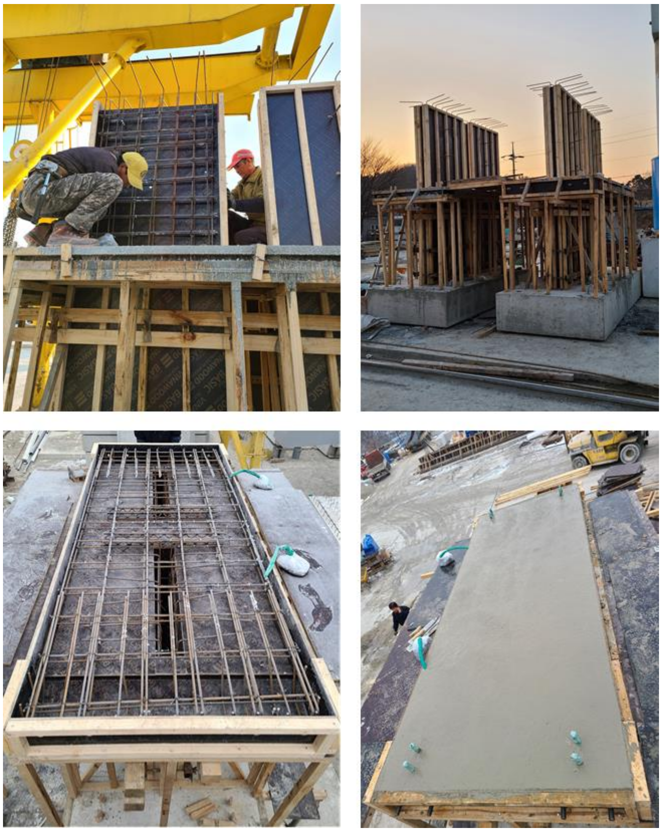

Figure 3-22 Construction Process of Upper Story

Figure 3-23 Removing Formwork at EPTC

3.4 Test Result

3.4.1 Material Strength Test

The material strength test of concrete was carried out on the day of test respectively. However, if the planned concrete strength and the results of the material test are significantly different, or if the concrete specimen is not properly cured due to steam curing, the strength is measured by extracting the core.

Table 3-3 Concrete Strength of Specimen

Specimen	Concrete Strength							
	Lower Slab-Wall				Upper Slab-Wall			
	1	2	3	Average	1	2	3	Average
SWB1	46	41	40	42.3	35	34	31	33.4
SWB2	31	30	28	30.0	41	42	33	38.4
SWB3	31	35	37	34.3	30	33	33	32.0
SWB4	31	35	37	34.3	35	19	34	29.0

Figures 3-26 shows the stress-strain Relationship of the reinforcing bar D10 and D13.

Table 3-4 Rebar Stress and Strain of Specimen

Diameter of Rebar	Rebar Number	Yield Strain	Yied Strength [Mpa]	Ultimate Strength [Mpa]
D10	1	0.0029	603	709
	2	0.0028	568	680
	3	0.0029	596	715
	Average	**0.0029**	**589**	**701**
D13	1	0.0027	553	671
	2	0.0028	565	691
	3	0.0027	549	679
	Average	**0.0027**	**555**	**680**

Figure 3-24 Material Test for Concrete

Figure 3-25 Material Test for Reinforcement (D10 and D13)

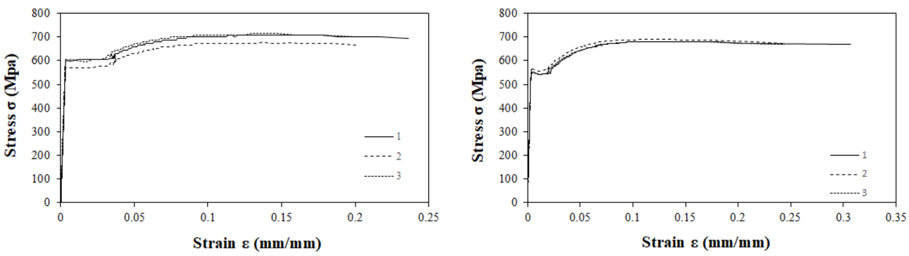

(a) D10 Rebar Stress – Strain Relationship

(b) D13 Rebar Stress – Strain Relationship

Figure 3-26 Stress- Strain Relationship of Reinforcement

3.4.2 Lateral Load-Drift Ratio (Displacement) Relationship

Figure 3-27 to Figure 3-30 show the lateral load-displacement (drift ratio) relationship of the specimen. The displacement was measured at the center of the upper slab, that is, at a height of 3500 mm. All of the specimens increased the load significantly compared to the results of the nonlinear finite element analysis (result is in Table 3-7). The tendency of the load -displacement graphs of all specimens is similar.

As can be seen from lateral load-drift ratio (displacement) Relationship, the ultimate shear strength of the specimen occurred in SWB1 and SWB2 during the positive force direction, while the maximum shear strength of the specimen occurred in SWB3 and SWB4 during the negative force direction.

In the case of SWB1, the ultimate strength of specimen in the positive force direction reached 333kN in step 8 (drift ratio 0.6%). The ultimate strength in the negative force direction reached -295kN in step 8 (drift ratio 0.6%). After step 10 (drift ratio 1.00%), concrete fauilure of the slab and wall was observed, and cyclic lateral loading step was performed only 2 cycles. In the first cycle of step 13 (drift ratio 2.0), 283kN occurred in the direction of positive force, which reached 86% of the ultimate strength. In addition, SWB1 shows ductile behavior as shown in Figure 3-27.

In the case of SWB2, the ultimate strength of specimen in the positive force direction reached 374kN in step 8 (drift ratio +0.6%). The maximum strength in the negative force direction reached -345kN in step 8 (drift ratio -0.6%). After step 10 (drift ratio 1.00%), concrete fauilure of the slab and wall was observed, and cyclic lateral loading step was performed only 2 cycles. In the first cycle of step 13 (drift ratio 2.0), 298kN occurred in the direction of positive force, which reached 80% of the maximum strength. In the second cycle of step 13 (drift ratio 2.0), 249kN occurred in the direction of positive force, which reached 67% of the ultimate strength. In addition, SWB2 shows ductile behavior as shown in Figure 3-28.

In the case of SWB3, the ultimate strength of specimen in the positive force direction reached 353kN in step 8 (drift ratio +0.6%). The maximum strength in the negative force direction reached -377kN in step 10 (drift ratio 1.00%). After step 10 (drift ratio 1.00%), concrete fauilure of the slab and wall was observed, and cyclic lateral loading step was performed only 2 cycles. In the first cycle of step 13 (drift ratio 2.0), 304kN occurred in the direction of negative force, which reached 81% of the ultimate strength. In addition, SWB3 shows ductile behavior as shown in Figure 3-29.

In the case of SWB4, the ultimate strength of specimen in the positive force direction reached 352kN in step 8 (drift ratio +0.6%). The maximum strength in the negative force direction reached -393kN in step 8 (drift ratio 0.6%). After step 10 (drift ratio 1.00%), concrete fauilure of the slab and wall was observed, and cyclic lateral loading step was performed only 2 cycles. In the first cycle of step 13 (drift ratio 2.0), 318kN occurred in the direction of negative force, which reached 81% of the ultimate strength. In addition, SWB4 shows ductile behavior as shown in Figure 3-30.

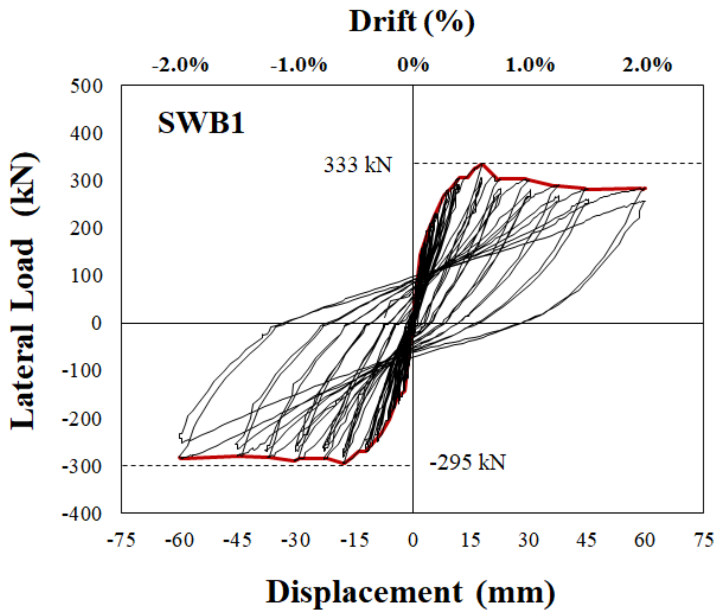

Figure 3-27 Lateral Load - Drift Ratio (Displacement) Relationship of SWB1

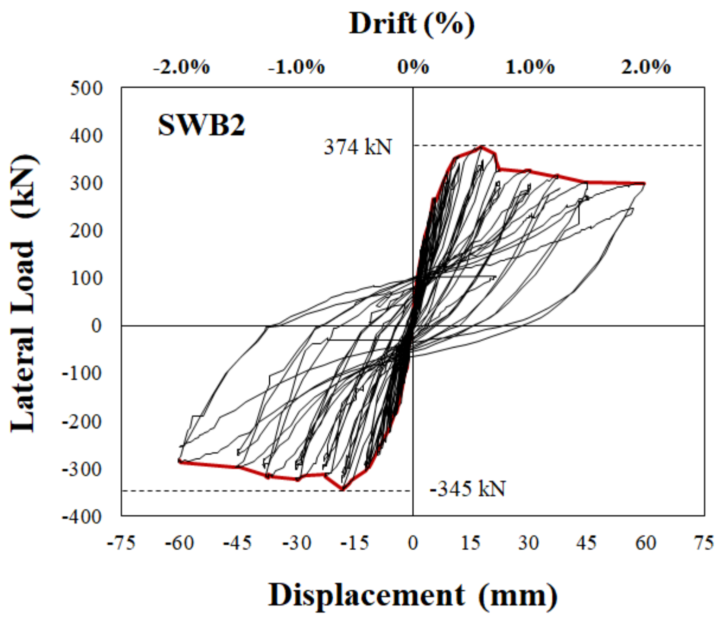

Figure 3-28 Lateral Load - Drift Ratio (Displacement) Relationship of SWB2

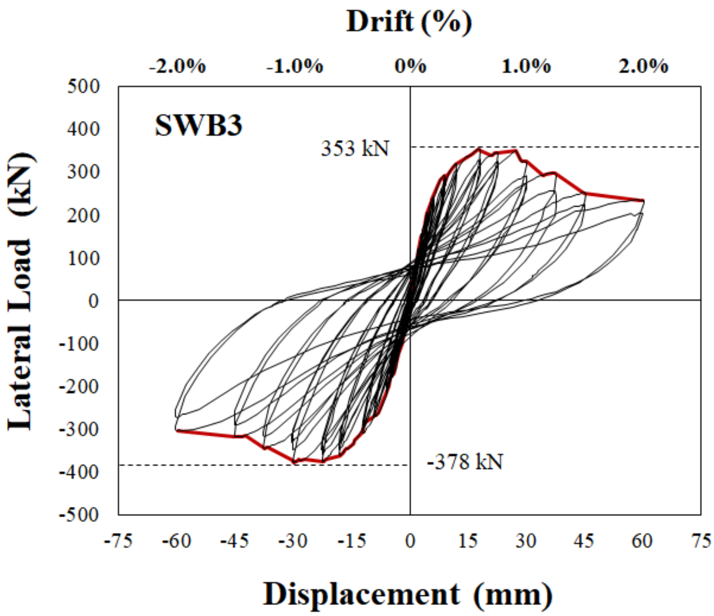

Figure 3-29 Lateral Load - Drift Ratio (Displacement) Relationship of SWB3

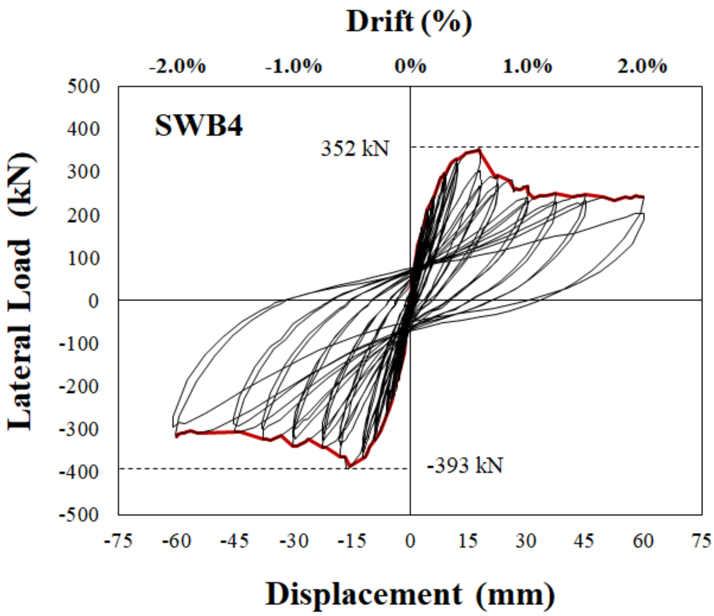

Figure 3-30 Lateral Load - Drift Ratio (Displacement) Relationship of SWB4

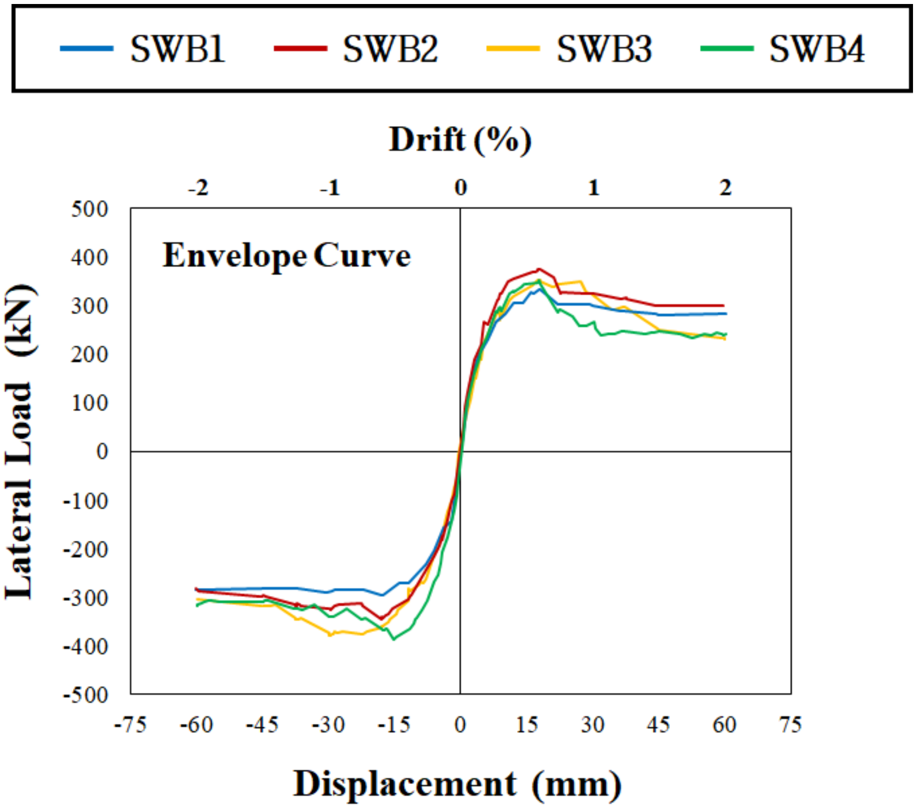

Figure 3-31 Envelope Curve of Specimens

The ultimate strength in the postive loading direction of the SWB2 with a slab thickness of 120mm is 120% compare to the SWB1 (374kN/334kN). The ultimate strength in the negative loading direction of the SWB2 specimen is 117% compare to the SWB1 (345kN/295kN). The thicker the slab, the greater the value of excess strength due to the slab-wall interaction.

The ultimate strength in the positive loading direction of the SWB3 specimen with an opening size of 600mm is 94% compare to the SWB2 specimen (353kN/374kN). The ultimate strength in the negative loading direction of the

SWB3 specimen is 109% compare to the SWB2 (377kN/345kN). The ultimate strength of the SWB3 specimen is 101% compare to the maximum strength of the SWB2. As the size of the opening increases, the ultimate strength does not increase (maximum strength increases by about 3 kN).

The ultimate strength in the positive loading direction of the SWB4 specimen, which is a lattice-shape of shear reinforcement arranged at the slab, is 94% compare to the the SWB2 (352kN/374kN). The ultimate strength in the negative loading direction of the SWB4 is 114% compare to the SWB2 (393kN/345kN). The ultimate strength of the SWB4 specimen is 105% compare to the ultimate strength of the SWB2 specimen (393kN/374kN). The ultimate strength was slightly increased due to the slab lattice-shaped of shear reinforcement, but there was no significant effect. (Maximum strength increased by about 19kN)

Figure 3-31 is the envelope curve of the specimen. As mentioned earlier, SWB1 and SWB2 had ultimate strength in the positive force direction, but SWB3 and SWB4 had ultimate strength in the negative force direction. Therefore, in order to accurately compare this, it is necessary to perform comparative analysis in the direction of the positive force of SWB1 and SWB2 and the negative force of SWB3 and SWB4. In chapter 3.5, by using following method, test will be analyzed.

3.4.3 Failure Mode

The specimen was fractured by the bending moment and shear acting on the slab as a load resistance mechanism. The specimen is dominated by shear force rather than by bending moment. Therefore, the failure mode occurred due to shear failure of the slab concrete, and the test was terminated (Refer to 3.5.2 Strain of Reinforcing Bar for details.). In all specimens, cracks such as punching shear occurred in the slab, and compression reinforcement buckling along with compression fracture of concrete at a drift ratio of 2.0% in the wall was fractured as shown in Figure 3-32 to Figure 3-39 in the last step which is step 13.

In the case of SWB1, the slab thickness is 80mm, compared to other specimens. As shown in Figure 3-36, a penetrating through the slab concrete failure mode occurred. In the case of SWB2, SWB3, and SWB4, fractures such as Figure 3-37, Figure 3-38, and Figure 3-39 occurred at the slab concrete.

In the case of walls, specimens show a similar tendency. In addition, the wall was integrally behaved by the slab, resulting in cracks as shown in Figures.

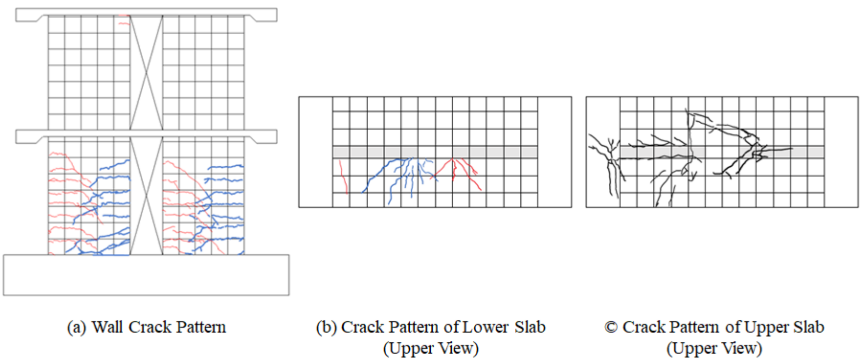

Figure 3-32 Wall and Slab Crack Pattern of SWB1

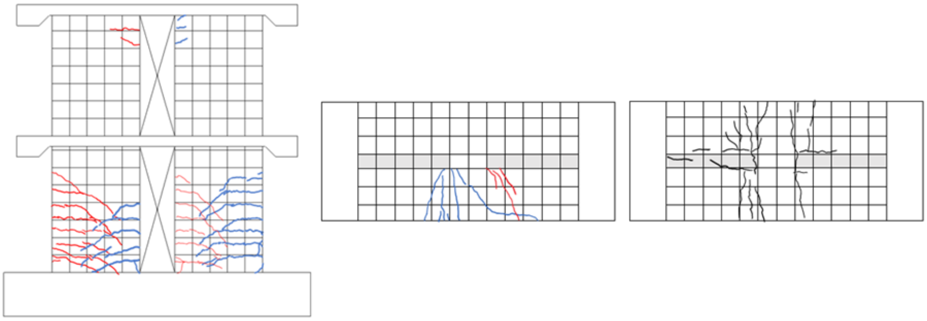

(a) Wall Crack Pattern

(b) Crack Pattern of Lower Slab (Upper View)

© Crack Pattern of Upper Slab (Upper View)

Figure 3-33 Wall and Slab Crack Pattern of SWB2

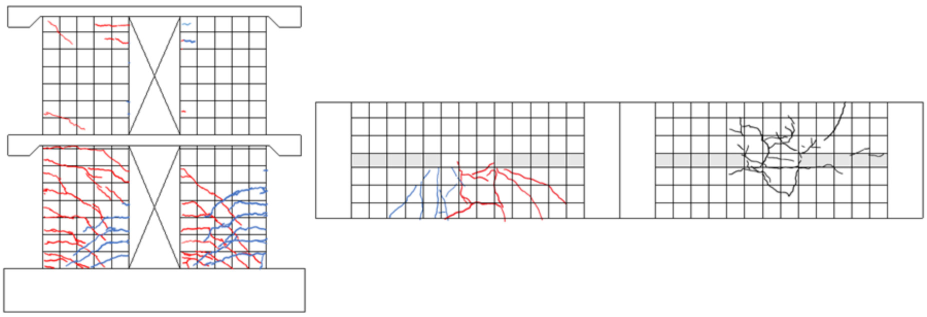

(a) Wall Crack Pattern

(b) Crack Pattern of Lower Slab (Upper View)

© Crack Pattern of Upper Slab (Upper View)

Figure 3-34 Wall and Slab Crack Pattern of SWB3

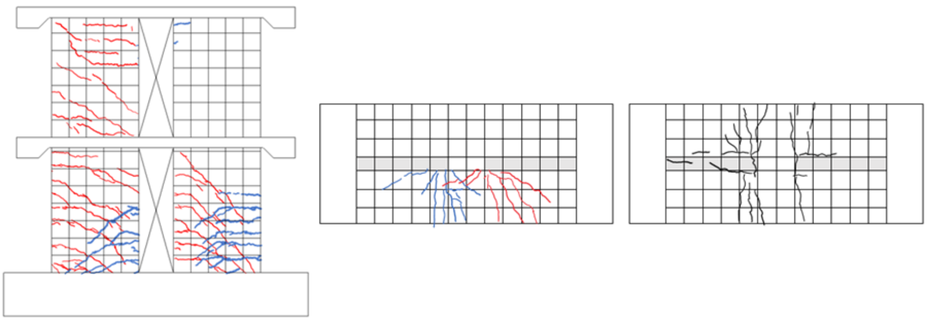

(a) Wall Crack Pattern

(b) Crack Pattern of Lower Slab (Upper View)

© Crack Pattern of Upper Slab (Upper View)

Figure 3-35 Wall and Slab Crack Pattern of SWB4

Figure 3-36 Failure Mode of SWB1

Figure 3-37 Failure Mode of SWB2

Figure 3-38 Failure Mode of SWB3

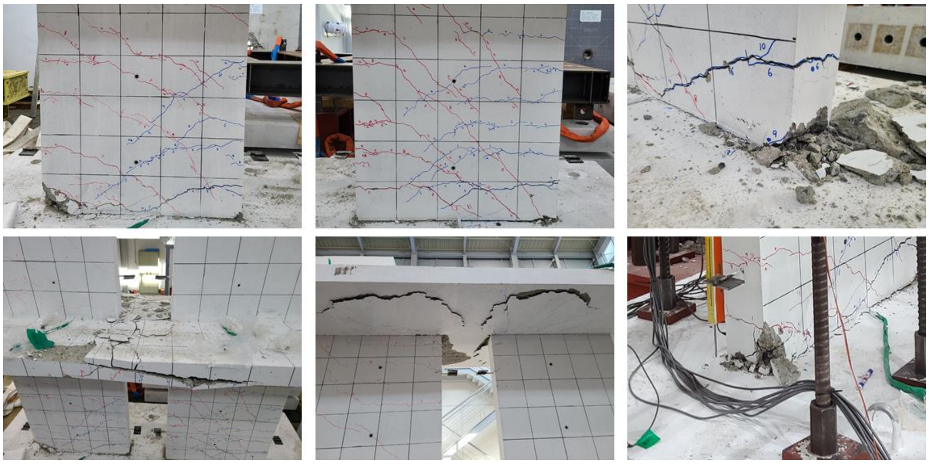

Figure 3-39 Failure Mode of SWB4

3.5 Test Analysis

3.5.1 Diaphragm Strength by Nonlinear Finite Element Analysis

By analyzing the Diaphragm model, which cannot be tested, the increase in the strength of the specimen due to the slab effect was verified. In the analysis using the diaphragm method, the slab is not used as a lateral load resistance system, and only the wall is used as a lateral load resistance system. Therefore, values less than the ultimate strength of the specimen with the slab will be analyzed. The larger the difference in strength between the diaphragm and the specimen, the more necessary a design method that considers the slab.

Analysis was performed by defining concrete and reinforced material models as shown in Figure 3-40 using the actual strength measured through the material test. ATENA is used as a nonlinear finite element analysis program, and the elements of each member are shown in Table 3-5.

Table 3-5 Element of Nonlinear Element Analysis member

Type of Member	Wall	Reinforcement	Loading Jig	Foundation	Diaphragm Slab
Element	Solid	1D Line Element	Elastic Solid	Elastic Solid	Elastic Solid

(a) Material Model

In order to simulate the two-story RC frame of slab-coupled wall specimens, an analysis model is modeled as the actual specimen. The analysis is performed using solid elements for concrete members and 1D line elements for reinforcing bars. In the case of analysis using the Diaphragm method in a nonlinear finite element analysis program, the slab is modeled as an elastic solid element having a thickness of 0.01m. Diaphragm slab uses an elastic solid material with a low modulus of elasticity.

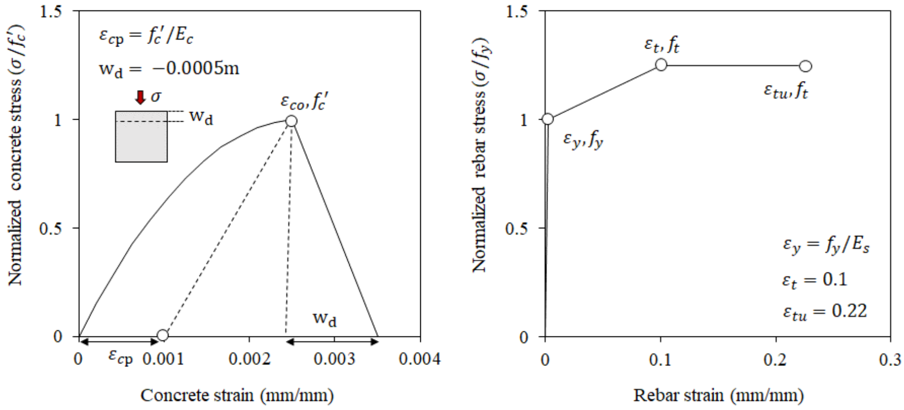

(a) Concrete stress-strain model (b) Rebar stress-strain model

Figure 3-40 Concrete and Rebar Stress-Strain Relationship in FEA

Table 3-6 Parameters of Constitutive Model

Parameter	Formula
Concrete Compression Strength [Mpa]	Depends on measured
Concrete Tensile Strength [Mpa]	$f_t = 1.40(\frac{f_{cl}}{f_{cko}})^{2/3}$
Poisson's Ratio	$\lambda = 0.2$
Elastic Modulus [Mpa]	$E = 4700\sqrt{f_{ck}}$
Fracture Energy [MN/m]	$G_F = 0.000025f_t$
Plastic Strain	$EPS_{CP} = F_{ck}/E$
Onset of Crushing [Mpa]	$F_{c0} = -2.1F_t$

(b) FEA Model of Diaphragm

The nonlinear finite element analysis model is shown in Figure 3-41. The size of the mesh does not exceed 0.2m, and in the case of the wall, which are thin members, the analysis is performed so that the out-of-plane load can be considered by dividing it into 4 equal parts in the thickness direction.

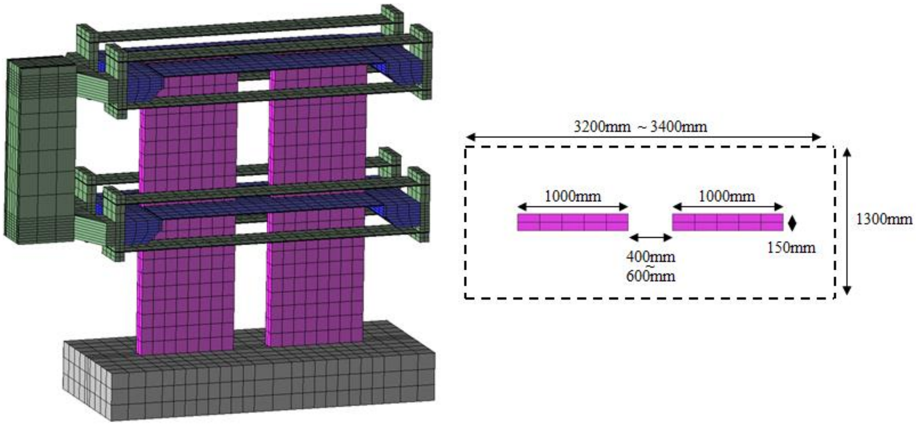

Figure 3-41 Diaphragm Model of Specimens in FEA

(c) Analysis of Diaphragm Model of Specimen

V_{test} is the test strength of the specimen and $V_{Diaphragm}$ is the diaphragm strength of the nonlinear finite element analysis.

Table 3-7 Comparison of Test and FEA Diaphragm Results

Specimen	V_{test}		$V_{Diaphragm}$		$V_{test}/V_{Diaphragm}$	
	Postive	Negative	Postive	Negative	Postive	Negative
SWB1	333	-295	244	-244	**1.36**	1.21
SWB2	374	-345	244	-244	**1.53**	1.41
SWB3	353	-378	244	-244	1.45	**1.55**
SWB4	352	-393	244	-244	1.44	**1.61**

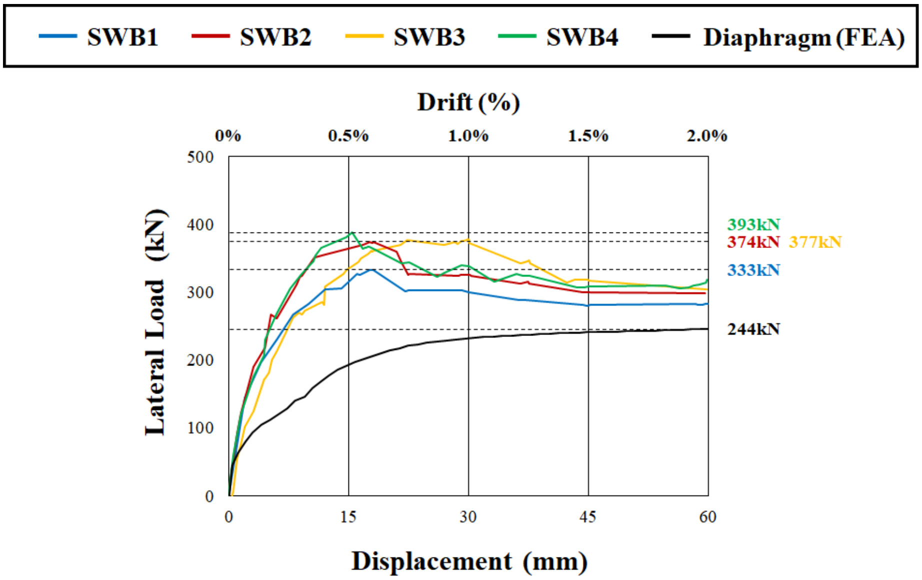

Figure 3-42 Envelope Curve of Specimens with Diaphragm

In the case of SWB3 and SWB4, the ultimate strength of the specimen occurred in the direction of the negative loading, so the graph was flipped up and down twist and turn left and right for an exact comparison.

The test strength of the specimen compared to the analysis strength is 136% for SWB1 (333kN/244kN), 153% for SWB2 (374kN/244kN), 155% for SWB3 (353kN/244kN), and 161% for SWB4 (352kN/244kN). The strength of specimens is greater than the result of the nonlinear analysis of Atena Diaphragm (black). In addition, the ultimate strength in the both loading direction of the test specimen showed greater results than the analysis result of diaphragm as shown in Table 3-7.

3.5.2 Strain of Reinforcing Bar

Figure 3-43 to Figure 3-66 show the strain distribution of the reinforcing bar of the specimens. The location of the strain measurement is located in the figure. The strain distribution was expressed as the lateral drift ratio of 0.3% (○ mark), 0.6% (□ mark), 1.0% (△ mark), 1.5% (◇ mark), and 2.0% (X mark). Also, permanent deformation after the yield strain of rebar distorts the strain shape, so it is excluded from the graph.

(a) Vertical Reinforcement of Lower Story Wall

Figure 3-43 to Figure 3-44 show the strain distribution of the reinforcing bar of lower story wall of the specimens. Because the wall is dominated by the bending behavior, the strain distribution of the wall before yielding shows an approximate linear distribution at a low lateral drift ratio. In structural analysis with the diaphragm method, the wall acts as an individual wall. Therefore, the strain of vertical reinforcement of the wall with the same stiffness should appear the same. However, it was confirmed that the strain of the compression reinforcing bar in the location of the loading part was smaller than that of the compression reinforcing bar in the opposite of the loading part that the coupling effect was generated between the walls by the slab. This is because, as mentioned earlier, when the slab acts as a lateral resistance system, the lateral load resistance mechanism generates the moment resistence frame effect of the slab. Due to the moment-resistance framing effect of the slab, axial force is generated on the wall, which causes tension on the wall in the direction of the loading part and compressive force on the wall in the opposite location of the loading part. Thereby, a coupling effect occurs and the wall is partially coupled.

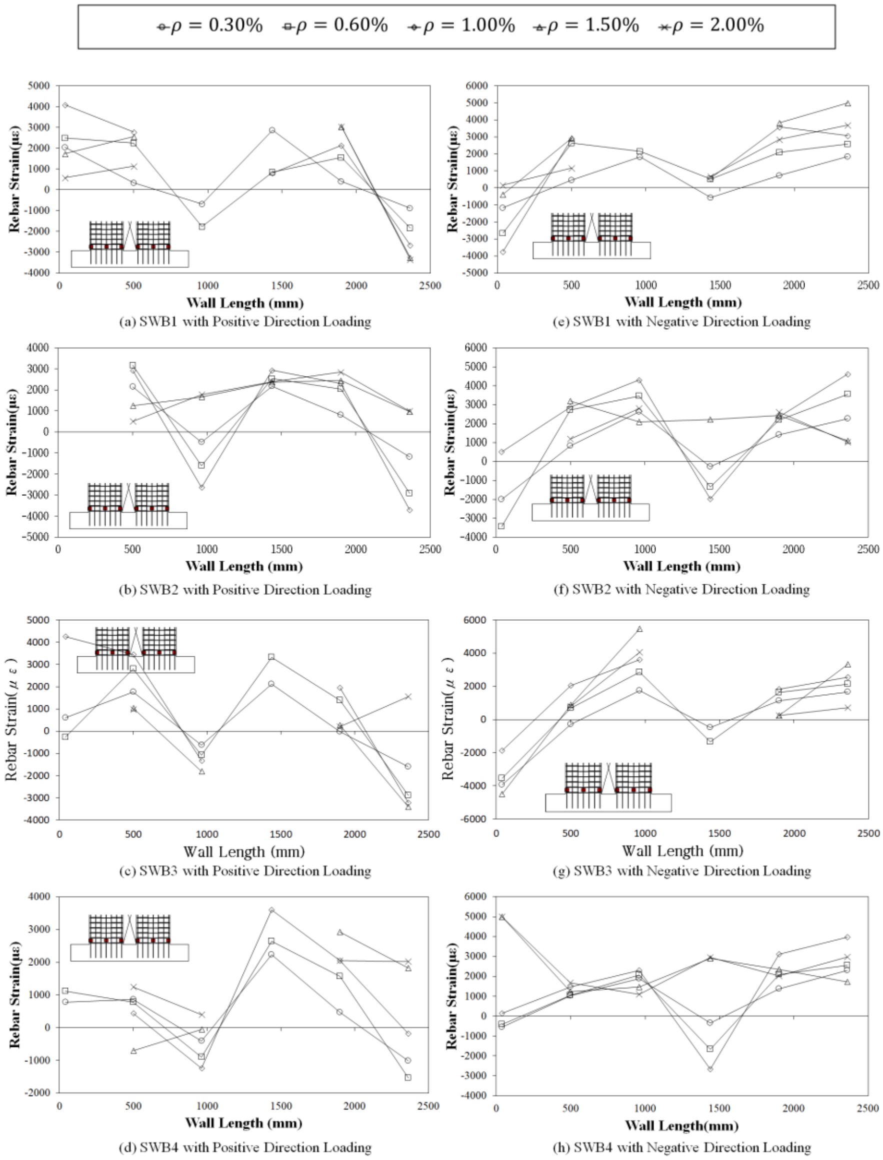

Figure 3-43 Strain Distribution of Vertical Bars of Lower Story Wall (Bottom)

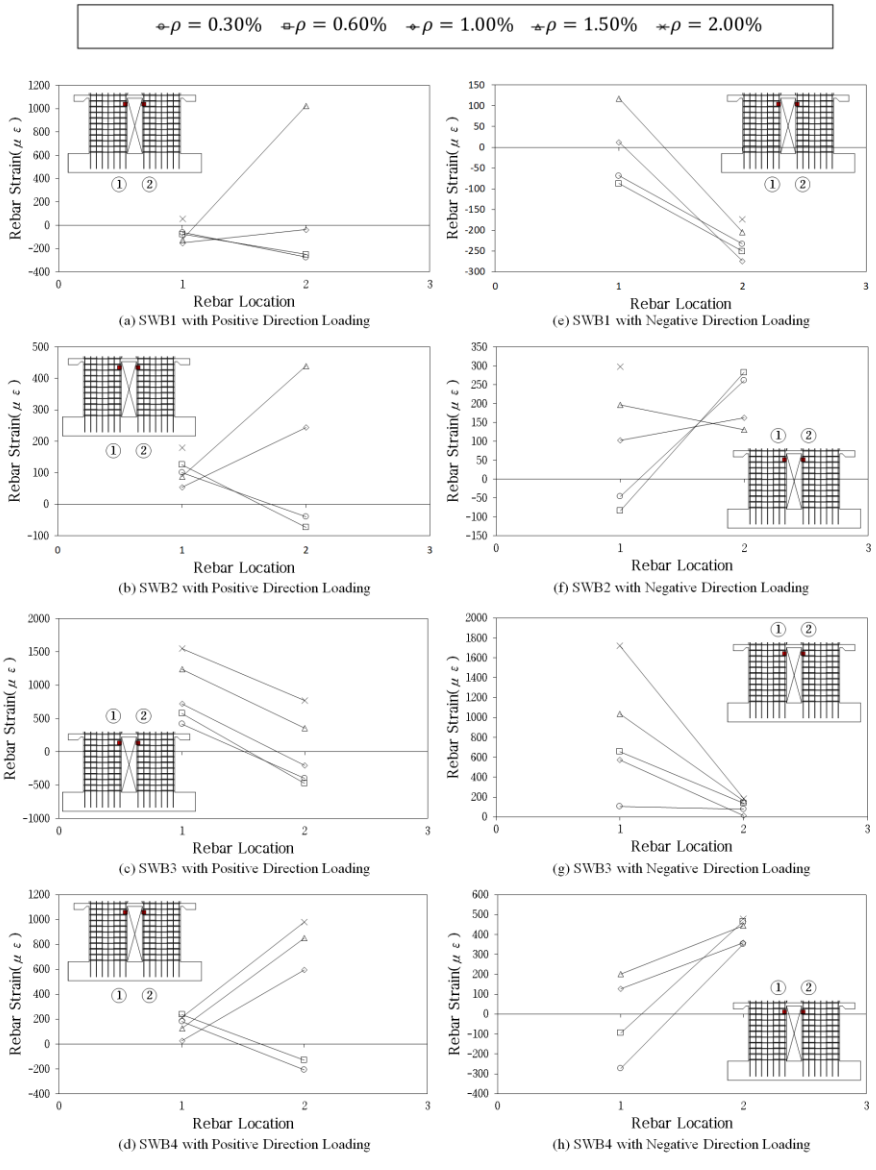

Figure 3-44 Strain Distribution of Vertical Bars of Lower Story Wall (Top)

(b) Vertical Reinforcement of Upper Story Wall

Figure 3-45 to Figure 3-46 show the strain distribution of the reinforcing bar of upper story wall of the specimens. The vertical reinforcement of the upper story wall did not reach the yield strength until the lateral drift ratio of 2.00% (step 13), and showed a linear distribution until the strain at the end of the test. The lateral drift ratio at which the outermost vertical reinforcement of the lower story wall reaches the yield strain is 0.05% to 0.20%. However, the upper story walls show less than 50% to yield strain at the same lateral drift ratio. In addition, it can be confirmed that the slab-wall interaction acts normally through the large strain occurring in the top of vertical reinforcing bar, and it shows the same tendency as the lower story wall.

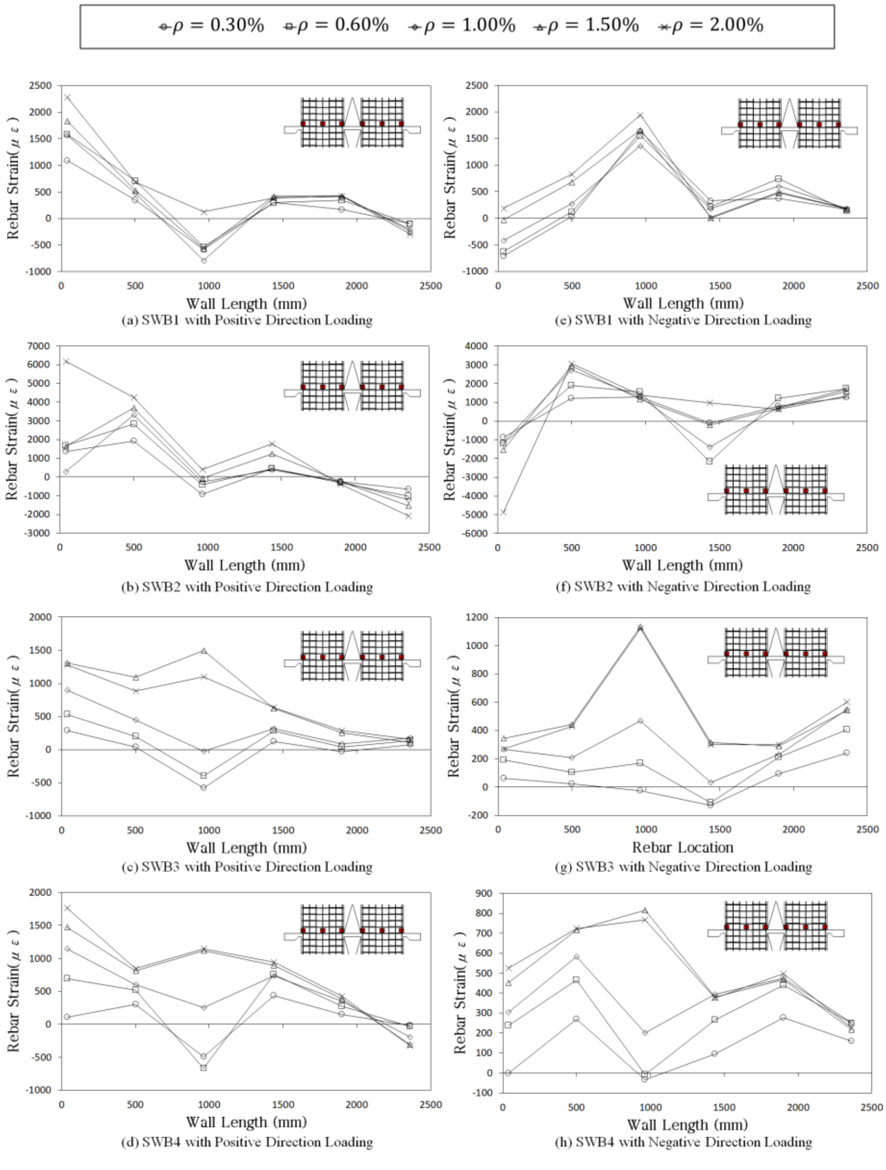

Figure 3-45 Strain Distribution of Vertical Bars of Upper Story Wall (Bottom)

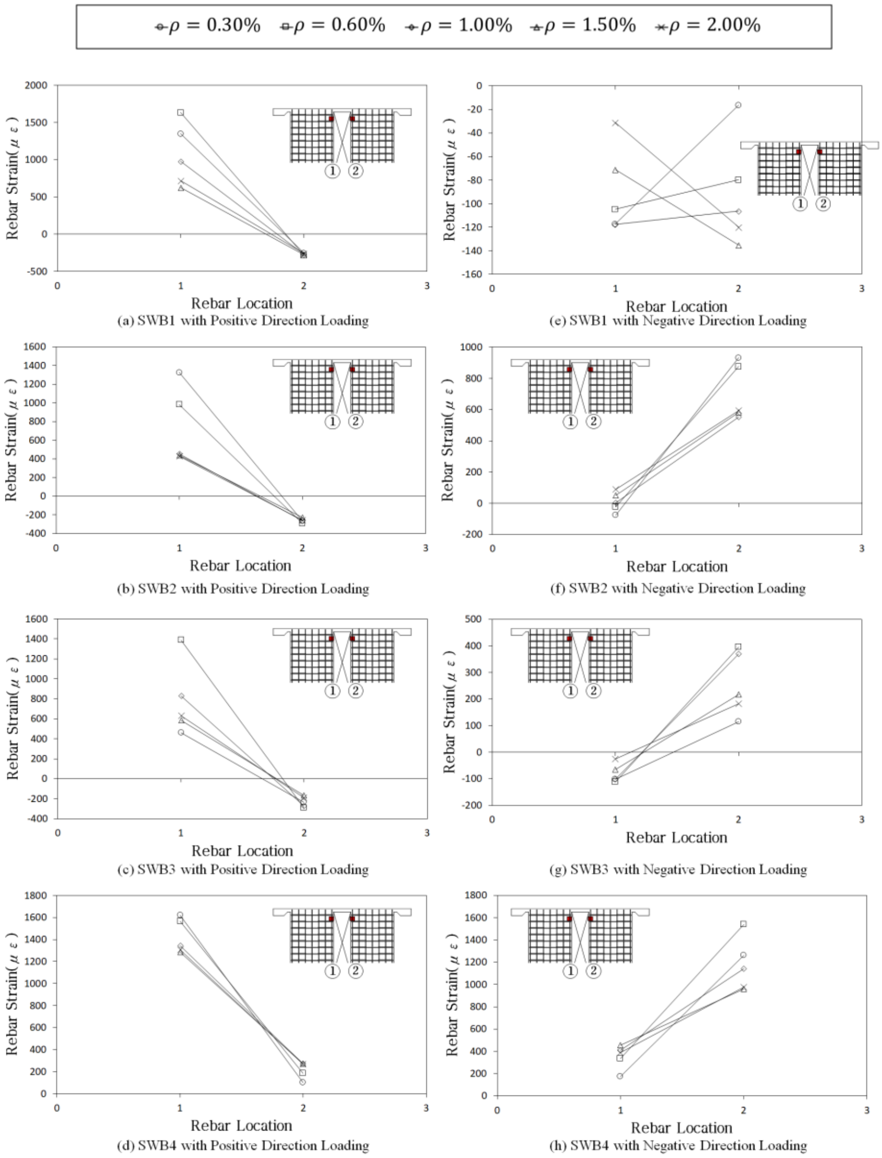

Figure 3-46 Strain Distribution of Vertical Bars of Upper Story Wall (Top)

(c) Horizontal Reinforcement of Wall

Figure 3-47 to Figure 3-48 show the strain distribution of the horizontal reinforcing bar of wall of the specimens. The strain of the horizontal reinforcing bars hardly occurred in the upper story wall of the specimen. However, the strain of the horizontal reinforcing bars was concentrated in the bottom of the lower story wall. If excessive strain is measured on the gauge of the upper story wall, it is judged as a measurement problem because the strain in the direction of positive loading and negative loading are the same. Therefore, the yield strain was not reached except for the bottom part of horizontal reinforcement of the SWB4 specimen.

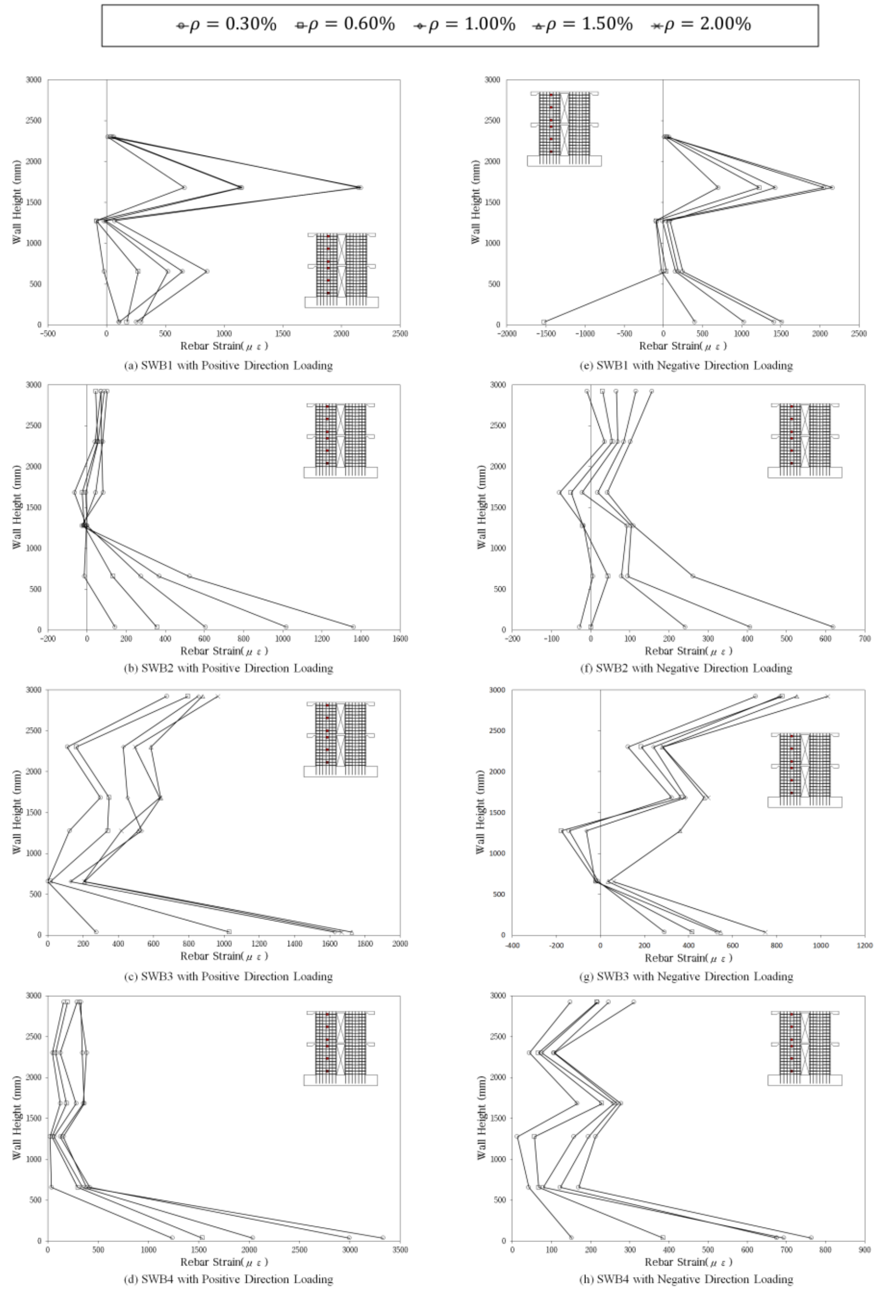

Figure 3-47 Strain Distribution of Horizontal Bars of Left Wall (Actuator Dir.)

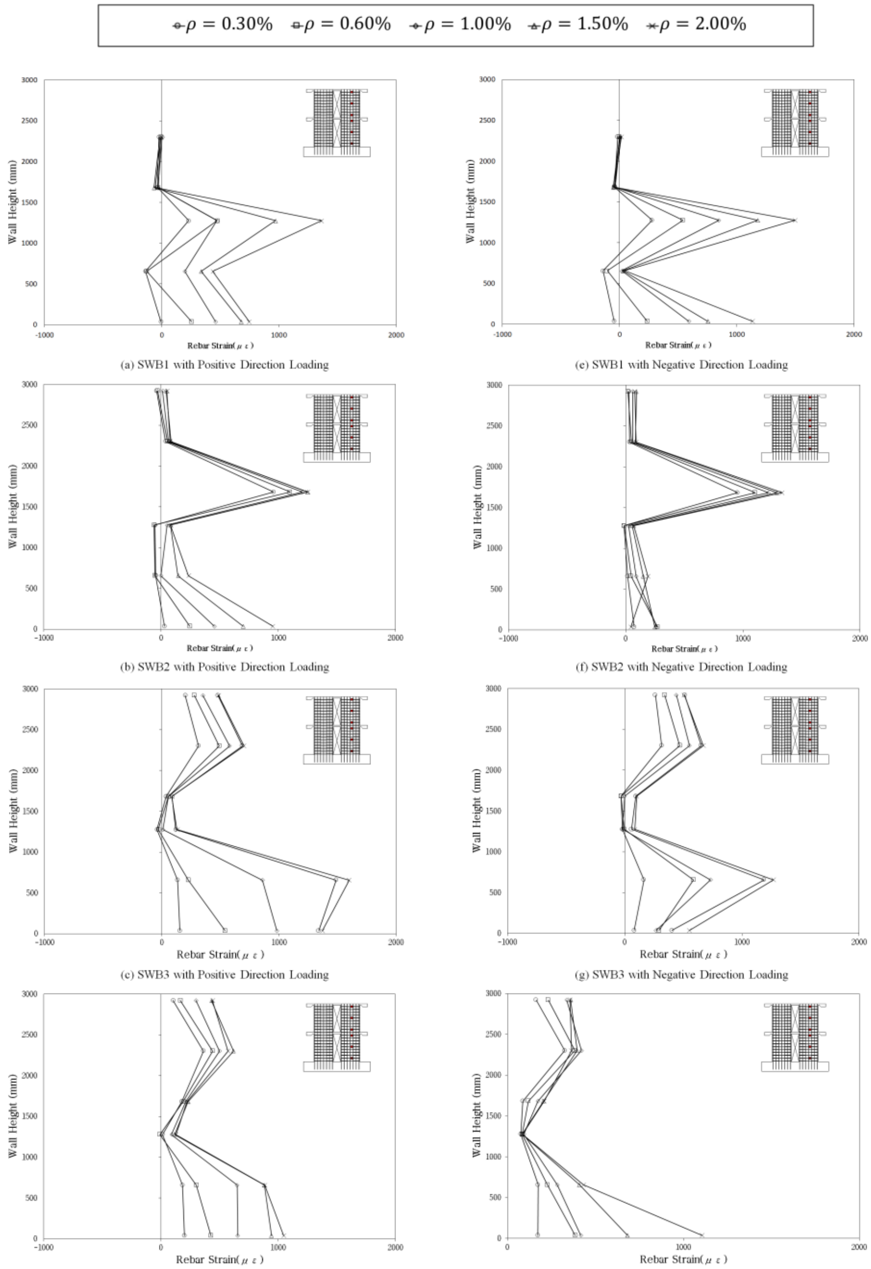

(a) SWB1 with Positive Direction Loading

(e) SWB1 with Negative Direction Loading

(b) SWB2 with Positive Direction Loading

(f) SWB2 with Negative Direction Loading

(c) SWB3 with Positive Direction Loading

(g) SWB3 with Negative Direction Loading

(d) SWB4 with Positive Direction Loading

(h) SWB4 with Negative Direction Loading

Figure 3-48 Strain Distribution of Horizontal Bars of Right Wall

(d) Reinforcement of Lower Story Slab of the Specimens

Among the reinforcing bars in the lower layer of the slab of the specimen, the strain of the rebar close to the wall did not yield or partially yielded at the lateral drift ratio of 2.0%. Among the reinforcing bars in the upper layer of the slab of the specimen, the strain of the rebar close to the wall did not yield or partially yielded at the lateral drift ratio of 1.0% to 1.5%.

As the reinforcing bar far from the center of slab-wall joint almost did not yield, it was confirmed that as the distance between the wall and the reinforcing bar increased, the effect of the slab flexural reinforcement decreased. Through this, it was confirmed that as the distance between the wall and the slab reinforcement increases, the effect of the flexural reinforcement on the slab-wall interaction decreases. This can be confirmed even in the failure mode of specimens, and cracks such as punching shear occurred.

The reason that the effect on the slab effect decreases as the distance from the wall increases is that cracks as punching shear and deformations are concentrated at the slab-wall joint. As the slab shear failure occurs locally, there is no significant effect on the flexural reinforcing bars. In addition, since the destruction occurs locally, the effect decreases as it is further away from the wall. Therefore, it is expected that the shear capacity of the slab is required rather than the bending moment capacity of the slab-wall structure. For a clear comparison, if the strain of SWB4, which reinforced the shear performance with rebars in the slab, is compared with SWB2, the results are not different. Through this, it can be seen that in slab-wall structures, the shear capacity of slab concrete has a dominant influence rather than arranging the shear reinforcing bars in slab. Even if the shear reinforcement yields, it is expected that the shear capacity of the slab is greatly reduced due to local damage to the slab concrete at the joint of wall. Thus, the effect is not greatly affected.

Compared to the other specimens of opening distance is 400mm, relatively more flexural reinforcing bars yielded at the position close to the slab-wall joint both the upper and lower story of the SWB3 specimen with a wide opening. This is because the shear force/bending moment ratio (V/M) applied to the slab decreases due to the increase in the arm length. Therefore, it is expected to have yielded relatively more than other specimens. However, because the shear force is also dominant, it seems that the concrete shear failure occurred at the slab-wall joint. Therefore, it is expected to have yielded relatively more than other specimens.

Through the following test analysis, it is expected indirectly that even if the flexural rebar ratio in the slab increases, it will be insignificant in the slab-wall structure. This is very consistent with the test results, and it can be seen that the influence of the slab thickness is the largest variable compared to others.

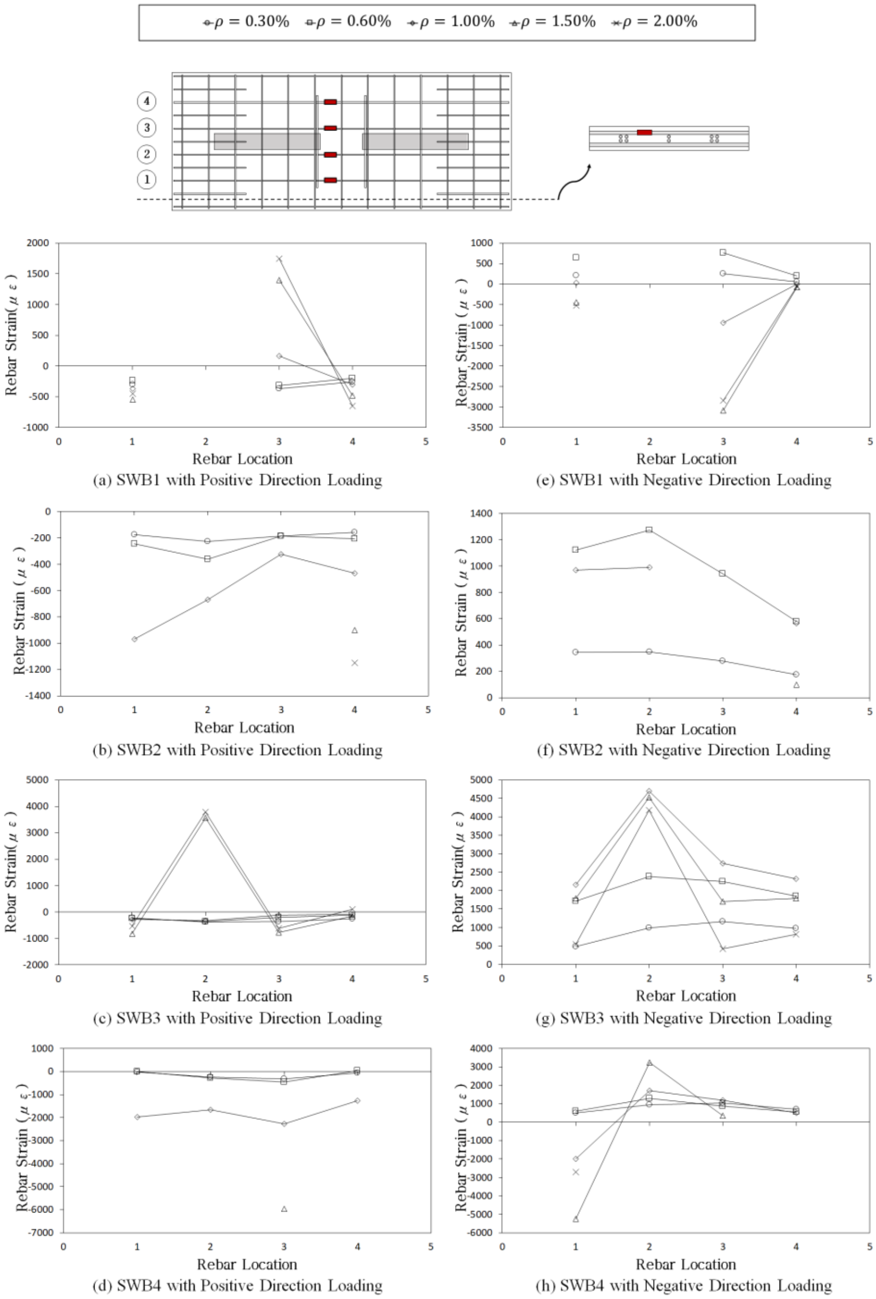

Figure 3-49 Reinforcement of Lower Story Slab

(Top Layer - In-Plane of Wall Direction Reinforcing Bars – Left)

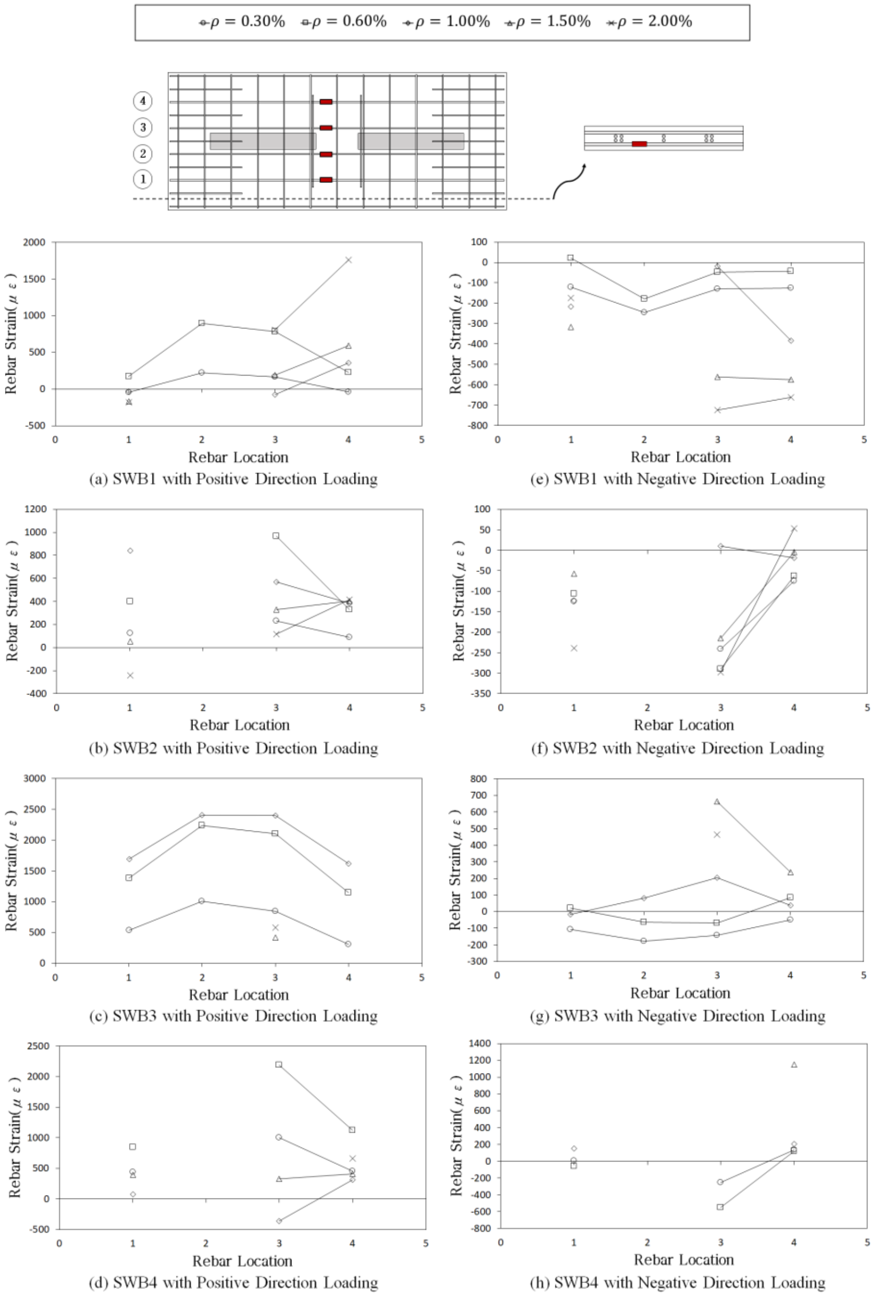

Figure 3-50 Reinforcement of Lower Story Slab

(Bottom Layer - In-Plane of Wall Direction Reinforcing Bars – Left)

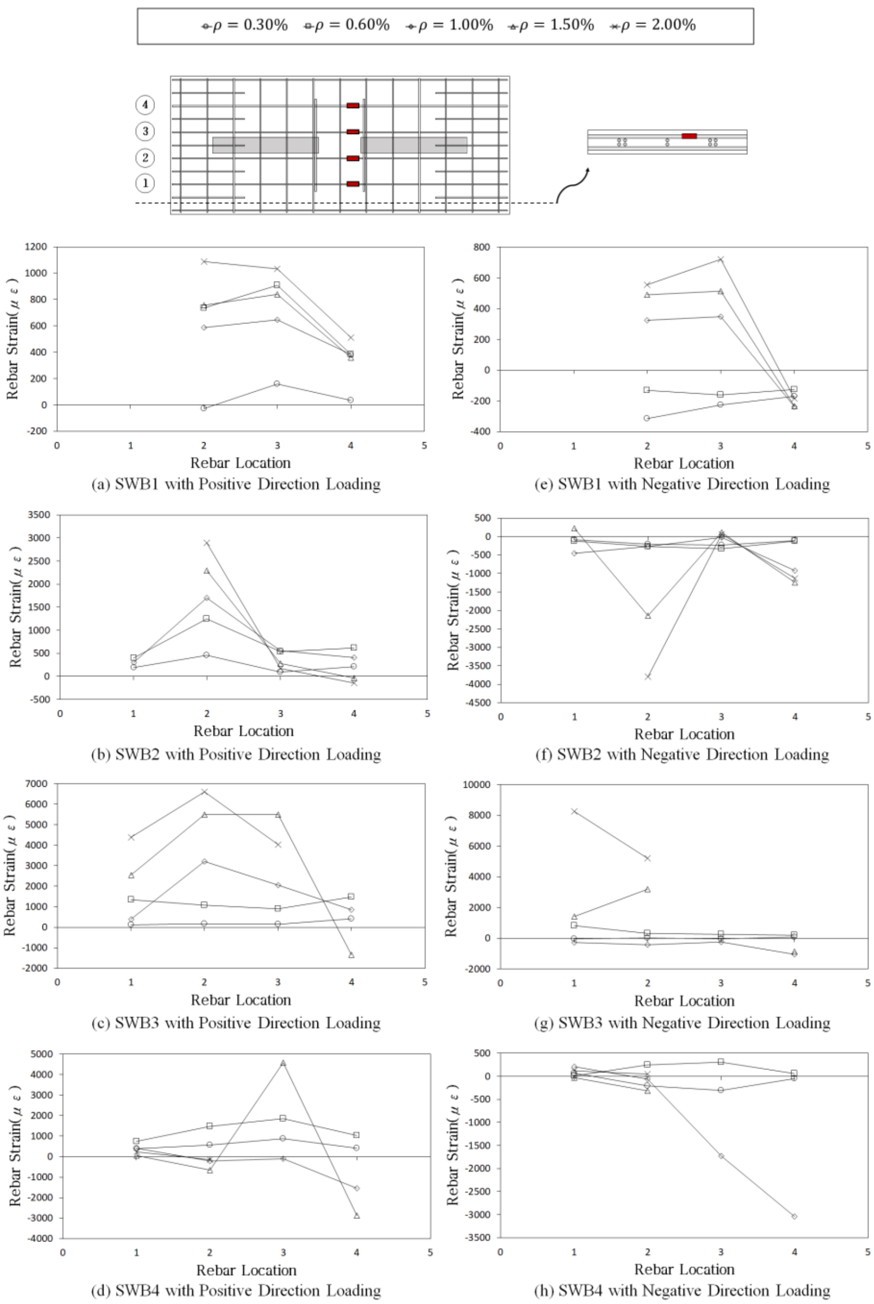

(a) SWB1 with Positive Direction Loading

(e) SWB1 with Negative Direction Loading

(b) SWB2 with Positive Direction Loading

(f) SWB2 with Negative Direction Loading

(c) SWB3 with Positive Direction Loading

(g) SWB3 with Negative Direction Loading

(d) SWB4 with Positive Direction Loading

(h) SWB4 with Negative Direction Loading

Figure 3-51 Reinforcement of Lower Story Slab

(Top Layer - In-Plane of Wall Direction Reinforcing Bars – Right)

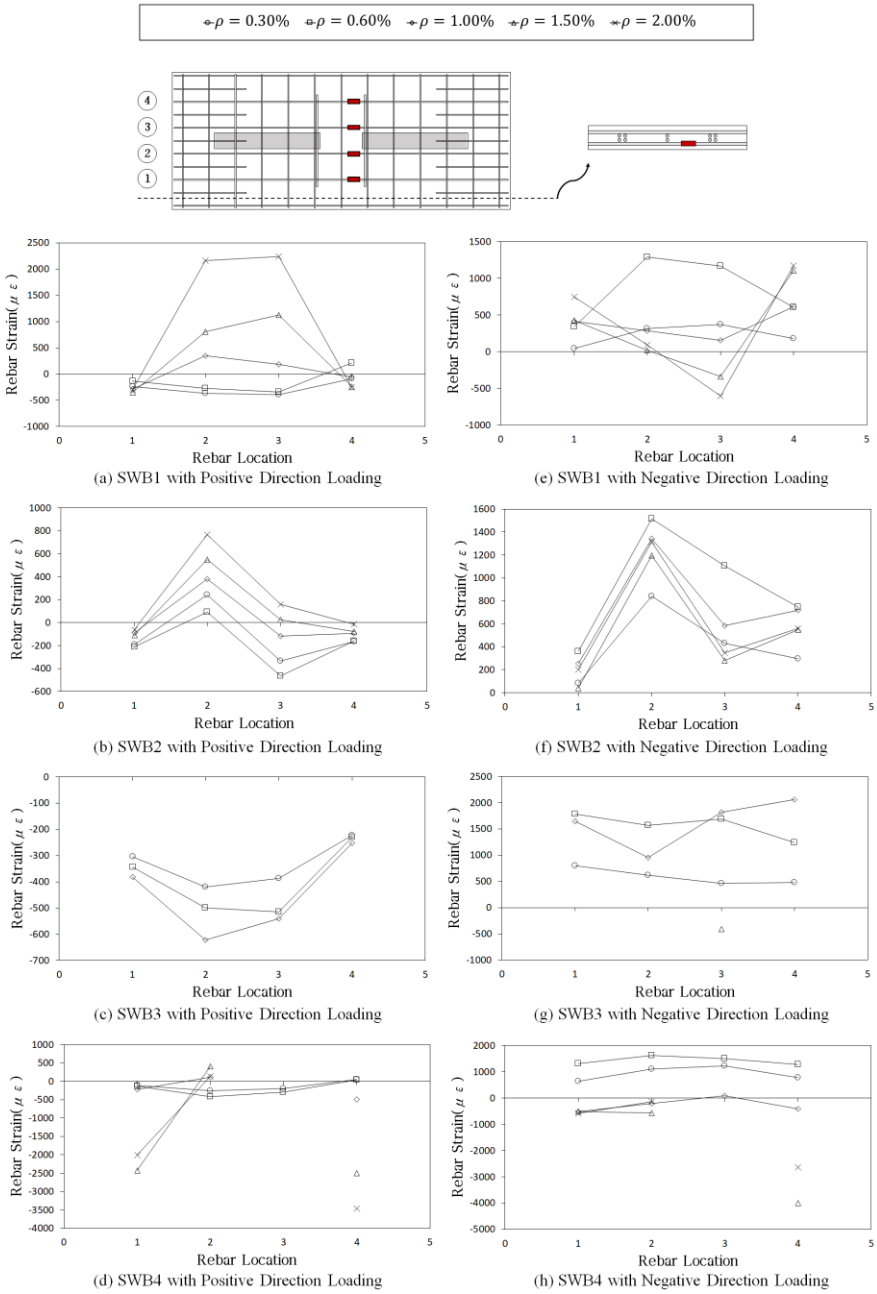

Figure 3-52 Reinforcement of Lower Story Slab

(Bottom Layer - In-Plane of Wall Direction Reinforcing Bars – Right)

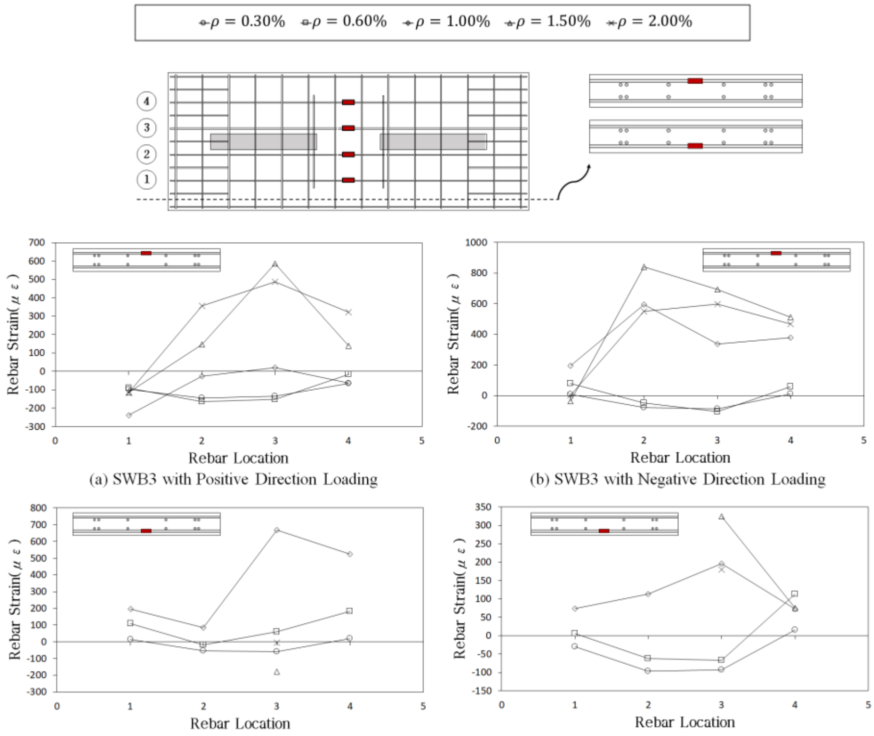

(a) SWB3 with Positive Direction Loading

(b) SWB3 with Negative Direction Loading

(c) SWB3 with Positive Direction Loading

(d) SWB3 with Negative Direction Loading

Figure 3-53 Reinforcement of Lower Story Slab (for SWB3 - Center)

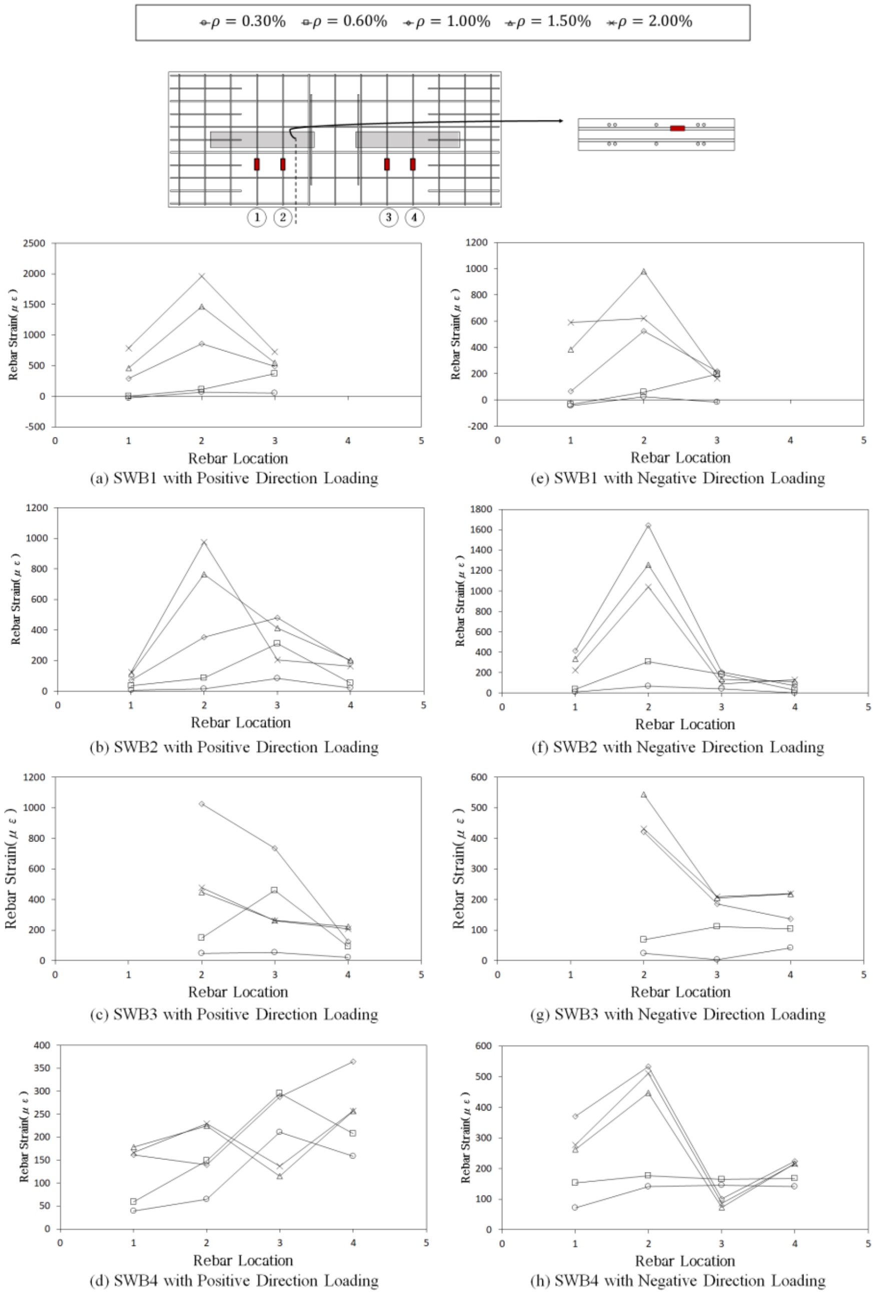

Figure 3-54 Reinforcement of Lower Story Slab

(Top Layer – Out-of-Plane of Wall Direction Reinforcing Bars - Side)

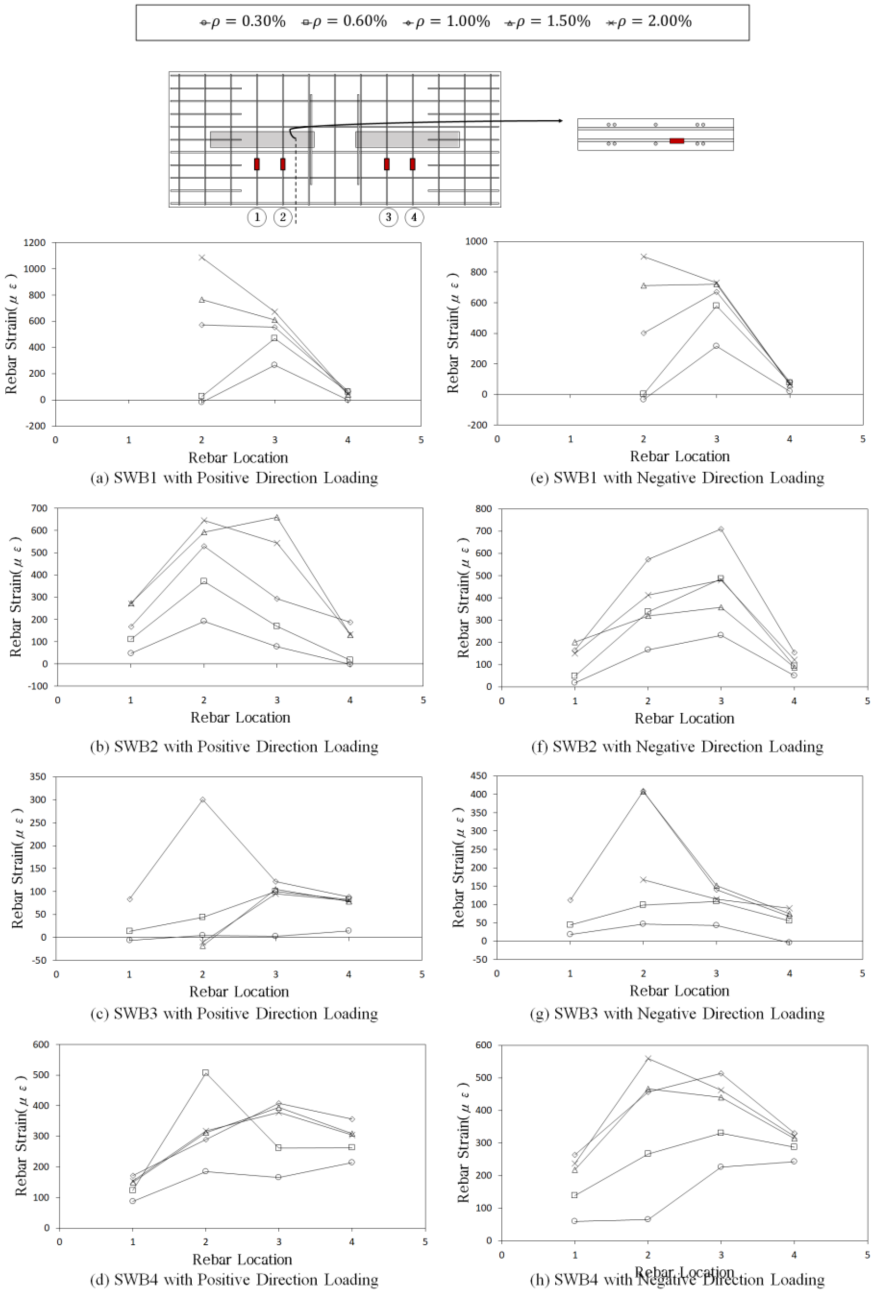

Figure 3-55 Reinforcement of Lower Story Slab

(Bottom Layer – Out-of-Plane of Wall Direction Reinforcing Bars - Side)

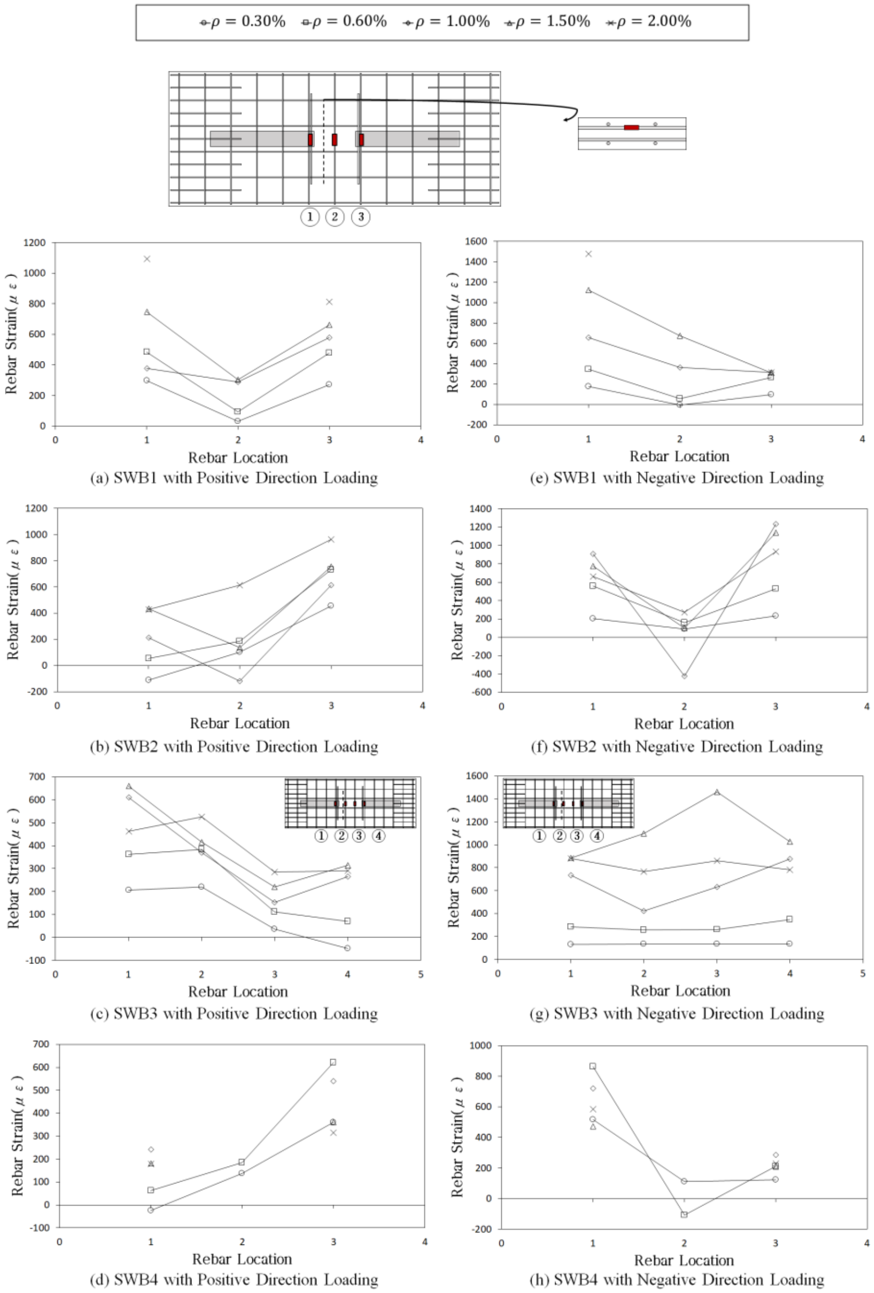

Figure 3-56 Reinforcement of Lower Story Slab

(Top Layer – Out-of-Plane of Wall Direction Reinforcing Bars - Center)

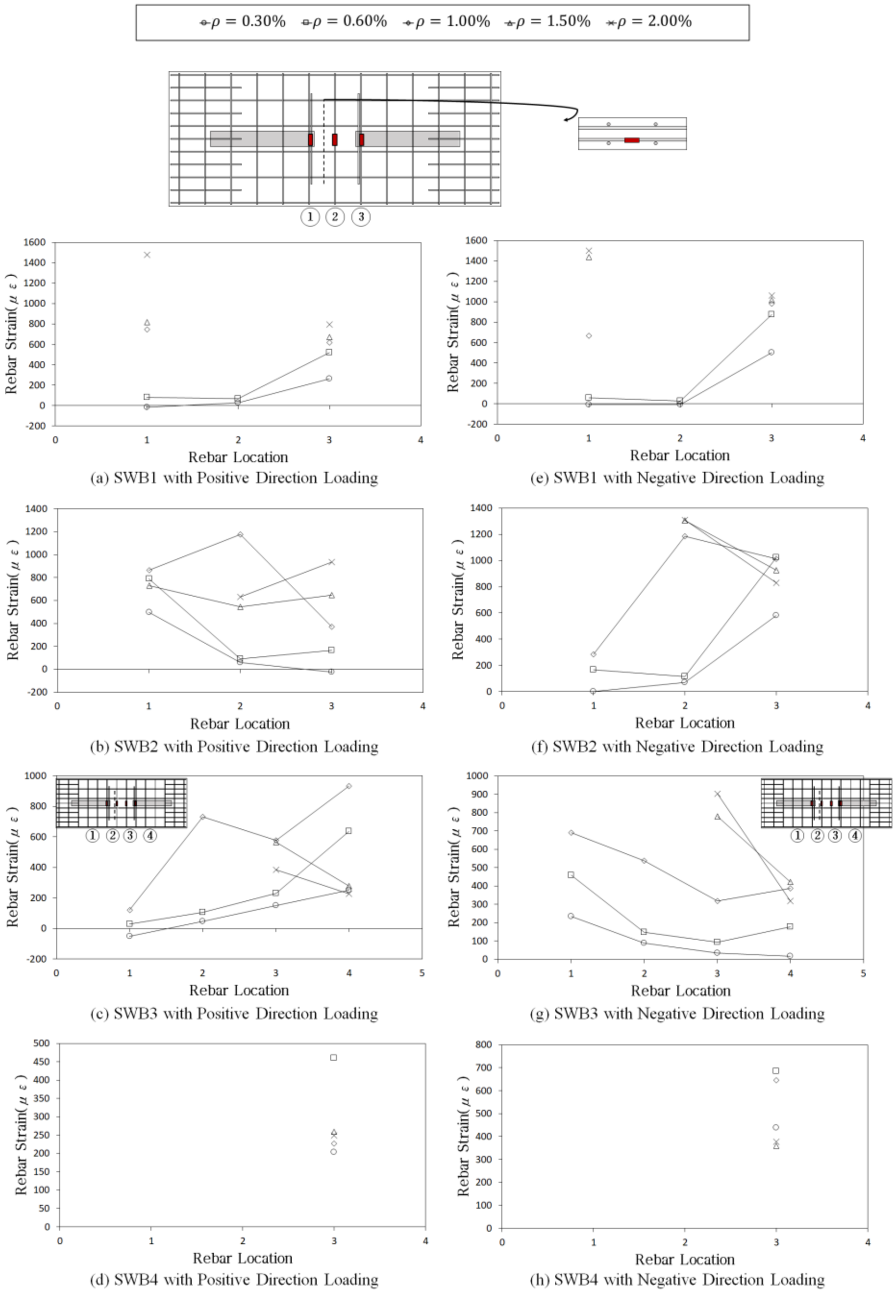

Figure 3-57 Reinforcement of Lower Story Slab

(Bottom Layer – Out-of-Plane of Wall Direction Reinforcing Bars - Center)

(e) Reinforcement of Upper Story Slab of the Specimens

Among the reinforcing bars in the lower and upper layer of the slab of the specimen, the yield of the rebar close to the wall did not occur or partially occurred at the lateral drift ratio of 1.0% ~ 1.5%. Among the reinforcing bars in the lower layer of the slab of the specimen, the yield of the rebar far from the wall did not occur until the lateral drift ratio of 2.0%. As the reinforcing bar far from the wall in the lower and upper layer of slab except SWB3 did not yield, it was confirmed that as the distance between the wall and the reinforcing bar increased, the effect of the slab flexural reinforcement decreased.

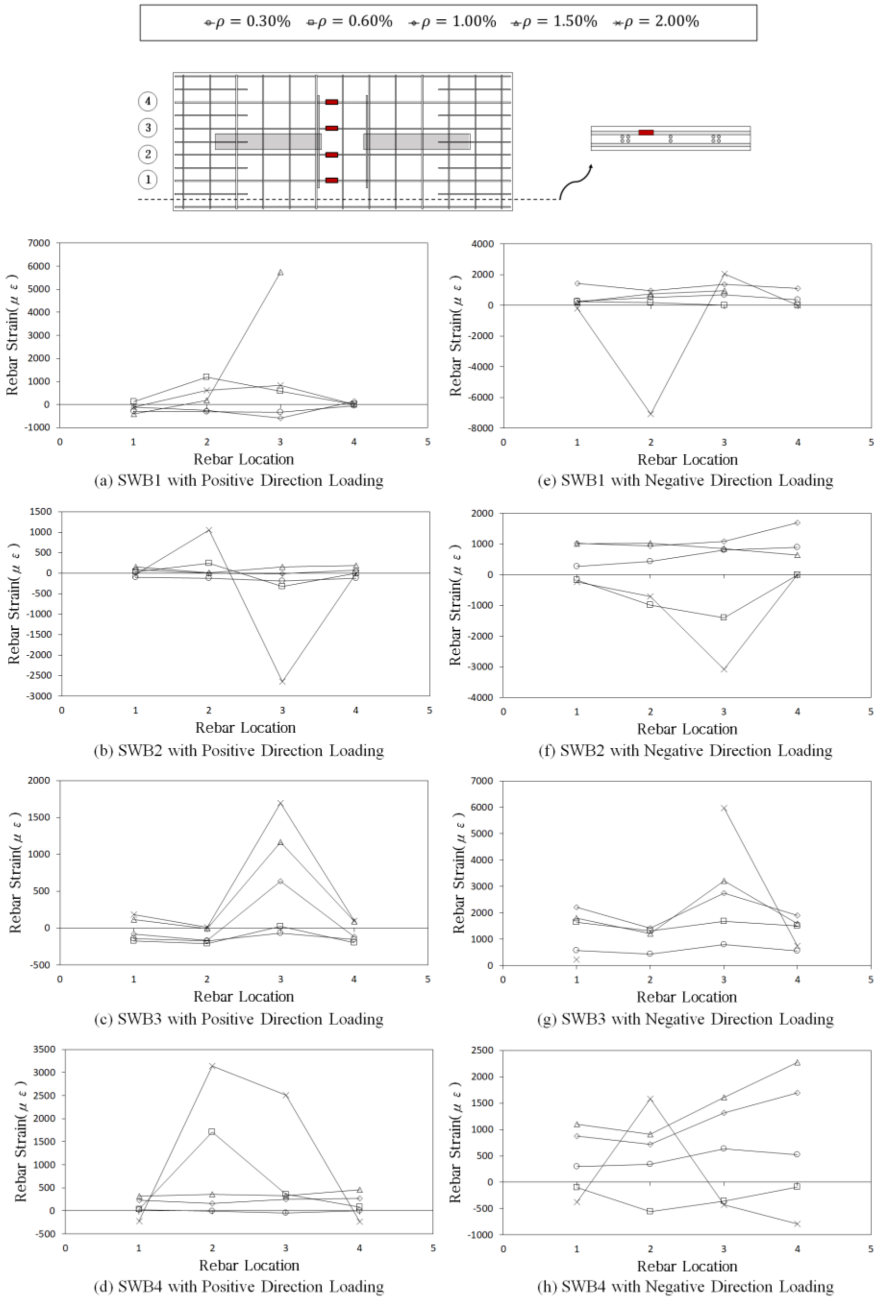

Figure 3-58 Reinforcement of Upper Story Slab

(Top Layer - In-Plane of Wall Direction Reinforcing Bars – Left)

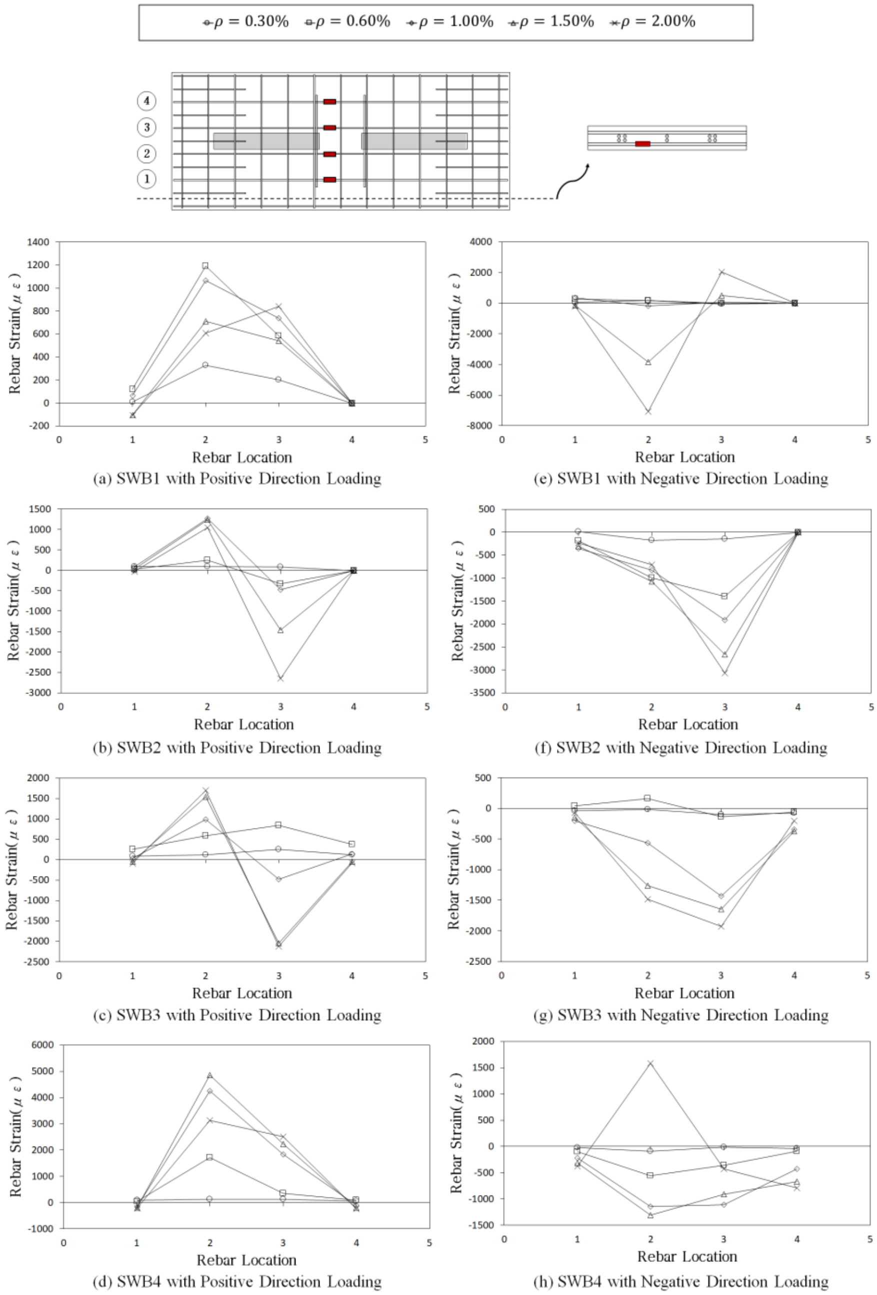

Figure 3-59 Reinforcement of Upper Story Slab

(Bottom Layer - In-Plane of Wall Direction Reinforcing Bars – Left)

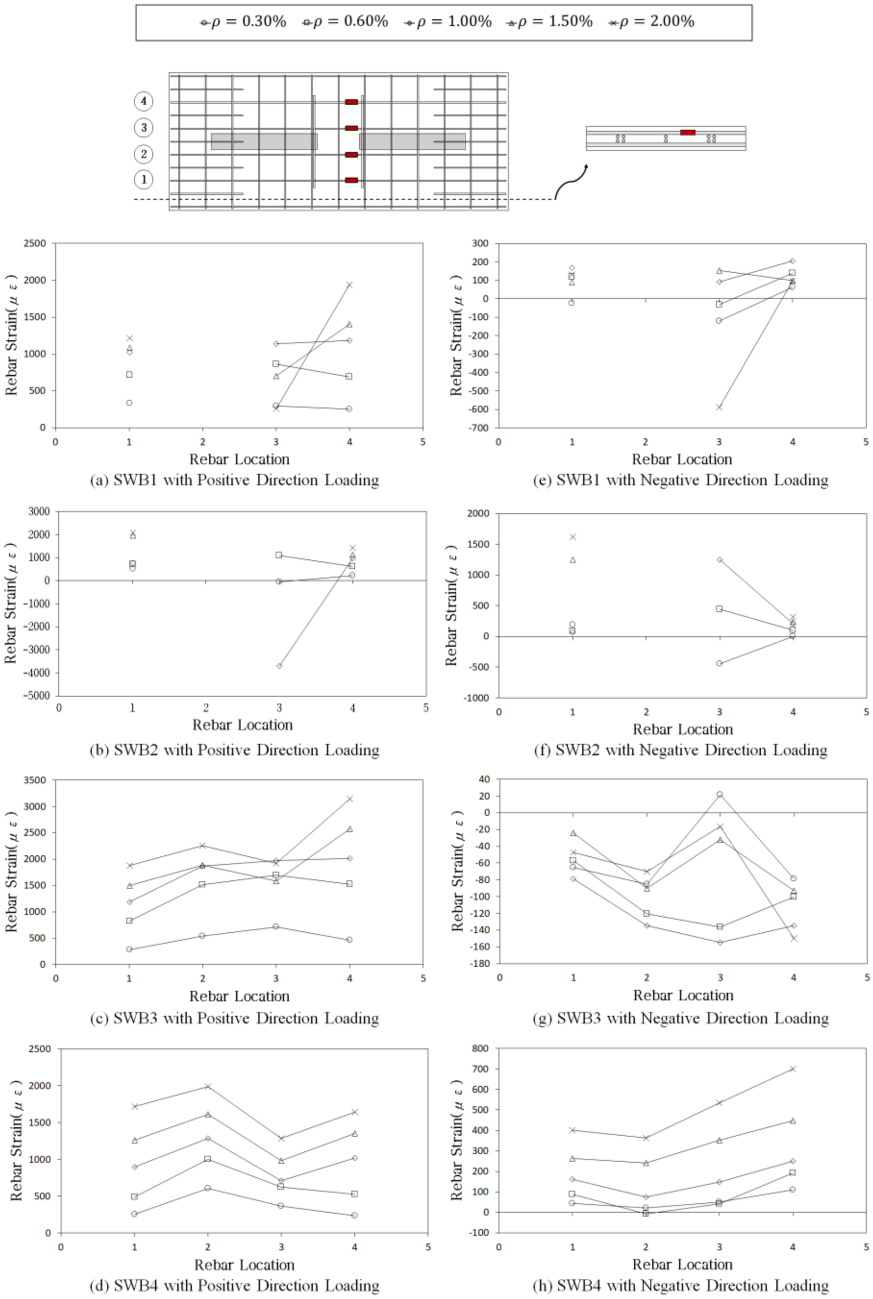

Figure 3-60 Reinforcement of Upper Story Slab

(Top Layer - In-Plane of Wall Direction Reinforcing Bars – Right)

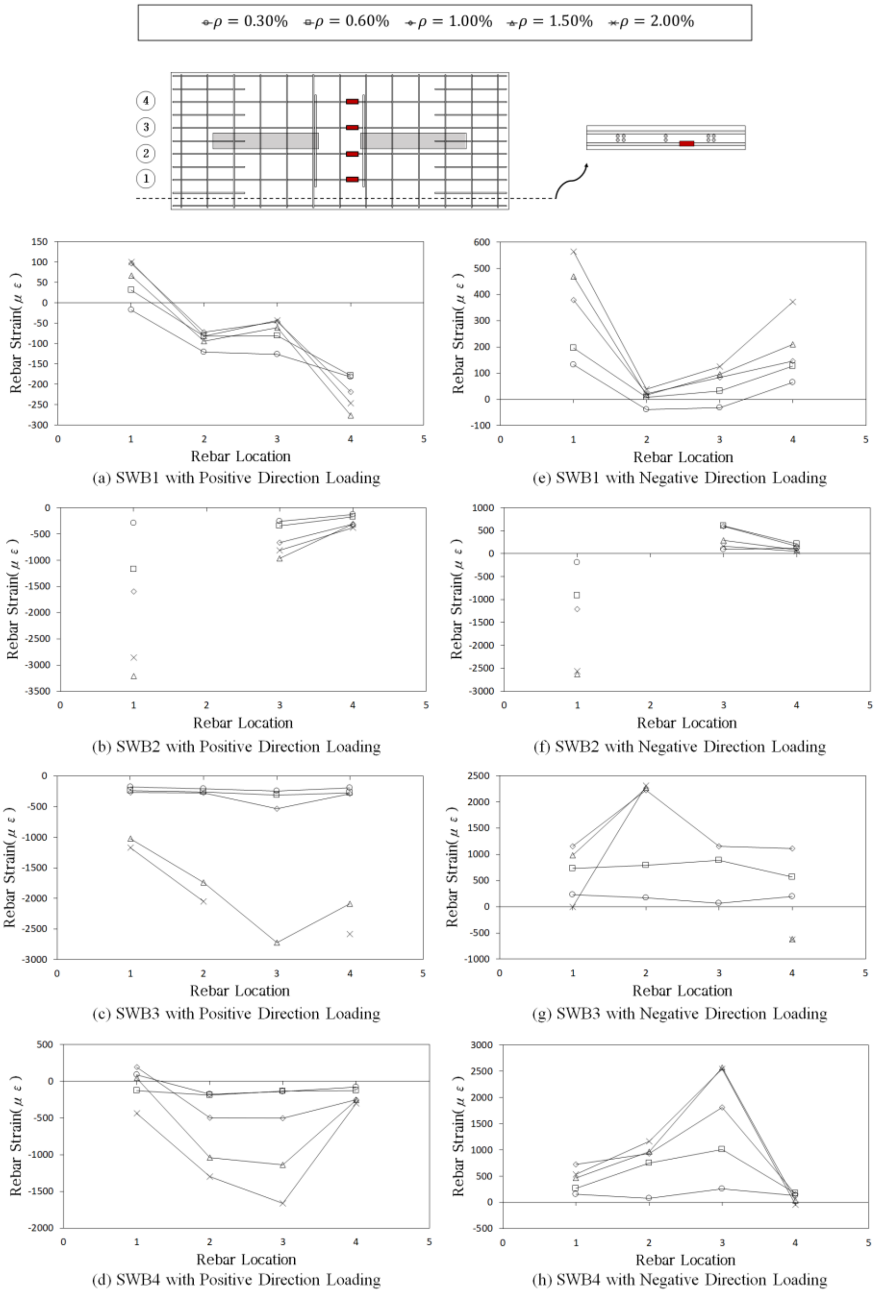

Figure 3-61 Reinforcement of Upper Story Slab

(Bottom Layer - In-Plane of Wall Direction Reinforcing Bars – Right)

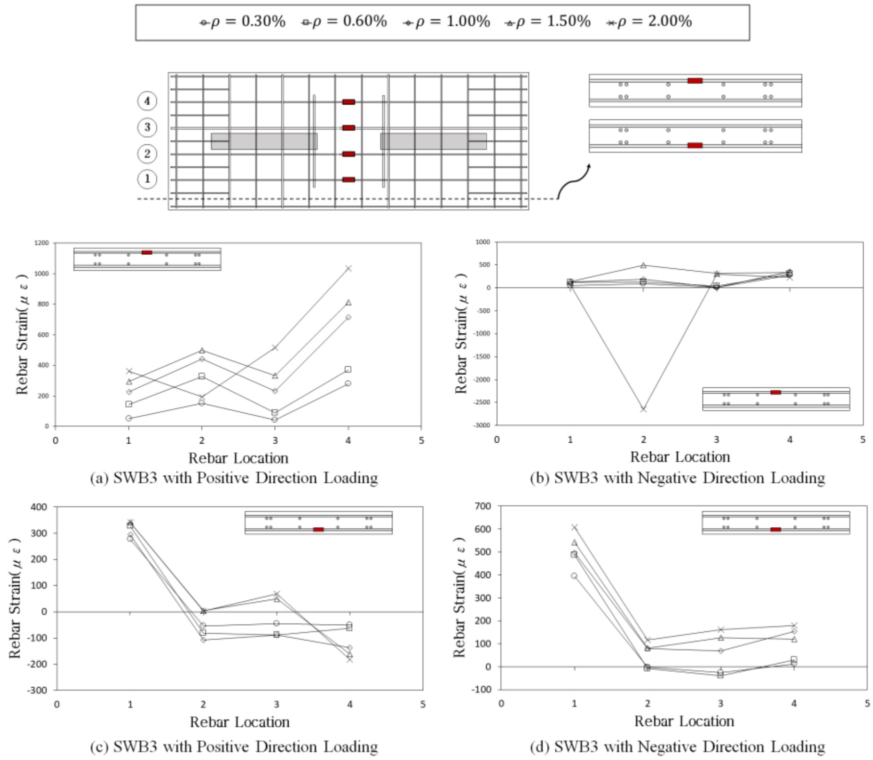

Figure 3-62 Reinforcement of Upper Story Slab (for SWB3 - Center)

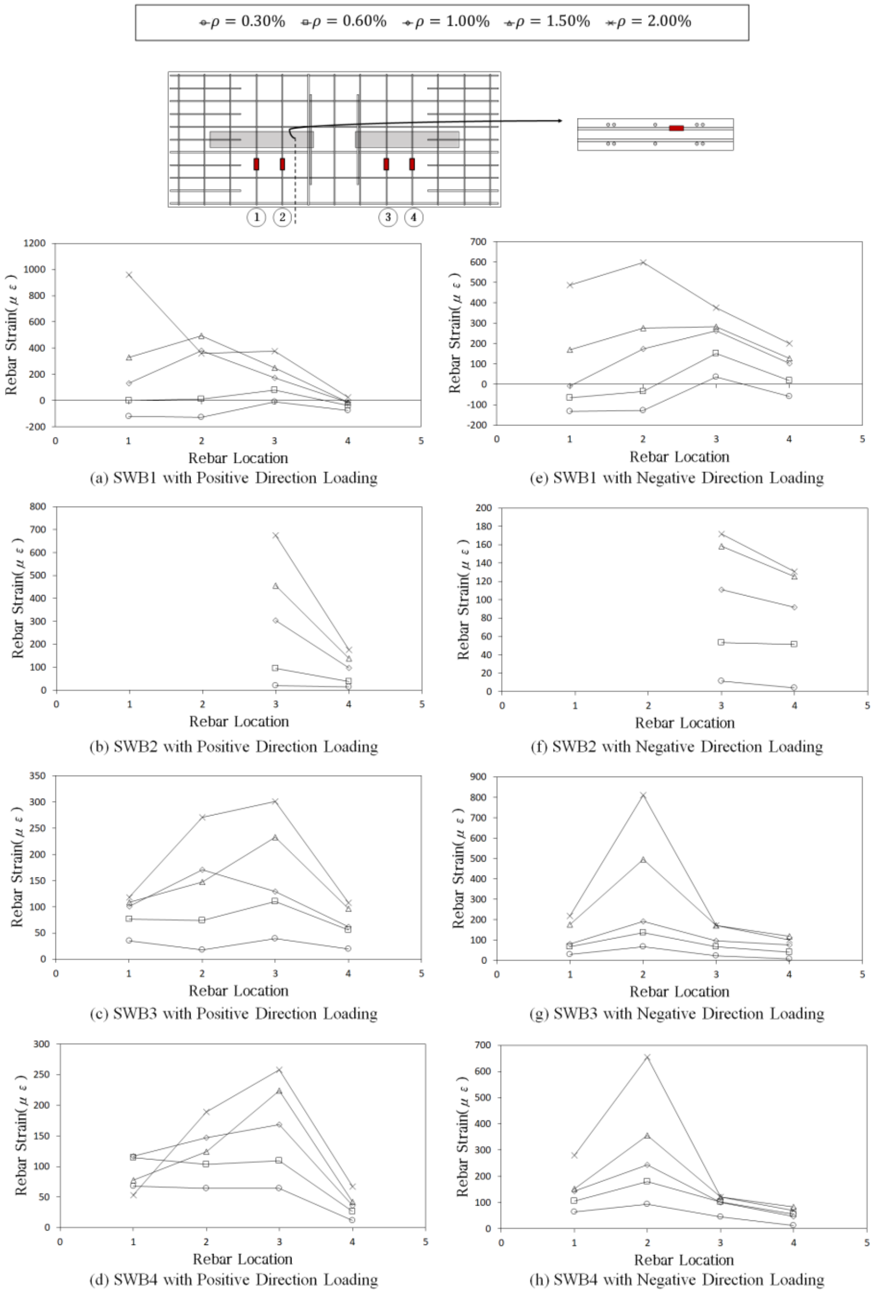

Figure 3-63 Reinforcement of Upper Story Slab

(Top Layer – Out-of-Plane of Wall Direction Reinforcing Bars - Side)

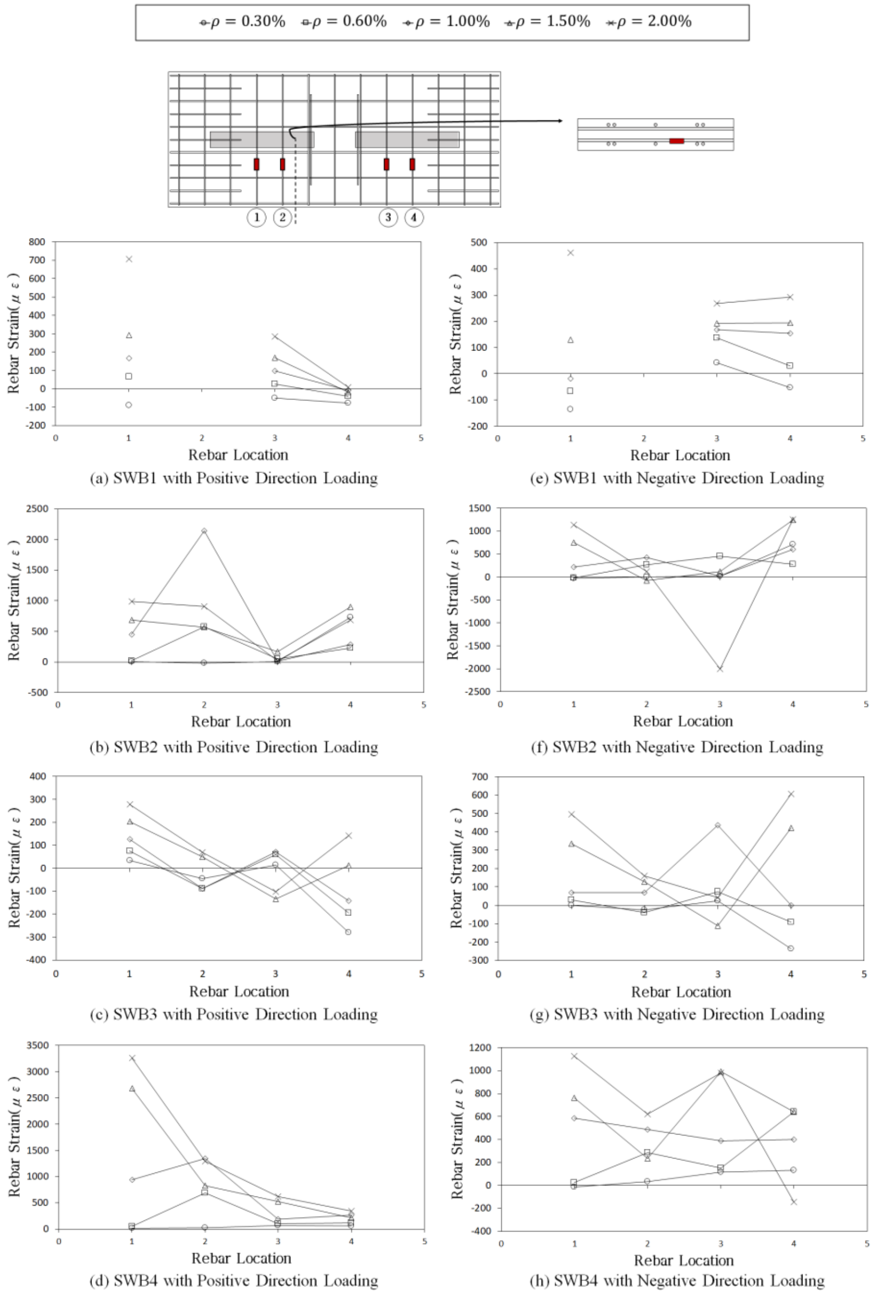

Figure 3-64 Reinforcement of Upper Story Slab

(Bottom Layer – Out-of-Plane of Wall Direction Reinforcing Bars - Side)

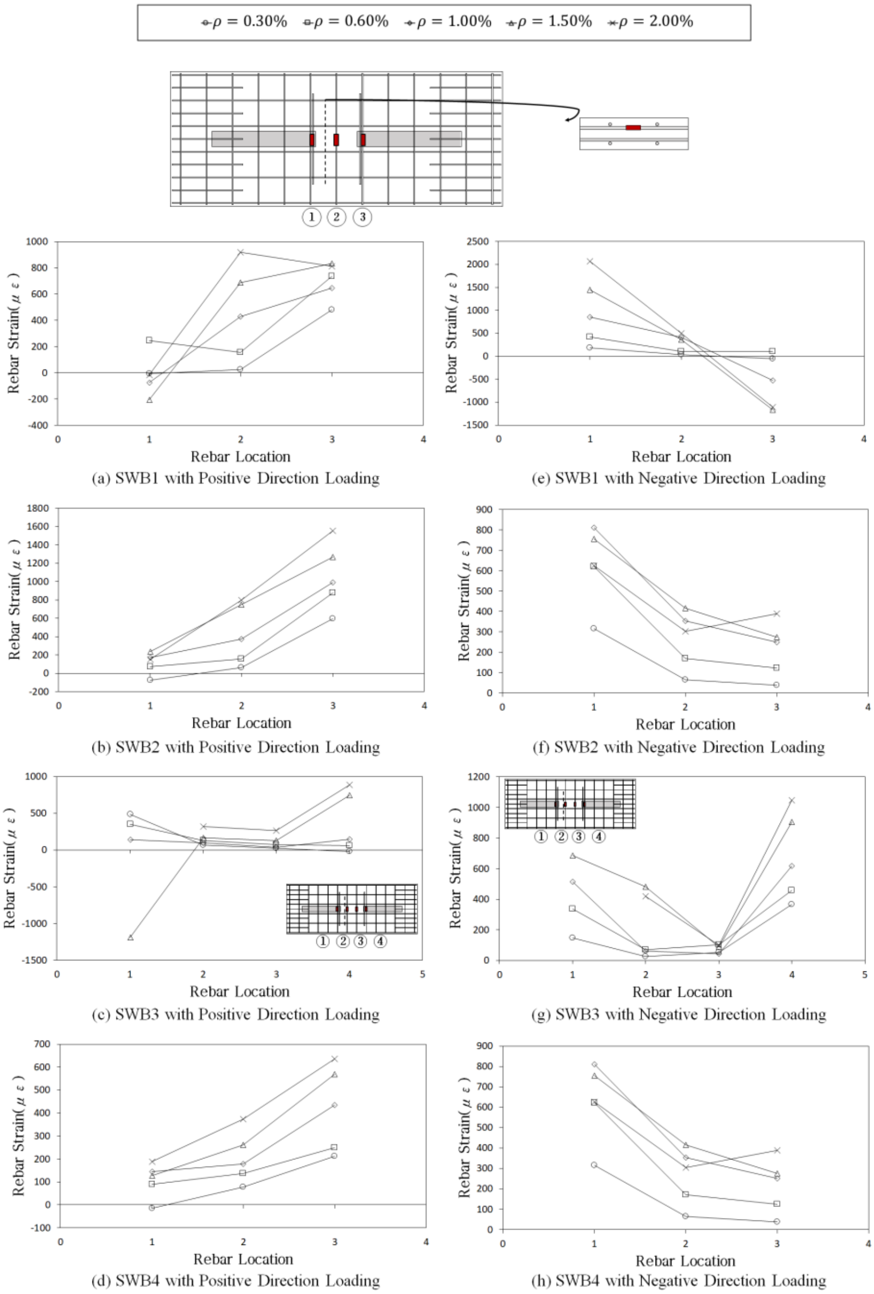

Figure 3-65 Reinforcement of Upper Story Slab

(Top Layer – Out-of-Plane of Wall Direction Reinforcing Bars - Center)

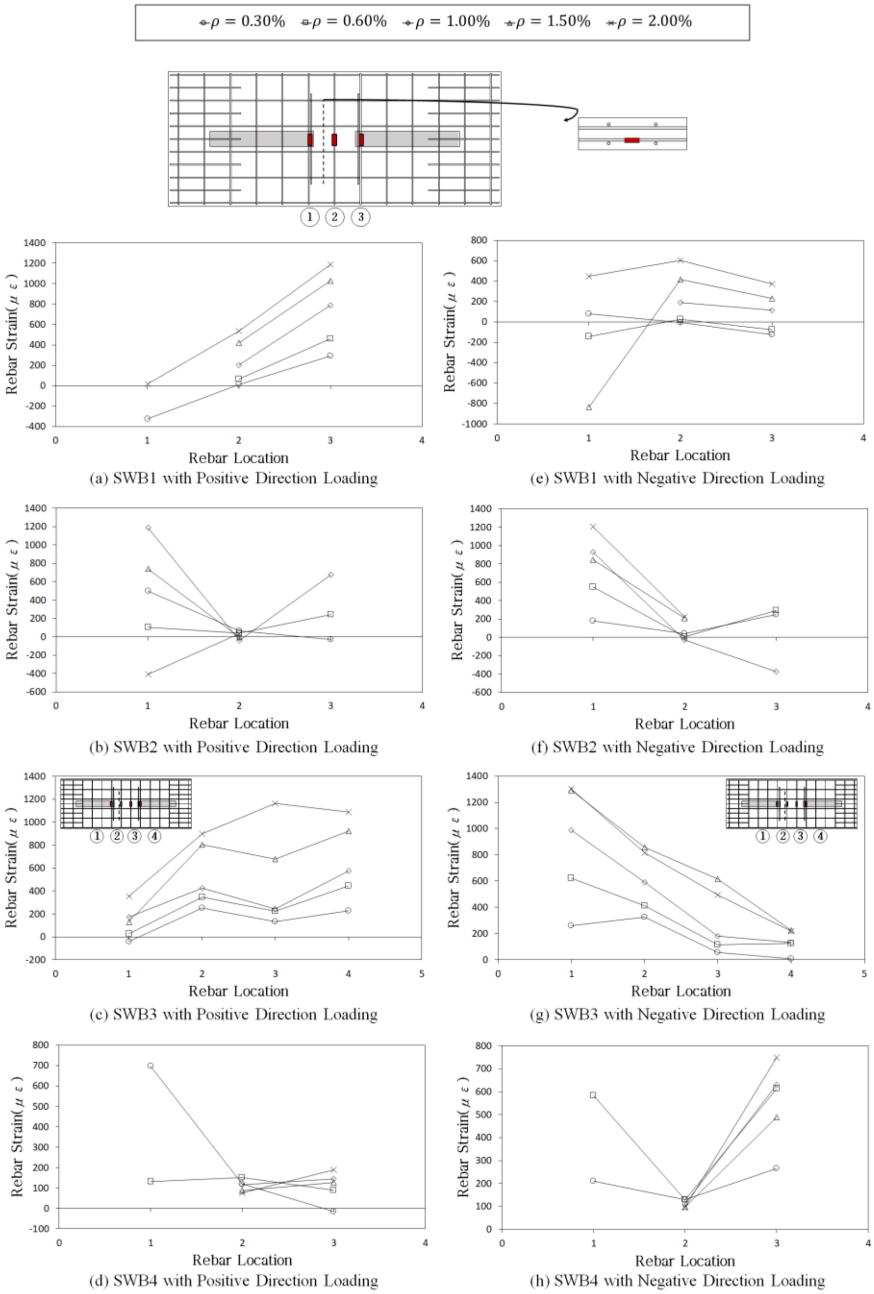

Figure 3-66 Reinforcement of Upper Story Slab

(Bottom Layer – Out-of-Plane of Wall Direction Reinforcing Bars - Center)

3.5.3 Energy Dissipation

Based on the test results, the energy dissipation capacity is evaluated. Reinforced concrete is a composite member of brittle material which is concrete and ductile material which is reinforcement. Therefore, reinforced concrete shows complex behavioral characteristics as pinching occurs along with strength and stiffness reduction due to cracking and inelastic behavior during cyclic load is applied. The energy dissipation capacity is an important evaluation that can reduce the damage of a structure under cyclic load such as earthquakes. By calculating the amount of energy dissipation of specimens by cycles and steps, the energy dissipation capacity of each specimen is evaluated and compared.

Table 3-8 Energy Dissipation Capacity of SWB1

Step	Drift	1 Cycle	2 Cycle	3 Cycle	Energy Dissipation By Step [kJ]	Cumulative Energy Dissipation [kJ]
1	0.05%	0.135	0.130	0.072	0.337	0.337
2	0.08%	0.161	0.171	0.097	0.429	0.765
3	0.10%	0.214	0.185	0.147	0.546	1.311
4	0.15%	0.335	0.315	0.127	0.778	2.089
5	0.20%	0.256	0.295	0.177	0.728	2.817
6	0.30%	0.778	0.628	0.370	1.776	4.593
7	0.40%	1.062	0.860	0.653	2.575	7.168
8	0.60%	3.259	2.470	1.797	7.526	14.695
9	0.75%	4.011	3.731	3.109	10.852	25.546
10	1%	6.647	6.217	5.407	18.272	43.818
11	1.25%	9.096	8.572	0.000	17.668	61.486
12	1.50%	12.078	11.486	0.000	23.565	85.051
13	2%	19.034	17.250	0.000	36.284	**121.334**

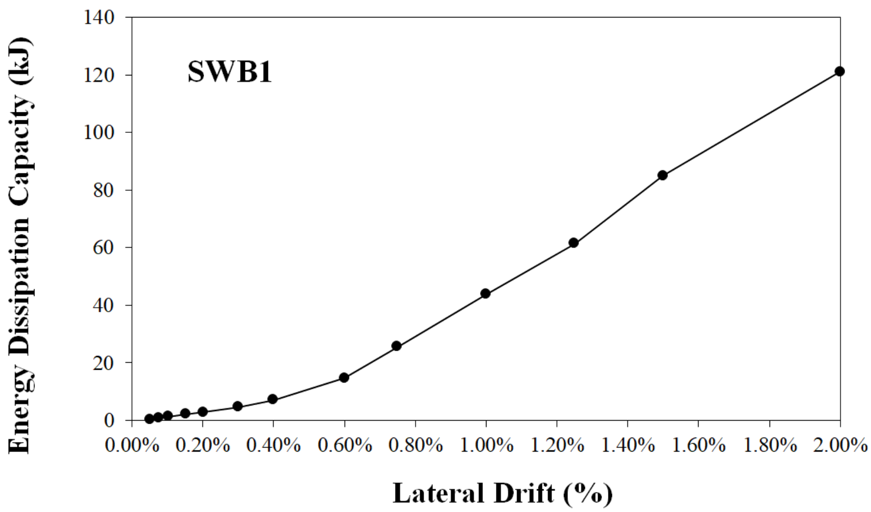

Figure 3-67 Energy Dissipation Capacity of SWB1

Table 3-9 Energy Dissipation Capacity of SWB2

Step	Drift	1 Cycle	2 Cycle	3 Cycle	Energy Dissipation By Step [kJ]	Cumulative Energy Dissipation [kJ]
1	0.05%	0.120	0.082	0.062	0.264	0.264
2	0.08%	0.131	0.121	0.104	0.356	0.619
3	0.10%	0.203	0.170	0.143	0.516	1.135
4	0.15%	0.348	0.297	0.167	0.813	1.948
5	0.20%	0.341	0.258	0.251	0.851	2.799
6	0.30%	0.885	0.573	0.418	1.876	4.675
7	0.40%	1.315	1.040	0.634	2.989	7.664
8	0.60%	3.707	2.407	1.708	7.823	15.487
9	0.75%	4.708	3.589	3.026	11.324	26.811
10	1%	6.873	5.958	5.194	18.024	44.835
11	1.25%	11.060	9.121	0.000	20.181	65.016
12	1.50%	12.700	11.497	0.000	24.197	89.213
13	2%	19.663	14.117	0.000	33.780	**122.993**

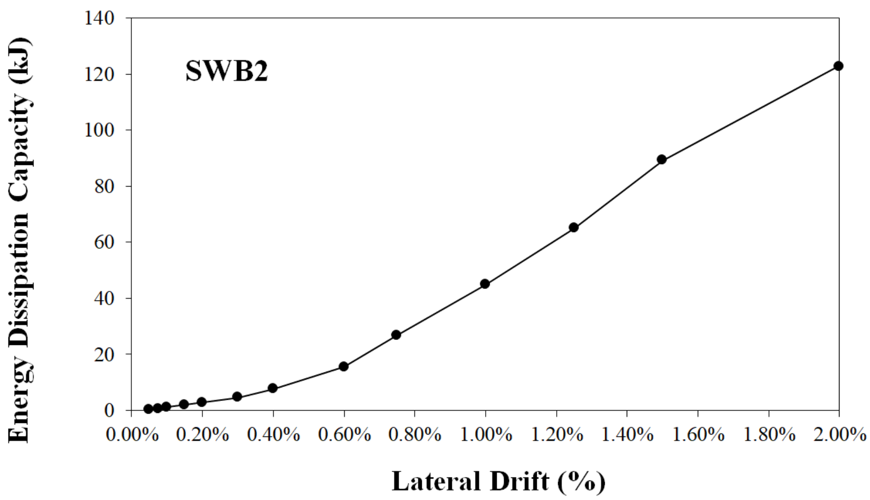

Figure 3-68 Energy Dissipation Capacity of SWB2

Table 3-10 Energy Dissipation Capacity of SWB3

Step	Drift	1 Cycle	2 Cycle	3 Cycle	Energy Dissipation By Step [kJ]	Cumulative Energy Dissipation [kJ]
1	0.05%	0.115	0.106	0.092	0.314	0.314
2	0.08%	0.197	0.185	0.175	0.557	0.871
3	0.10%	0.306	0.312	0.260	0.878	1.748
4	0.15%	0.594	0.575	0.461	1.629	3.378
5	0.20%	0.803	0.774	0.662	2.240	5.617
6	0.30%	1.638	1.498	1.270	4.406	10.023
7	0.40%	2.450	2.231	2.060	6.741	16.764
8	0.60%	5.207	4.461	3.806	13.473	30.237
9	0.75%	6.073	6.622	6.608	19.304	49.541
10	1%	11.752	9.682	8.694	30.128	79.668
11	1.25%	13.384	11.831	0.000	25.215	104.883
12	1.50%	14.694	13.007	0.000	27.701	132.584
13	2%	19.908	15.027	0.000	34.935	**167.519**

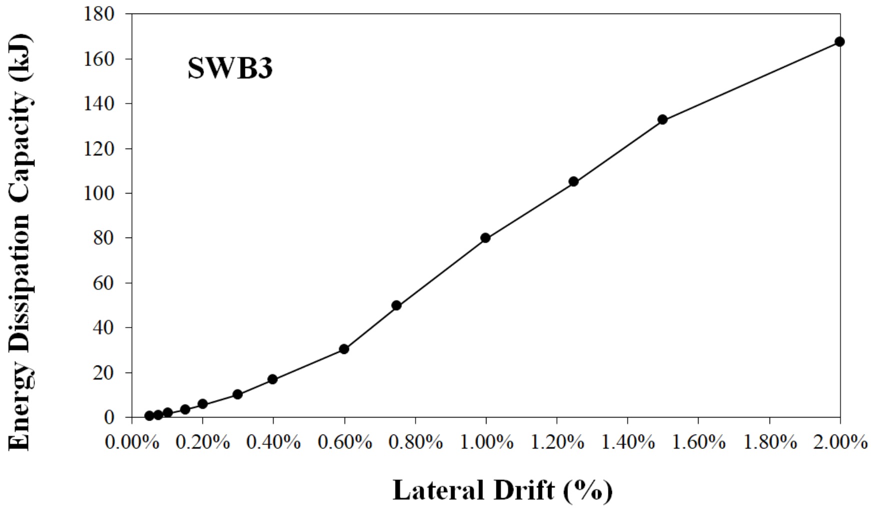

Figure 3-69 Energy Dissipation Capacity of SWB3

Table 3-11 Energy Dissipation Capacity of SWB4

Step	Drift	1 Cycle	2 Cycle	3 Cycle	Energy Dissipation By Step [kJ]	Cumulative Energy Dissipation [kJ]
1	0.05%	0.141	0.126	0.118	0.385	0.385
2	0.08%	0.220	0.211	0.192	0.623	1.008
3	0.10%	0.336	0.332	0.288	0.957	1.966
4	0.15%	0.592	0.584	0.489	1.665	3.630
5	0.20%	0.806	0.788	0.702	2.296	5.926
6	0.30%	1.602	1.376	1.168	4.147	10.073
7	0.40%	2.406	2.136	1.768	6.310	16.383
8	0.60%	5.156	4.233	3.593	12.983	29.366
9	0.75%	6.008	5.918	5.575	17.502	46.867
10	1%	10.163	8.651	7.556	26.371	73.239
11	1.25%	11.889	10.809	0.000	22.698	95.937
12	1.50%	14.150	13.264	0.000	27.415	123.351
13	2%	21.157	17.382	0.000	38.539	**161.890**

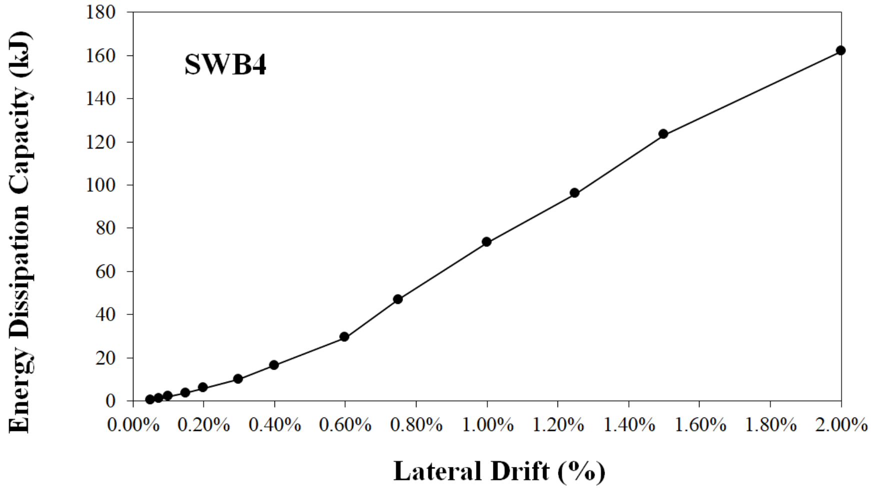

Figure 3-70 Energy Dissipation Capacity of SWB4

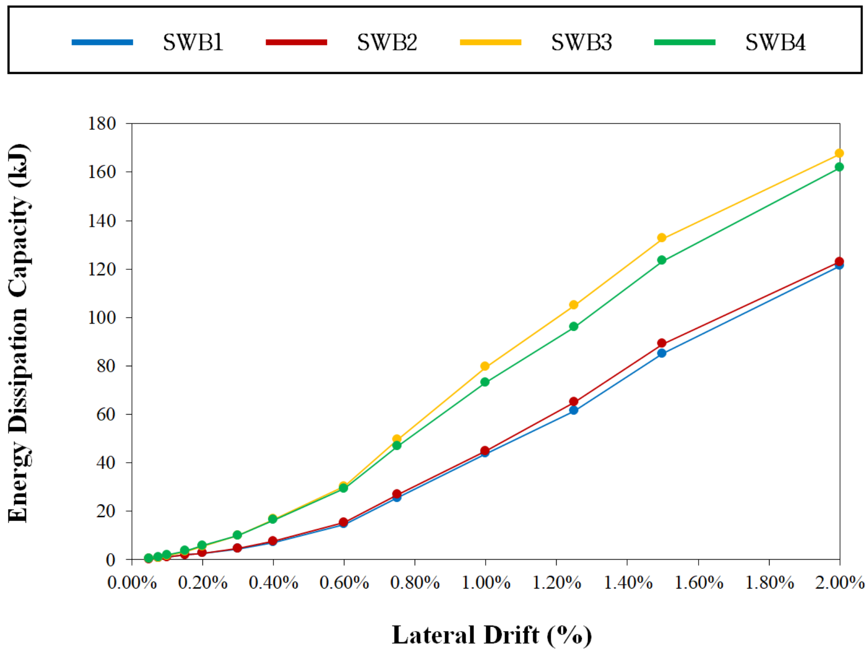

Figure 3-71 Energy Dissipation of Specimens

The failure mode of specimens is shear failure of the slab concrete. The energy dissipation capacity of the specimen compared to the SWB2 is 99% for SWB1 (121kJ/123kJ), 136% for SWB3 (168kJ/123kJ), and 131% for SWB4 (162kJ/123 kJ). SWB3, which has a wide opening, has a lower stiffness than SWB2, but the length of the arm is longer, so the degradation of stiffness and strength of the specimen occurs later. As a result, the shear failure of the slab concrete in SWB3 occurred late, and the energy dissipation capacity increased by about 36.2% compared to SWB2. The energy dissipation capacity of SWB4 is increased by 31.6% compared to SWB2 by lattice-shaped slab shear reinforcement even after slab concrete shear failure occurs.

3.6 Discussion

The failure mode of two-story RC frame of slab-coupled wall structures is shear failure of slab concrete. All failure mode of the specimens occurred in the lower slab, and it was confirmed that cracking patterns were observed like punching shear. At the joint of the slab-wall, the fracture pattern through which the slab penetrates appeared, and the deformation of the slab-wall joint is also the greatest in slab.

The strength improvement by the slab-wall interaction was the most affected by the slab thickness. In slab-wall structures, the shear capacity of the slab is more dominant than the flexural capacity of the slab. Among them, the shear performance capacity of slab concrete is dominant. In the case of the specimen with increased spacing between the walls, the initial stiffness of the specimen is lower than that of the other specimens due to the long arm length. Also, the degradation of strength and stiffness occurs later. However, the shear capacity of the slab concrete also dominates the structural performance of specimens. In addition, when the lattice-shaped shear reinforcement reinforcement was placed in the slab, there was a slight increase in strength, but there was no significant effect because the shear capacity of the slab concrete was dominant.

As the thickness of the slab increased from 80mm to 120mm, the ultimate strength increased by 12% (41kN, SWB1 vs SWB2). As the wall thickness increased from 400mm to 600mm, the ultimate strength increased by 1% (4kN, SWB2 vs SWB3), and the ultimate strength was reached in Step 10 (drift ratio 1.0%). The ultimate strength is increased by 4% (14kN) at the shear reinforcement of the opening. (SWB2 vs SWB4)

The variable that has the greatest influence on the ultimate strength is the thickness of the slab. The change in strength is insignificant when the spacing between walls is increased or when shear reinforcement is reinforced at the opening. This can be identified through the failure mode, strain distribution of slab and wall, and behavior of the specimen.

The test strength of the specimen compared to the analysis strength is 136% for SWB1 (333kN/244kN), 153% for SWB2 (374kN/244kN), 155% for SWB3 (377kN/244kN), and 161% for SWB4 (393kN/244kN).

The energy dissipation capacity of the specimen compared to the SWB2 is 99% for SWB1 (121kJ/123kJ), 136% for SWB3 (168kJ/123kJ), and 131% for SWB4 (162kJ/123 kJ).

Chapter 4. Numerical analysis of Specimens

4.1 Introduction

Based on the results of the test, the following study of the analysis of the specimens is carried out to establish a structural design manual for the procedure and method to consider the effect of slab in the structural analysis of wall-type structure. 1) The mechanism of the slab-wall interaction structure should be identified through finite element analysis, and 2) the effective stiffness of the slab and wall in the elastic analysis and the effective stiffness of the slab and wall in the program for application to performance-based design should be verified.

Therefore, it is intended to verify the following analysis and design results by performing structural analysis on the specimen and comparing it with the test results.

(1) Perform nonlinear finite element analysis and verify the validity of the nonlinear analysis model by comparing the results with the test results. In addition, the slab effect was verified by comparing the model using the Diaphragm and the model using the slab model.

(2) Linear elastic analysis was performed to verify the reliability of the slab 35% effective stiffness (Seismic Load Analysis Model) and slab 15% effective stiffness (Ultimate Strength Design Method).

4.2 Nonlinear Finite Element Analysis of Specimens

4.2.1 Material Model

Analysis was performed by defining concrete and reinforced material models as shown in Figure 4-1 using the actual strength measured through the material test. ATENA is used as a nonlinear finite element analysis program, and the elements of each member are shown in Table 4-1.

Table 4-1 Element of Nonlinear Element Analysis member

Type of Member	Wall and Slab	Reinforcement	Loading Jig	Foundation	Diaphragm Slab
Element	Solid	1D Line Element	Elastic Solid	Elastic Solid	Elastic Solid

The reliability of the nonlinear analysis model is verified by comparing and analyzing the test results with the nonlinear finite element analysis. In order to simulate the two-story RC frame of slab-coupled wall structure specimens, an analysis model is modeled as the actual specimen. The analysis is performed using solid elements for concrete members and 1D line elements for reinforcing bars. In the case of analysis using the diaphragm method in a nonlinear finite element analysis program, the slab is modeled as an elastic solid element having a thickness of 0.01m. Diaphragm slab uses an elastic solid material with a low modulus of elasticity.

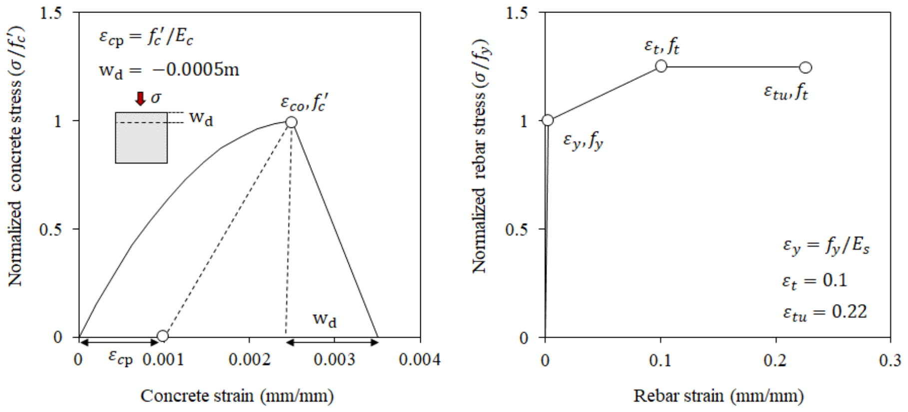

(a) Concrete stress-strain model (b) Rebar stress-strain model

Figure 4-1 Concrete and Rebar Stress-Strain Relationship in FEA

Table 4-2 Formulas of Constituitive Model in FEA

Parameter	Formula
Concrete Compression Strength [Mpa]	Depends on measured
Concrete Tensile Strength [Mpa]	$f_t = 1.40(\frac{f_{cl}}{f_{cko}})^{2/3}$
Poisson's Ratio	$\lambda = 0.2$
Elastic Modulus [Mpa]	$E = 4700\sqrt{f_{ck}}$
Fracture Energy [MN/m]	$G_F = 0.000025f_t$
Plastic Strain	$EPS_{CP} = F_{ck}/E$
Onset of Crushing [Mpa]	$F_{c0} = -2.1F_t$

4.2.2 Nonlinear Finite Element Analysis Model of Specimens

The nonlinear finite element analysis model is shown in Figure 4-2. The mesh size does not exceed 0.03m. The reason for this is that punching shear occurs in the slab near the junction between the wall and the slab. In the case of the slab, it is very thin and fracture occurs intensively near the slab-wall joint. In order to analyze it considering punching shear failure of slab, the analysis is performed by dividing the mesh into 10 equal elements of the slab in the wall thickness direction. Also, the mesh size does not exceed 0.03m because the aspect ratio of the element is set to about 2 or less.

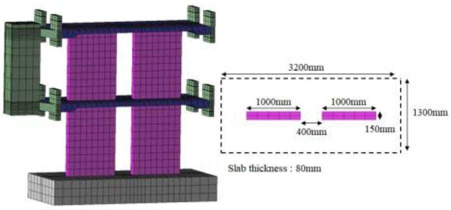

(a) FEA Model of SWB1

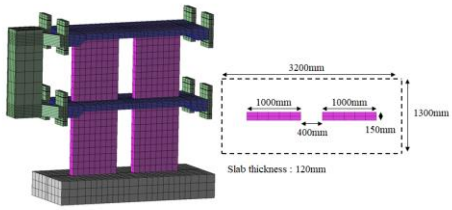

(b) FEA Model of SWB2

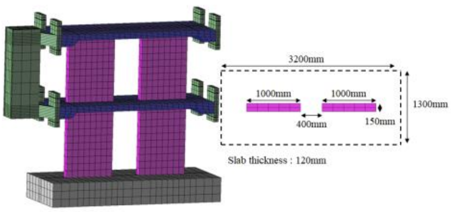

© FEA Model of SWB3

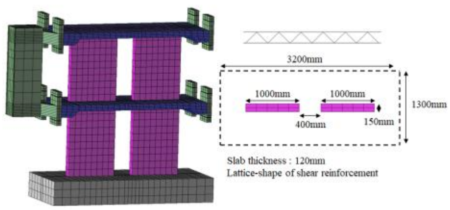

(d) FEA Model of SWB4

Figure 4-2 Nonlinear Finite Element Analysis Model of Specimens

4.2.3 FEA Result

V_{Test} is the ultimate strength result of cyclic loading test. V_{FEA} and V_{Diap} is the ultimate strength result of the nonlinear finite element analysis. As can be seen from Table 4-3, V_{Test}/V_{FEA} is close to 1 and the error does not occur significantly (less than 10%). In addition, the reliability of the nonlinear finite element analysis is proved through the load-displacement relationship graphs in Figure 4-3 to Figure 4-6. Conversely, T/D is much greater than 1. Through this, it can be seen that the strength improvement effect by the slab is much greater than diaphragm method.

Table 4-3 Result of Test and FEA Results

Specimen	Test Strength (Cyclic Test) V_{Test}		Strength Prediction (Static Loading) V_{FEA}		V_{Test}/V_{FEA}		V_{Test}/V_{Diap}	
	Pos [kN]	Neg [kN]	Flexural Strength V_{FEA} [kN]	Shear Strength V_n [kN]	Pos	Neg	Pos	Neg
Diaphragm	-	-	244	1351	-	-	-	-
SWB1	333	-295	318	1351	1.05	0.93	1.36	1.21
SWB2	374	-345	377	1351	0.99	0.92	1.53	1.41
SWB3	353	-378	368	1351	0.96	1.03	1.45	1.55
SWB4	352	-393	392	1351	0.90	1.00	1.44	1.61

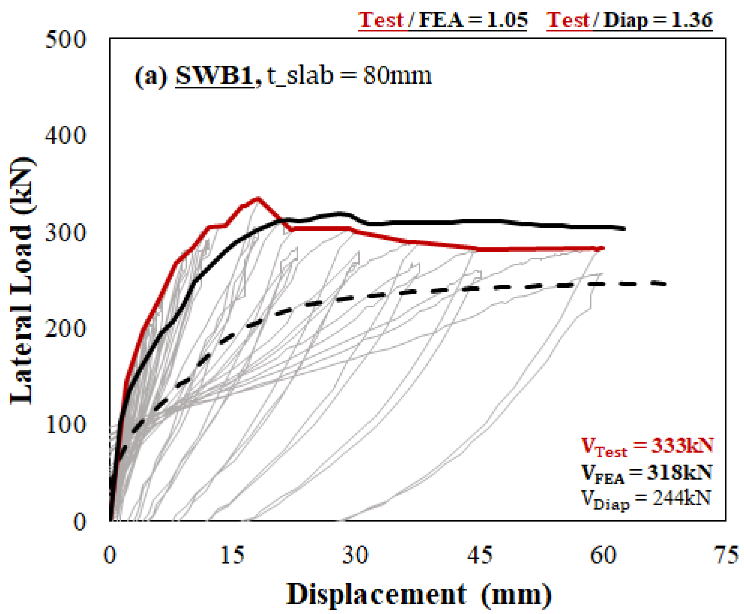

Figure 4-3 Test Results of SWB1 with FEA and Diaphragm

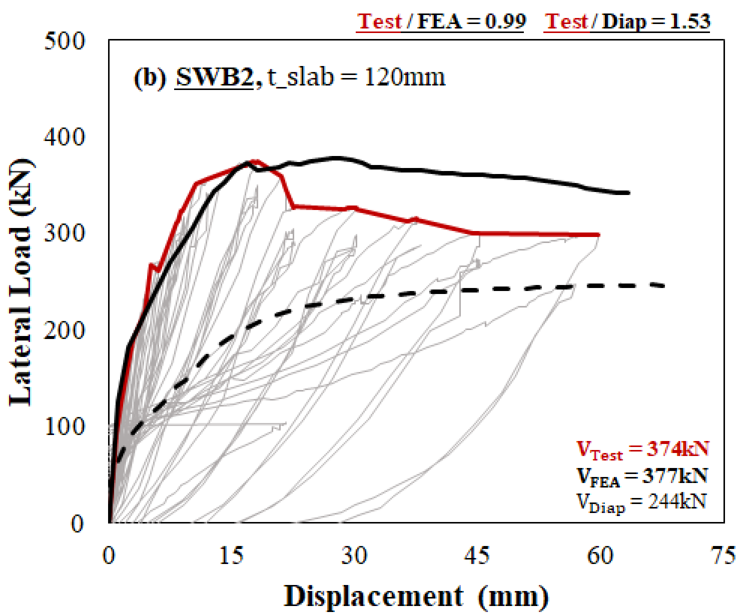

Figure 4-4 Test Results of SWB2 with FEA and Diaphragm

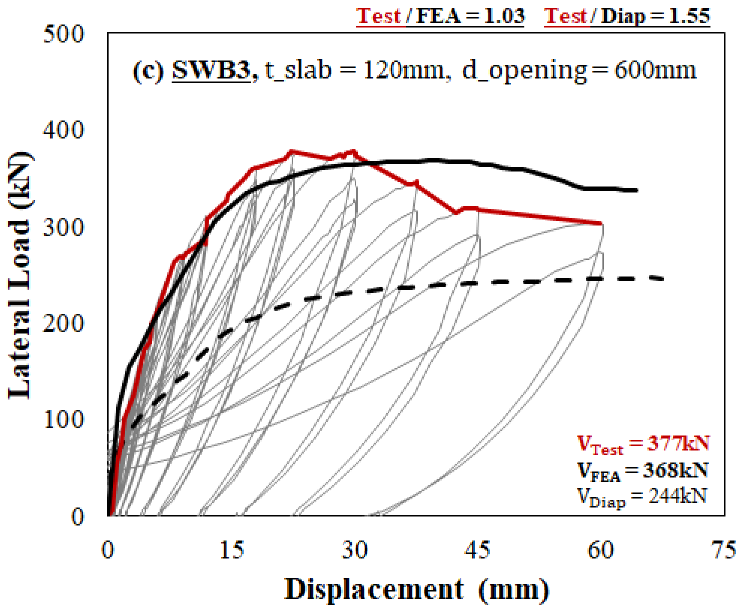

Figure 4-5 Test Results of SWB3 with FEA and Diaphragm

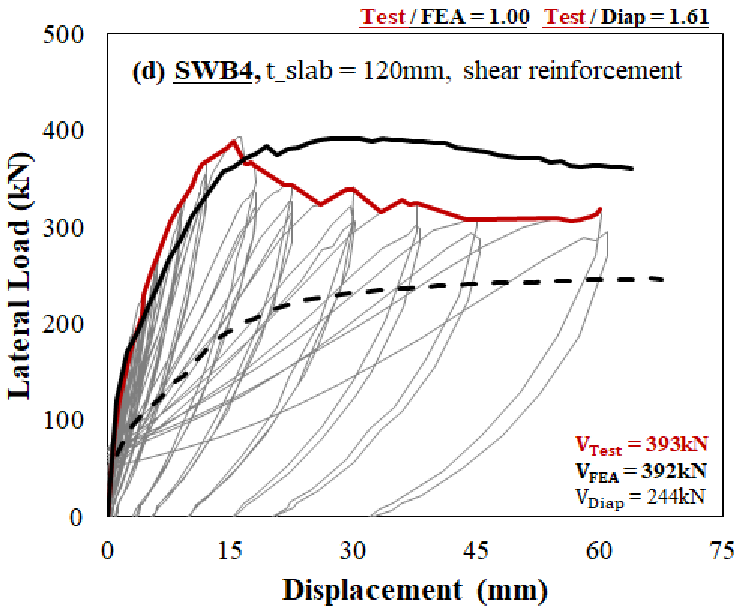

Figure 4-6 Test Results of SWB4 with FEA and Diaphragm

When comparing the ultimate strength of the FEA result and the test result, it can be confirmed that the error rate is less than 5%. Also, it can be seen that the reliability of the test results was confirmed through the similarity of the FEA results and the lateral load-displacement relationship of the test results.

The test strength of the specimen compared to the FEA strength is 105% for SWB1 (333kN/318kN), 99% for SWB2 (374kN/277kN), 103% for SWB3 (378kN/368kN), and 100% for SWB4 (393kN/392kN). The strength of specimens is greater than the result of the nonlinear analysis of Atena (black). In addition, the ultimate strength in the both loading direction of the test specimen is similar to the analysis result of FEA as shown in Table 4-3.

4.2.4 Test Analysis with FEA

(a) Load Resistance Mechansim

The load resistance mechanism of the specimen is shown in Figure 4-7 (a). When a lateral load is applied to two-story RC frame of slab-wall structure, rotation occurs in the walls of each floor. As the wall is rotated, the slab is also deformed and the bending moment is applied. When a bending moment occurs in the slab, a corresponding shear force is generated in the slab, and accordingly, an axial force is transmitted in the wall. The axial force acts as a tensile force and a compressive force on each wall, and through this, the wall of the specimen is coupled.

In case of diaphragm, it behaves like a cantilever as shown in Figure 4-7 (b). This means that the walls behave like individual walls, and the effect of the slab cannot be expected.

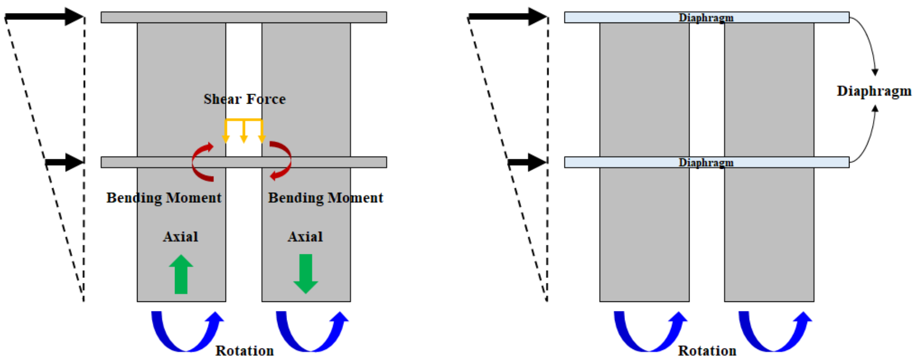

(a) Load Resistance Mechanism of Specimen (b) Load Resistance Mechanism of Diaphragm

Figure 4-7 Load Resistance Mechanism

(b) Bending Moment and Shear Force of Slab

According to the load resistance mechanism, a bending moment occurs in the slab as rotation occurs in the wall. Through this, a shear force corresponding to the bending moment is generated in the slab. Figure 4-8 shows that the bending moment showed a slight decrease in the drift ratio at which the ultimate strength occurs and the drift ratio at which the fracture of specimens occurs, but there is no significant difference. From the following results, it can be seen that the influence of the bending moment of the slab is not dominant on the specimen.

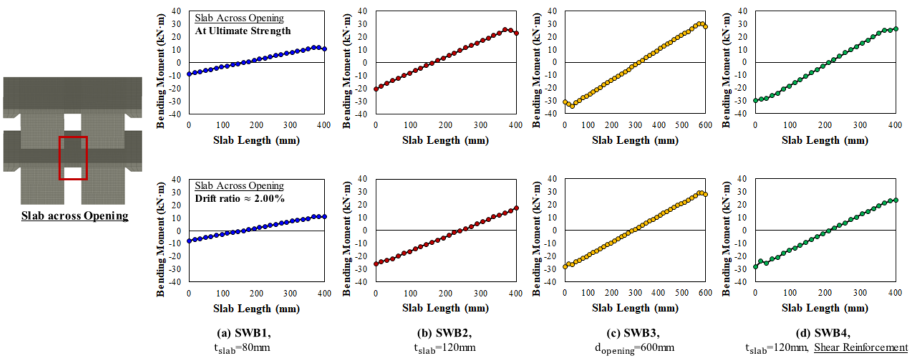

Figure 4-8 Bending Moment of Slab Across Opening

Figure 4-9 is a graph showing the shear force generated at the slab across opening when ultimate strength occurs and when the drift ratio is 2.00%. In the case of Figure 4-10, the shear force generated at the center of across opening is a graph showing when ultimate strength occurs and when the drift ratio is 2.00%. Through Figure 4-9 and Figure 4-10, it can be predicted that the shear force generated in the slab decreases after the ultimate strength occurs. The reduced shear force in Figure 4-9 is similar to the reduced shear force in Figure

4-10, so it can be expected that most concrete fractures occurred near the slab-wall joint. To confirm this, Figure 4-11 to Figure 4-14 shows the crack pattern and deformation of the specimen in the nonlinear analysis.

From Figure 4-11 to Figure 4-14, it can be seen that the failure mode of the specimen was caused by shear failure of the slab concrete at the slab-wall joint. This shows a similar tendency to the actual test failure mode.

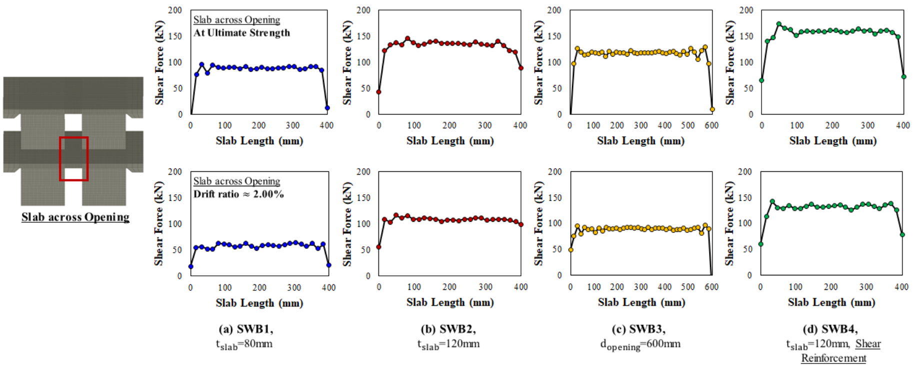

Figure 4-9 Shear Force of Slab Across Opening

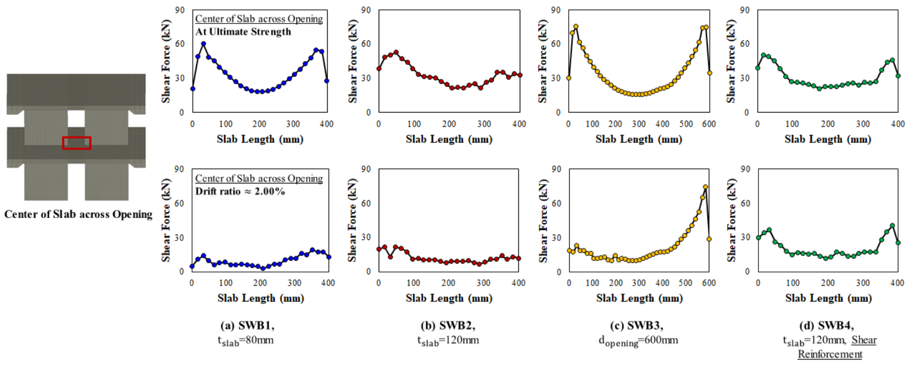

Figure 4-10 Shear Force of Center of Slab Across Opening

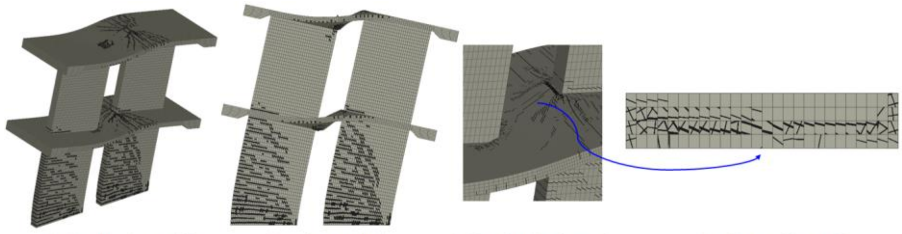

(a) Deformation of FEA Model (b) Crack Pattern of Wall (c) Slab Deformation of Lower Floor (d) Crack Pattern of Center Slab

Figure 4-11 Deformation and Crack Pattern of SWB1

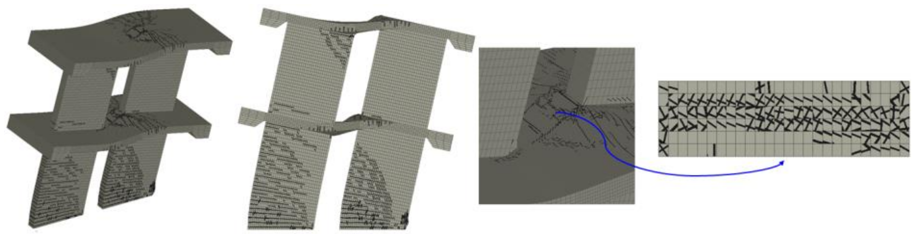

(a) Deformation of FEA Model (b) Crack Pattern of Wall (c) Slab Deformation of Lower Floor (d) Crack Pattern of Center Slab

Figure 4-12 Deformation and Crack Pattern of SWB2

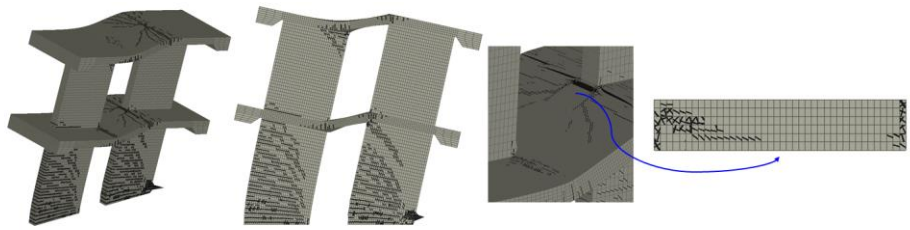

(a) Deformation (b) Crack Pattern of Wall (c) Slab Deformation of Lower Floor (d) Crack Pattern of Center Slab

Figure 4-13 Deformation and Crack Pattern of SWB3

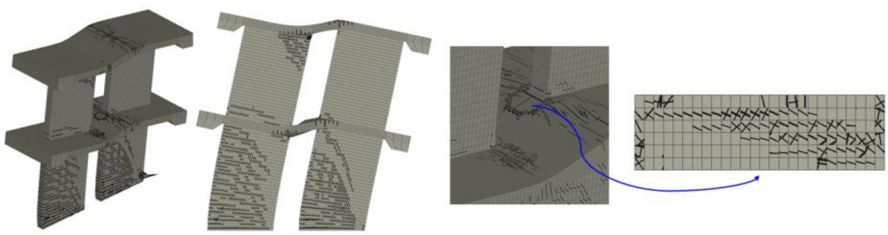

(a) Deformation (b) Crack Pattern of Wall (c) Slab Deformation of Lower Floor (d) Crack Pattern of Center Slab

Figure 4-14 Deformation and Crack Pattern of SWB4

(c) Axial Force of Wall (Slab Effect)

As the load-resisting system works as shown in Figure 4-7 (a), the specimen behaves like a frame and an axial force is generated in the wall. As the axial force is applied, the wall will be partially coupled. In Chapter 3, the axial force generated by the slab is defined as the slab effect. Therefore, the difference in the axial force generated by the lateral load excluding the gravity load was compared for each variable of the specimen using the nonlinear finite element analysis. This can be confirmed through Figure 4-15.

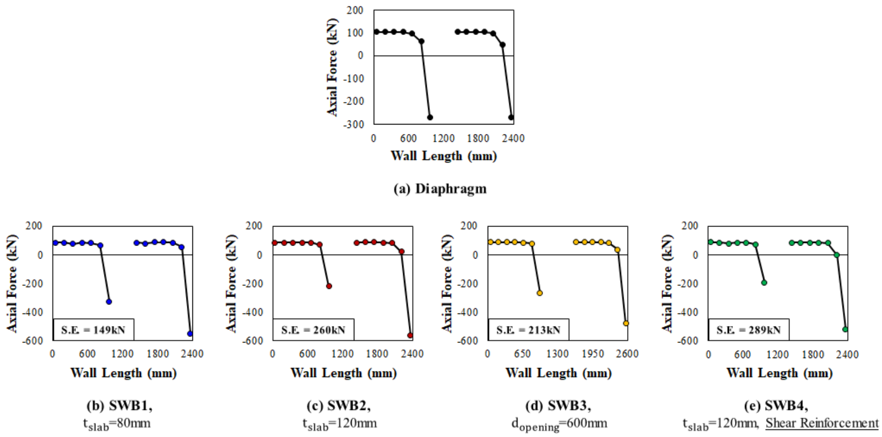

Figure 4-15 Comparison of Slab Effect (Axial Force of Wall)

Through the graph in Figure 4-15, it can be confirmed that the walls of the slab-wall structure partially behave integrally. Conversely, the walls of the diaphragm behave individually. The slab effect occurs greatly in the order of SWB4, SWB2, SWB3, and SWB1, and the difference in axial force between the walls (slab effect) is 289kN, 260kN, 213kN, and 149kN, respectively.

4.3 Elastic Analysis of Specimens for Seismic Load and Design

4.3.1 Synopsis of Elastic Analysis of Specimens

Midas Gen was used as a linear elastic analysis program, and the model is shown in Figure 4-16. Shell elements are used for walls and slabs. In the case of a wall, it should be divided by the slab mesh, so it is set as one connected element. The thickness of the wall and slab was used for the thickness of the specimen. The effective stiffness of the slab and wall was adjusted by applying the wall stiffness scale factor for wall and the plate stiffnese scale factor for slab. In order to simulate the double curvature of the slab, the slab of the wall opening is divided into 0.1m length in the longitudinal direction of the opening. In order to apply the same load as in the test, the ultimate strength was divided so that the load was distributed at a ratio of 2:1 between the upper and lower story slabs. The loading plan of the test was simulated by inputting two nodal loads to each slab (Refer to Figure 4-16).

In order to control the in-plane bending stiffness in the program of Midas Gen, plane stress, is used, so the analysis was performed by adjusting the axial stiffness as well.

Table 4-4 Formulas of Constituitive Model in Linear Elastic Analysis

Parameter	Formula
Concrete Compression Strength [Mpa]	Depends on measured
Elastic Modulus [Mpa]	$E = 4700\sqrt{f_{ck}}$

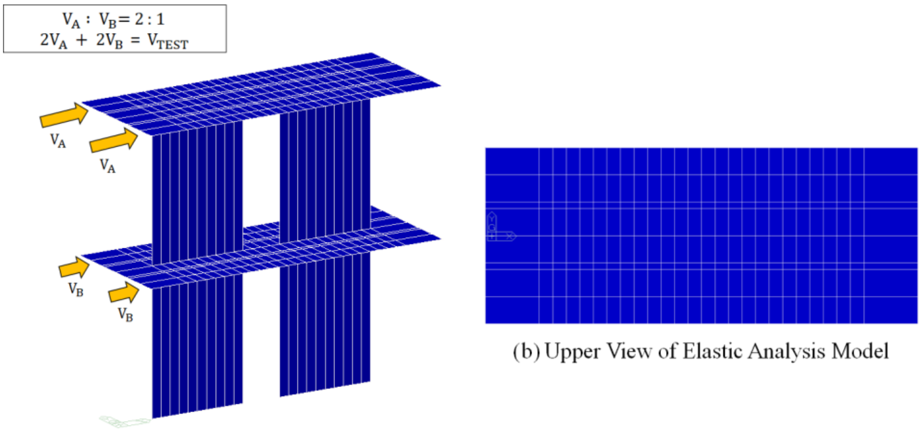

(a) Elastic Analysis Model

(b) Upper View of Elastic Analysis Model

Figure 4-16 Elastic Analysis Model of Specimens

4.3.2 Elastic Model for Fundamental Period Estimation

In order to design an actual building, it is necessary to determine the fundamental period for seismic load calculation. The fundamental period for structure is determined by referring to 2.1.2 Korea Building Code 2016 in Chapter 2. In the case of diaphragm model, dynamic analysis is performed on the elastic analysis model to find out the natural period, and then calculate the fundamental period according to the KBC 2016. Then, the seismic load corresponding to the fundamental period is calculated and the design is carried out by applying the seismic and gravity load into the analysis model.

When designing the wall considering slab-wall interaction, the slab should be added to the analysis model to constrain each story instead of using diaphragm. When the slab is modeled, the stiffness of the structure increases, and the natural period becomes less compared to the model of the diaphragm. However, if the natural period is calculated using 100% of the effective stiffness of the wall and slab, the excessive seismic load is applied to the structure. Since this does not consider the early yielding of the slab, which is thin member, it may result in an overdesigned design. In order to consider this case, the effective stiffness is adjusted to establish an elastic analysis model for fundamental period estimation. In order to properly adjust the effective stiffness, it was determined and confirmed by referring to 2.1.5 ‘Bending Moment and Compression Design Criteria of Concrete Structure’ in Chapter 2.

When the effective stiffness of ‘Bending Moment and Compression Design Criteria of Concrete Structure’ is applied to slabs and walls, analysis is performed to check whether the analysis model has adequate stiffness.

In the modeling of the actual wall-type strucuture, there is a gravity load which is vertical force to members, so effective stiffness of non-cracked wall (70% of effective stiffness) is applied to walls in the in-plane direction. However, since the test specimen does not have a vertical load (gravity load), 35% effective stiffness (cracked wall) in in-plane direction is applied in elastic analysis. In the case of slab, analysis is performed by applying only out-of-plane bending effective stiffness of beam which is 35%. In the linear elastic analysis model, by measuring the displacement at the same location as the test, the stiffness in the elastic analysis was obtained using the "Lateral Load/Displacement" of the analysis model.

In order to control the in-plane bending stiffness in the program of Midas Gen, plane stress, is used, so the analysis was performed by adjusting the axial stiffness as well.

Table 4-5 Element of Nonlinear Element Analysis member

Type of Member	Wall	Slab	Loading Plan	Boundary Condition
Element	Shell (35% of In-plane Effective Stiffness)	Shell (35% of Out-of-plane Effective Stiffness)	2 Nodal Loads per Floor	Fixed

4.3.3 Elastic Model for Design

A model for fundamental period estimation and a model for design were separately considered. If the design proceeds with the analysis model for the fundamental period calculation determined previously, the slab will be subjected to excessive stress because the required strength steadily increases without considering yielding due to the characteristics of the elastic analysis. In this case, unlike the previous diaphragm, overestimated design is made in the slab where the slab-wall interaction occurs. Also, as a result of the test, the slab concrete shear capacity was dominant rather than the bending moment capacity of the slab of the specimen when a lateral load was applied. Therefore, in order to economically design a building, linear elastic analysis should be performed by setting the effective stiffness of slab and wall in consideration of the above results.

When the effective stiffness of 'Bending Moment and Compression Design Criteria of Concrete Structure' is applied to walls, analysis is performed to check whether the analysis model has adequate stiffness except for slab.

In the modeling of the actual wall-type strucuture, there is a gravity load which is vertical force to members, so effective stiffness of non-cracked wall (70% of effective stiffness) is applied to walls in the in-plane direction. However, since the test specimen does not have a vertical load (gravity load), 35% effective stiffness (cracked wall) in in-plane direction is applied in elastic analysis. In current practice, when considering slabs, in order to consider the yield strength of the slab and prevent overdesigning the slab, the effective stiffness of the slab is used as 10-20%. In addition to the above, the slab is a thin member, and early yielding due to out-of-plane demands is expected. Therefore, the effective stiffness should be determined considering the redistribution of the force. In order to verify the validity of the effective stiffness, the analysis was performed by applying 15% to the out-of-plane bending stiffness of the slab.

In order to control the in-plane bending stiffness in the program of Midas Gen, plane stress, is used, so the analysis was performed by adjusting the axial stiffness as well.

Table 4-6 Element of Nonlinear Element Analysis member

Type of Member	Wall	Slab	Loading Plan	Boundary Condition
Element	Shell (35% of In-plane Effective Stiffness)	Shell (35% of Out-of-plane Effective Stiffness)	2 Nodal Loads per Floor	Fixed

4.4 Analysis Result of Specimens

4.4.1 Initial Stiffness of Specimens

The results of the linear elastic analysis of SWB1~SWB4 (35% wall, 35% slab effective stiffness) are compared with the nonlinear finite element analysis results and test results as shown in Table 4-7.

The stiffness of the linear elastic analysis model is an average of 89% of the initial stiffness of the nonlinear finite element model, which is smaller than the stiffness of the nonlinear finite element model. (SWB1: 81%, SWB2: 96%, SWB3: 84%, SWB4: 95%) The stiffness of the linear elastic analysis model of SWB2 and SWB4 was very similar to the initial stiffness of the nonlinear finite element model, and the stiffness of the linear elastic analysis model of SWB1 and SWB3 was lower than the initial stiffness of the nonlinear finite element model.

The stiffness of the linear elastic analysis model is an average of 101% of the initial stiffness of the test results. Initial stiffness, which is similar than the stiffness of the nonlinear finite element model. (SWB1: 111%, SWB2: 90%, SWB3: 101%, SWB4: 101%) The initial stiffness of the test results was determined through the displacement of the specimen under a load of about 40 kN. This is because the specimen was judged to be an elastic part at a load of about 40 kN.

Table 4-7 Initial Stiffness of Specimens (Elastic Analysis, FEA and Test)

	Elastic Analysis K_E [kN/mm]	FEA K_{FEA} [kN/mm]	TEST (About 40kN) K_{TEST} [kN/mm]	$\frac{K_E}{K_{FEA}}$	$\frac{K_E}{K_{TEST}}$
SWB1	69.1	85.8	62.44	0.81	1.11
SWB2	100.0	104.2	110.8	0.96	0.90
SWB3	78.9	93.9	78.3	0.84	1.01
SWB4	95.3	100.7	94.2	0.95	1.01

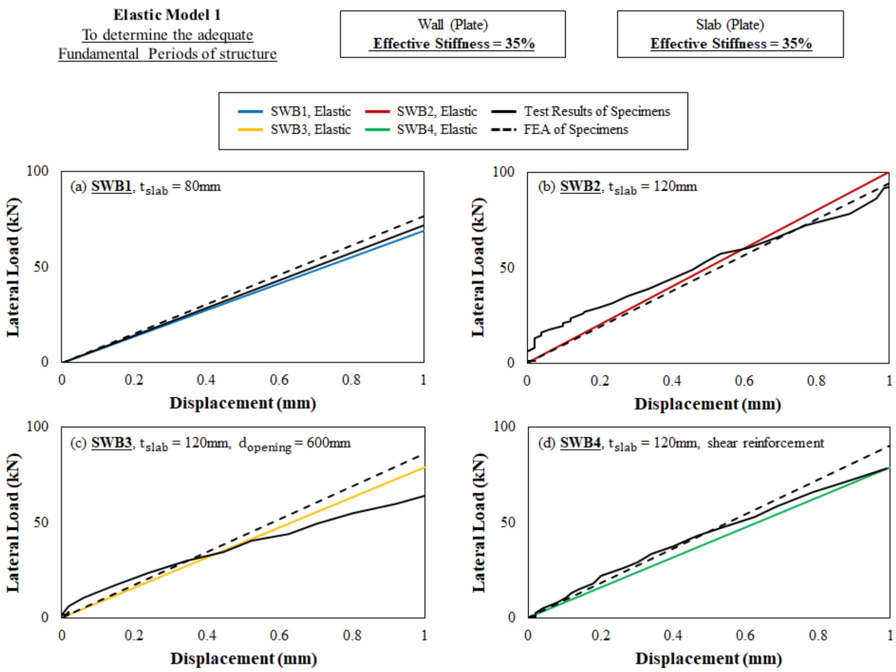

Figure 4-17 Initial Stiffness Comparison of Test, FEA and Elastic Analysis

4.4.2 Design of Specimens Wall

The slab is a thin and wide member, and although the stiffness in the in-plane direction is very strong, it is very weak in the out-of-plane direction, so premature yielding in the out-of-plane direction is expected. This results in load redistribution, and in order to take this into account, it is necessary to properly set the effective stiffness of the slab and wall in the design model. Therefore, it proves its suitability as a design model by comparing the PM curve of the wall subjected to the actual test and the demand on the walls in the analysis result simulated by the elastic analysis of the actual test.

The PM curve of the wall of the test specimen was compared with the axial force-moment relationship in the analysis model to check whether the appropriate load distribution for wall design was performed in the elastic analysis model. Also, cut and check the slab-wall joint that receives the most demand in the 15% effective stiffness model in the out-of-plane direction of the slab. Through this, it is compared whether the demand of the slab exceeds the design capacity of the slab.

Figure 4-18 shows the design strength and required strength of the load concentration part of the specimen slab. In all specimens, the required strength at the load concentration area exceeds the slab capacity, but the demands on the entire width of the slab(1.3m) is smaller than the entire width of the slab capacity. The above results well simulate that the failure of the slab did not occur due to flexural failure. At the slab-wall joint, not only moment but also shear force is concentrated. However, in the case of the slab, the shear reinforcement of the slab is not arranged, and thus local punching shear is expected. Similarly, since shear failure of the slab concrete occurred in the actual test, it was judged that the test results were properly simulated. Since the slab is fractured due to shear failure, it is judged that the behavior of the slab is not different according to the increase in the reinforcement ratio.

Figure 4-19 shows the PM Curve and elastic analysis results of the specimens. The specimens are a coupled wall arrangement, and the PM curve of both walls and the elastic analysis result are compared. In all specimens, in the direction of the positive loading direction, the left wall receives tensile and right wall compressive forces, and in the direction of the negative loading, it acts opposite to the positive loading direction. When the following occurs, a moment of similar demand is distributed to both walls.

For all walls, there is no difference between the boundary of the PM curve and the analysis result. Through this, it can be seen that the required strength of elastic analysis and the performance strength of the tested specimen wall show similar strength.

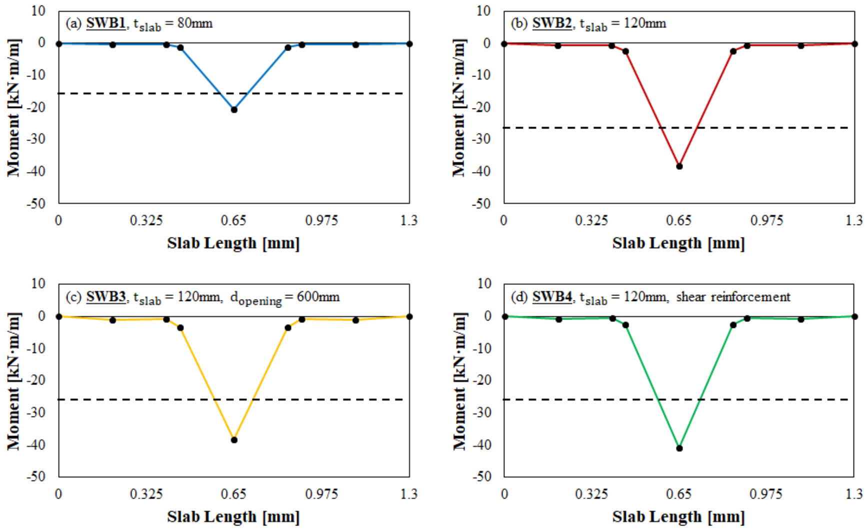

Figure 4-18 Slab Bending Moment in Elastic Design Model

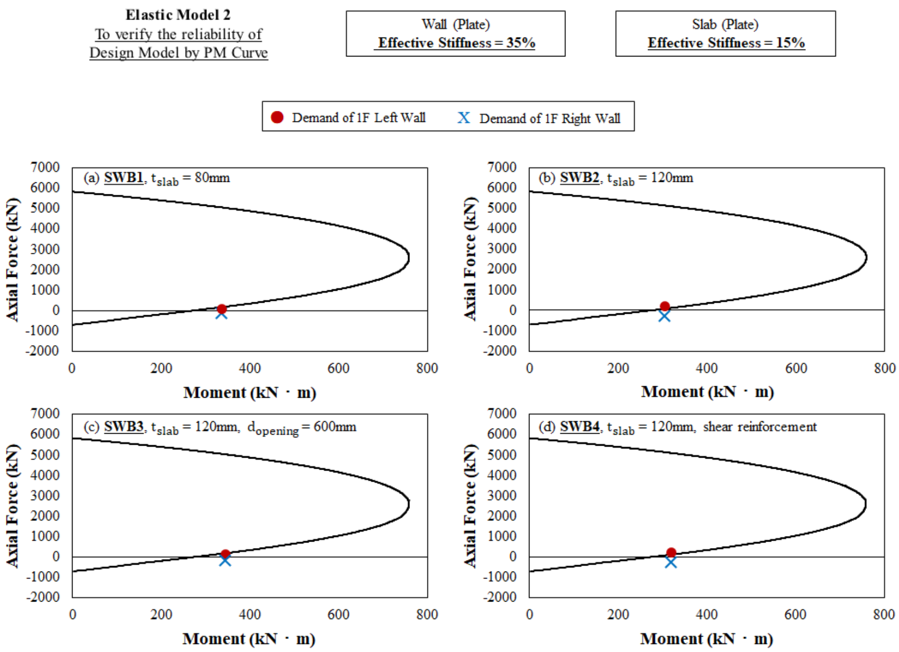

Figure 4-19 PM Curve of Wall and Demand of the Elastic Design Model

4.5 Discussion

Among the linear elastic models of 35% wall and 35% slab, which is elastic model for fundamental period esitimation, SWB2 and SWB4 showed the almost same initial stiffness as that of the Atena inelastic finite element model and test. The initial stiffness of the nonlinear finite element model compared to the stiffness of the linear elastic analysis model averaged 89%. The average of the initial stiffness of the test results compared to the stiffness of the linear elastic analysis model is 101%.

When comparing the demands of the linear elastic analysis with the performance strength of the tests, the required strength of the linear elastic analysis is located near the boundary of the P-M performance curve. The demand of wall in elastic analysis and the performance strength of the specimen in test shows similar strength. As a result, the test results are adequately simulated by linear elastic analysis.

In the wall effective stiffness 35% and slab effective stiffness 15% model which is elastic model for design, the required strength per unit length of the slab exceeds the capacity of the slab in the small area connected to the wall. However, the demand of the entire slab is less than the overall capacity of the slab. As a result, it is expected that no additional reinforcement is required for the slab.

As a result, the reliability of the elastic analysis model was proven through 35% of effective stiffness of slab (Seismic Load Analysis Model) and 15% of effective stiffness of slab (Ultimate Strength Design Method).

Chapter 5. Elastic Design of Prototype Model Considering Slab Effect

5.1 Introduction

According to the height of general wall-type structure, they are classified into low-rise, middle-rise, and high-rise. Also, according to the shape of the floor plan, it is classified into - shaped and L-shaped wall-type structure. As a result of examining the effects of analysis variables on the elastic analysis model before selecting the research target building, the effect of increasing the stiffness due to the slab effect increases as the story increases. For effective research, a total of 4 apartment houses were selected as research buildings, each of which had each two types of mid-rise and high-rise buildings with - shaped and L shaped plans. For mid-rise buildings, it is a 17-story building, and for a high-rise building, it has 24 or 25 story building. In addition, for all wall-type structures, design and analysis are performed for a private area where one generation has $59m^2$.

Based on the results from Chapter 3, it can be confirmed that the demand on the wall is reduced when designing considering the slab-wall interaction. Also, the numerical analysis was conducted based on the test results in Chapter 4. Two elastic analysis models (model for fundamental period estimation and model for design) that can simulate the load redistribution were determined through specimen analysis, and reliability was vertified. Therefore, the design method considering the slab-wall interaction proposed by Chapter 5 is applied to the prototype model to show that the reinforcement quantity of walls is reduced in general wall-type structures. This proves that the proposed design method is more economical and reasonable than the existing design method which is diaphragm.

5.2 Prototype Model

5.2.1 Model

Figure 5-1 to Figure 5-4 are prototype models to which the proposed design method proven in Chapter 4 is applied. Figure 5-1 and Figure 5-2 are mid-rise buildings and Figure 5-3 and Figure 5-4 are high-rise buildings. Also, Figure 5-1 and Figure 5-3 are buildings with plan of - shape, and Figure 5-2 and Figure 5-4 are buildings with plan of L shape.

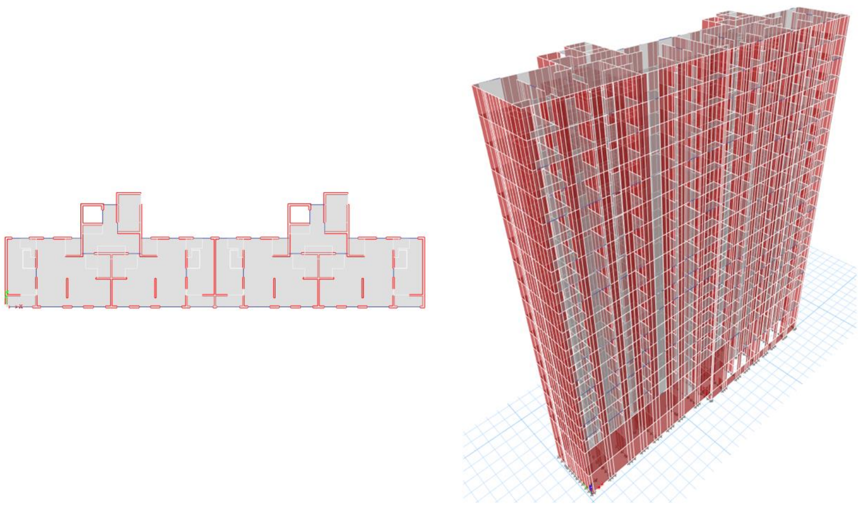

(a) Plan of Prototype Model (b) Prototype Model

Figure 5-1 – Shaped Mid-rise Structure

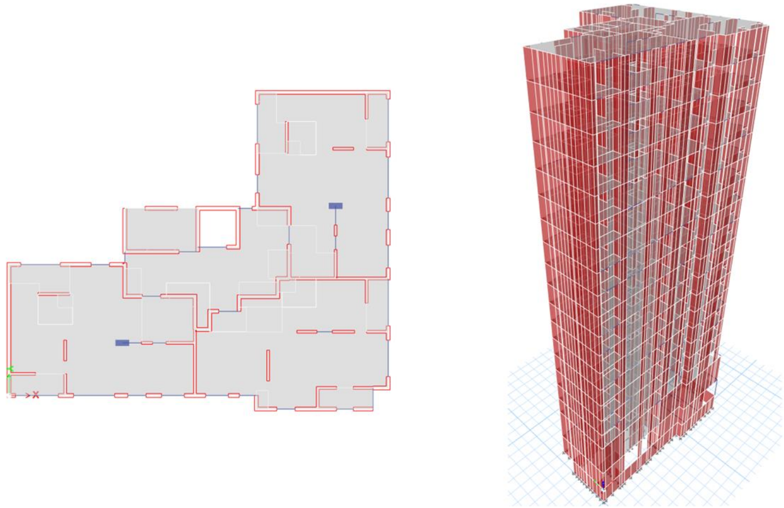

(a) Plan of Prototype Model (b) Prototype Model

Figure 5-2 L Shaped Mid-rise Structure

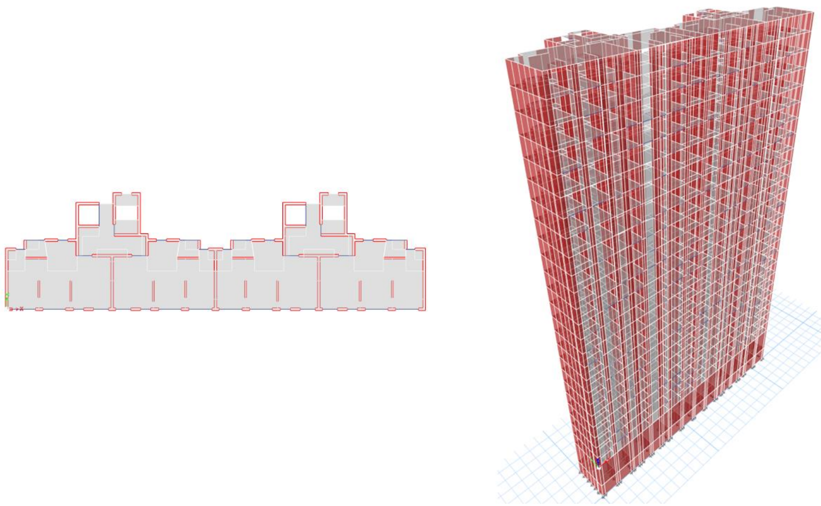

(a) Plan of Prototype Model (b) Prototype Model

Figure 5-3 – Shaped High-rise Structure

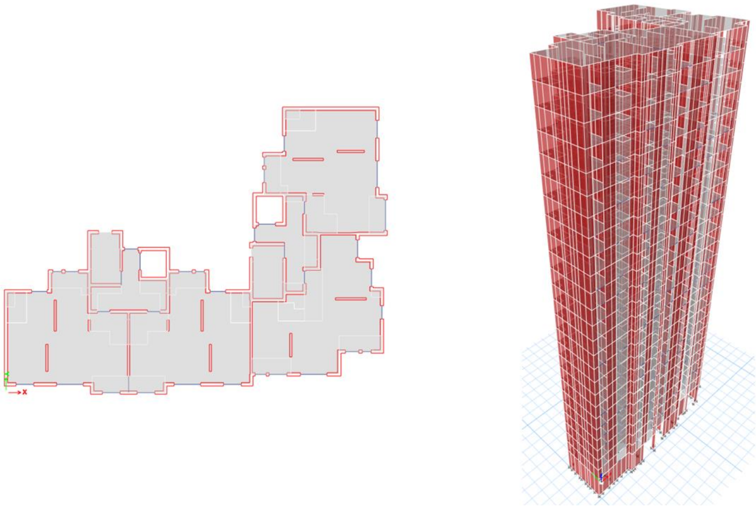

(a) Plan of Prototype Model (b) Prototype Model

Figure 5-4 L Shaped High-rise Structure

5.2.2 Design Load

The gravity load for the prototype of diaphragm model and slab model is shown in Table 5-1 to Table 5-4. Dead load and live load also considered the weight of the member. Line loads such as windows, masonry, exterior wall joints, handrails, light-weight partitions, and partial walls were replaced with area loads for convenience in slab model. The error of reaction does not occur much (Refer to 5.4.4 Reaction). The design load of the slab model was considered by increasing it by a specific amplication factor from the diaphragm model.

Table 5-1 Typical Floor Design Load of mid-rise structures - shaped structure

List	Dead Load (kN/m^2)		Live Load (kN/m^2)	
	Diaphragm	Slab Model	Diaphragm	Slab Model
Living Rooom	6.445	8.31	2	2
Stair	7.852	10.124	5	5
Stair pace	4.595	5.925	5	5
Balcony	5.739	7.4	3	3
Extended Balcony	6.665	8.593	3	3
Equipment (150mm)	3.6	4.462	1	1
Equipment (210mm)	5.04	6.498	1	1
Entrance	7.125	9.187	2	2
Hall	4.595	5.925	3	3
Bathroom	4.595	5.86	2	2

Table 5-2 Typical Floor Design Load of mid-rise structures L shaped structure

List	Dead Load (kN/m²)		Live Load (kN/m²)	
	Diaphragm	Slab Model		Diaphragm
Living Rooom	6.445	8.632	2	2
Stair	7.852	10.517	5	5
Stair pace	4.595	6.154	5	5
Balcony	5.739	7.686	3	3
Extended Balcony	6.665	8.927	3	3
Equipment (150mm)	3.6	4.822	1	1
Equipment (210mm)	5.04	6.75	1	1
Entrance	7.125	9.543	2	2
Hall	4.595	6.154	3	3
Bathroom	4.595	6.087	2	2

Table 5-3 Typical Floor Design Load of high-rise structures - shaped structure

List	Dead Load (kN/m²)		Live Load (kN/m²)	
	Diaphragm	Slab Model	Diaphragm	Slab Model
Sleeve	3.531	5.202	1	1.054
Sleeve (130mm)	3.06	4.508	1	1.054
Stair Pace	4.526	6.667	5	5.27
Balcony	6.568	9.676	3	3.162
Generation Entrance	6.943	10.228	2	2.108
Outdoor Unit	4.943	7.282	5	5.27
Bathroom	9.46	13.936	2	2.108
Room and Kitchen	6.353	9.359	2	2.108
Hall	4.741	6.984	3	3.162
Bathroom	4.46	6.57	2	2.108

Table 5-4 Typical Floor Design Load of high-rise structures L shaped structure

List	Dead Load (kN/m^2)		Live Load (kN/m^2)	
	Diaphragm	Slab Model	Diaphragm	Slab Model
Living Rooom	6.4	8.714	2	2
Stair	7.852	10.691	5	5
Stair pace	4.595	6.256	5	5
Balcony	5.985	8.149	3	3
Equipment (150mm)	3.6	4.902	1	1
Equipment (210mm)	5.04	6.862	1	1
Entrance	7.239	9.856	2	2
Hall	4.595	6.256	3	3
Bathroom	4.475	6.093	2	2

The seismic load conditions were set as shown in Table 5-5. Since wind load is critical for high-rise structures, consideration of design wind load was not given to the prototype.

Table 5-5 Analysis Setting of Seismic Loads

Seismic Load Parameters	Factor
Seismic Zone	1
0.2 Sec Spectral Acceleration (S_s)	0.44
1 Sec Spectral Acceleration (S_1)	0.176
Site Class	S_d
F_a	1.448
F_v	2.096
S_{DS}	0.4247
S_{D1}	0.2459
Importance Factor (I)	1.2
Response Modification Coefficient (R)	4
Seismic Design Category	D
Response Spectrum	KBC 2016

5.2.3 Material

The wall and slab thickness and concrete strength are shown in Table 5-6. The types of reinforcing bars used in the design of the prototype model are shown in Table 5-7.

Table 5-6 Thickness and Concrete Strength of Wall and Slab

	Wall Thickness [mm]	Slab Thickness [mm]	Wall Concrete Strength [Mpa]	Slab Concrete Strength [Mpa]
Mid-rise - shaped	250 (Exterior Wall or Core) / 180 (Wall)	210	24 (High floor) / 27 (Low floor)	24
Mid-rise L shaped	250 (Exterior Wall or Core) / 180 (Wall)	210	24 (High floor) / 27 (Low floor)	24
High-rise - shaped	300 (Exterior Wall or Core) / 200 (Wall)	210	24 (High floor) / 27 (Low floor)	24
High-rise L shaped	300 (Exterior Wall or Core) / 200 (Wall)	210	24 (High floor) / 27 (Low floor)	24

Table 5-7 Type of Rebar

Type of Rebar	Grade	F_y
Lower than D13 Higher than D16	SD500 SD600	500 Mpa 600 Mpa

5.3 Overview of Design

5.3.1 General

When the effective stiffness of the wall and slab is set to 100%, the seismic load is excessively increased. Therefore, the effect of reducing the quantity of rebar is hardly occurred. When considering the flexural stiffness of the slab, an analysis model similar to the actual structure should be used. If the effective stiffness of the wall and slab is set to be 100%, it is judged to be excessively safe. Therefore, it is desirable to use the effective stiffness within the range allowed by the structural standards. In the analysis model, 70% of wall flexural stiffness and 35% of slab (effective stiffness of structural standards) should be used to control excessive reduction in natural period. Through this, reasonalbe and economical design is possible. In relation to the period calculation of the analysis model, the earthquake-resistant design standards for buildings suggest that the deformation characteristics and structural characteristics should be considered when calculating the period. ASCE also suggested to consider the effect of cracks in concrete in modeling. The verification of effective stiffness is performed on the specimen by performing the test results and elastic analysis in Chapter 4.

For a given seismic load, the design model uses 70% effective stiffness for walls and 15% for slabs. The following results were compared and analyzed with the model constrained by the diaphragm method with 100% effective stiffness for walls which is the existing design method.

5.3.2 Scope of Application

- Wall type apartment composed of slab-shear walls
- Shear wall structure in which most slabs are surrounded by walls
- Apartment with 15 stories and 45m or more in height

5.3.3 Analysis and Design Program

- It is necessary to use a program whose reliability has been secured whether it satisfies the requirements of the following analysis and design.
- The function of the existing structural analysis program that can be used for structural analysis of shear wall structures must have a function that can implement plate bending elements. It can also be modeled as a grid beam instead of a plate bending element.
- If the out-of-plane bending stiffness of the wall is to be considered, a shell element should be included.
- In the case of a wall, the influence of a deformed shape wall should be considered in the design.
- If the function of designing the deformed shape wall as an integrated wall is not included, each unit wall element can be designed independently, but economical design is difficult to achieve.
- When the out-of-plane bending moment is considered in the wall, this effect should be reflected in the design.

- For slabs, bending moment design of slabs should be possible.

5.3.4 Definition of Terms

- Plate bending element: A finite element that exhibits out-of-plane bending stiffness effect in order to consider the effect of bending stiffness of the slab.

- In-plane stress element (membrane element, plane stress element): A plane element that considers only in-plane stiffness. Out-of-plane deflection can be used in the analysis of walls that do not need to consider the effect.

- Shell element: A finite element that can consider the effects of in-plane stiffness and out-of-plane flexural stiffness. It can be used for the analysis of walls that need to consider out-of-plane bending.

- Grid beam model: A method of modeling a slab plate using closely arranged grid beams instead of plate bending elements representing the bending stiffness of the slab. Since the linear element is used, the plastic hinge model can be applied in the nonlinear analysis, so it can be used in the nonlinear analysis.

- Diaphragm model: A model that uses a slab as an in-plane rigid body element. The flexural stiffness effect of the slab cannot be considered. In general moment frames with beams, there is no need to consider the effect of bending stiffness of the slab, and the diaphragm model can be used.

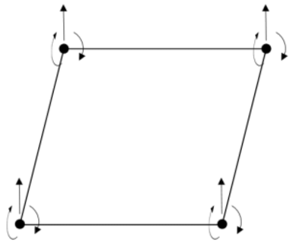

Figure 5-5 Plate Bending Element

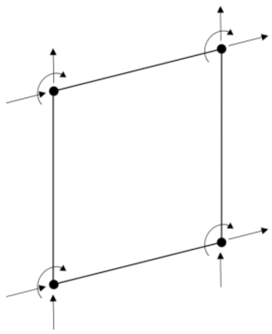

Figure 5-6 Membrane Element (Plane Stress Element)

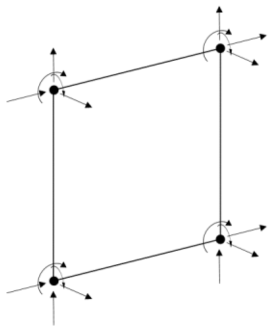

Figure 5-7 Shell Element

5.3.5 Design Strategy

(a) General

- When using the bending stiffness of the slab, the interaction between the wall and the slab is considered, so the span between the shear walls is not large. Therefore, it is applied to the structural system that has a great effect on the bending and torsional stiffness of the slab.

- If a lot of additional reinforcing bars are used in the slab, economical efficiency and constructability are reduced, so there is no practical benefit. Design so that additional reinforcing bars are not required or minimized as much as possible in the slab.

- As a strategy to retain economic feasibility, the secant stiffness of the slab should be as small as possible (15% of the elastic stiffness) to maintain the quantity of reinforcing bars in the slab against gravity load (minimum reinforcing bar: SD500 D10 @300) and minimize the increased rebar used in slab.

- If the slab reinforcement does not increase or if the wall reinforcement is to be further reduced, a larger secant stiffness can be used.

- Considering the slab effect, structurally, there is no need to increase the section area of shear wall per floor because the stiffness and strength are significantly increased. In order to improve economic efficiency, it is desirable to consider the slab effect and adjust the section area of wall per floor.

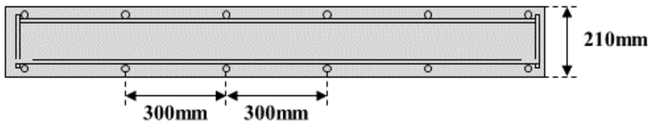

Figure 5-8 Slab Reinforcement of Typical Floor

(b) Linear Elastic Analysis

- Evaluate the period using the effective stiffness of the wall and slab to prevent excessive seismic load due to the underestimation of the dynamic analysis period when calculating the seismic load. In this case, 70% of wall and 35% of slab, which is the effective stiffness suggested in the current concrete design standards, is used.

- In the structural analysis for the design for the seismic load determined by the above, the reduced secant flexural stiffness is used for the slab to redistribute the load after premature yielding of the slab. Therefore, the design model uses 70% of wall and 15% of slab.

- If excessive additional reinforcement is required for the slab, lower the secant stiffness of the slab.

- If the bending moment locally exceeds the capacity of the slab, the average bending moment can be calculated by considering the redistribution of the bending moment in the relevant area (1/4 of the smallest span). In case of using grid beam, bending moment corresponding to the width of grid beam appears, so it can be averaged automatically.

- If the lateral drift of the building exceeds 1%, the diaphragm model must be used because the bending effect cannot be considered due to the premature failure of the slab.

(c) Seismic Force Estimation

- The dynamic analysis period is determined using the effective flexural stiffness ratio (effective flexural stiffness to elastic stiffness) of wall 70% and slab 35%.

(d) Determination of the Fundamental Period for Equivalent Static Load

- In the case of approximate fundamental period, $0.049h_n^{\frac{3}{4}}$ is used for both x and y direction of structure.

- If the natural period is between the upper limit period and the approximate fundamental period, the natural period is used as the equivalent static load period.

- If the natural period is shorter than the approximate fundamental period, the approximate fundamental period is used as the equivalent static load period.

- If the natural period is longer than the upper limit period, the upper limit period is used as the equivalent static load period.

5.4 Results of Analysis and Design

5.4.1 Natural Period

The results of the mode analysis method are shown in Figure 5-9 and Table 5-8 to Table 5-11.

In the case of natural period, it is the analysis result of the model for fundamental period estimation (Slab 35% and Wall 70%). On the other hand, in the case of modal participation mass ratios, it is the analysis result of the model for design (Slab 15% and Wall 70%). In the case of the slab model, the lateral resistance capacity increased by the slab, and the period decreased compared to the diaphragm model. Modal participation mass ratio was considered to be over 90%, and Table 5-8 to Table 5-11 show up to mode 12 to compare the slab model and the diaphragm model.

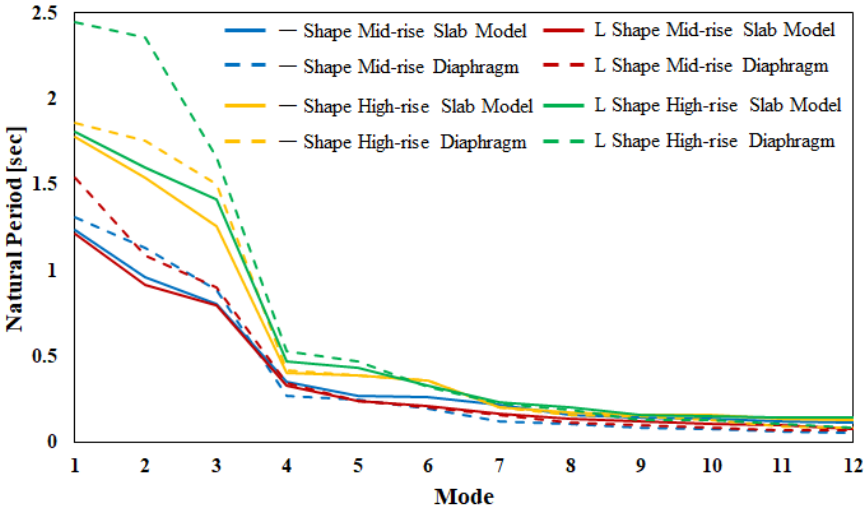

Figure 5-9 Natural Period of Diaphragm and Slab Model

Table 5-8 Modal Analysis Result of – Shaped Mid-rise Structure

Mode	Period [sec]	Diaphragm Model			Slab Model		
		Sum UX	Sum UY	Sum RZ	Sum UX	Sum UY	Sum RZ
1	1.237	0.0021	0.5454	0.1105	0.0002	0.542	0.1202
2	0.958	0.4188	0.5674	0.3083	0.3412	0.5979	0.3652
3	0.808	0.6413	0.6568	0.6271	0.6535	0.653	0.64
4	0.351	0.7881	0.7115	0.6272	0.6549	0.653	0.6402
5	0.269	0.8205	0.8223	0.6783	0.7024	0.7765	0.6478
6	0.26	0.8363	0.8597	0.8308	0.8029	0.8007	0.693
7	0.216	0.9065	0.865	0.8313	0.8248	0.835	0.8242
8	0.159	0.9084	0.9167	0.8398	0.8257	0.835	0.8244
9	0.144	0.9124	0.9266	0.9042	0.8257	0.8351	0.8244
10	0.135	0.9454	0.9283	0.9057	0.8915	0.8416	0.8246
11	0.121	0.9459	0.9516	0.9071	0.895	0.8896	0.8363
12	0.117	0.9632	0.9516	0.9078	0.8951	0.8898	0.8364

Table 5-9 Modal Analysis Result of L Shaped Mid-rise Structure

Mode	Period [sec]	Diaphragm Model			Slab Model		
		Sum UX	Sum UY	Sum RZ	Sum UX	Sum UY	Sum RZ
1	1.217	0.0091	0.5165	0.0967	0.0172	0.5169	0.0724
2	0.917	0.4826	0.5818	0.1744	0.4637	0.5831	0.159
3	0.798	0.6385	0.6554	0.5876	0.6239	0.6178	0.6148
4	0.334	0.6394	0.8411	0.6271	0.6263	0.7726	0.6445
5	0.239	0.846	0.8425	0.6276	0.8038	0.7809	0.6496
6	0.215	0.8468	0.8759	0.794	0.8112	0.7981	0.8047
7	0.168	0.8478	0.9337	0.8141	0.8144	0.8704	0.816
8	0.135	0.9242	0.9337	0.8159	0.8153	0.8704	0.8161
9	0.121	0.9242	0.9421	0.816	0.8859	0.8715	0.8163
10	0.108	0.929	0.9443	0.8958	0.892	0.882	0.8385
11	0.101	0.9581	0.9443	0.897	0.8922	0.9085	0.8846
12	0.079	0.9588	0.9444	0.8982	0.8922	0.9094	0.885

Table 5-10 Modal Analysis Result of – Shaped Mid-rise Structure

Mode	Period [sec]	Diaphragm Model			Slab Model		
		Sum UX	Sum UY	Sum RZ	Sum UX	Sum UY	Sum RZ
1	1.778	0.0059	0.6002	0.0093	0.0018	0.6204	0.0004
2	1.541	0.0215	0.6125	0.5852	0.0419	0.6205	0.5898
3	1.257	0.6372	0.6161	0.6064	0.6635	0.6226	0.6245
4	0.404	0.7617	0.6168	0.6071	0.6757	0.7856	0.6273
5	0.391	0.762	0.8078	0.6073	0.7412	0.8081	0.6725
6	0.36	0.7655	0.8079	0.7941	0.7813	0.8089	0.7964
7	0.203	0.8214	0.808	0.795	0.8291	0.809	0.8
8	0.174	0.8214	0.8862	0.795	0.8291	0.8834	0.8
9	0.161	0.8258	0.8863	0.8749	0.8354	0.8834	0.8714
10	0.158	0.8641	0.8863	0.8763	0.8354	0.8838	0.8717
11	0.139	0.8642	0.9288	0.8764	0.8354	0.8838	0.8717
12	0.131	0.8954	0.929	0.8877	0.8692	0.8838	0.8742

Table 5-11 Modal Analysis Result of L Shaped Mid-rise Structure

Mode	Period [sec]	Diaphragm Model			Slab Model		
		Sum UX	Sum UY	Sum RZ	Sum UX	Sum UY	Sum RZ
1	1.805	0.5551	0.0056	0.0834	0.3984	0.2761	7.53E-06
2	1.603	0.5618	0.4861	0.2311	0.5544	0.4838	0.3157
3	1.418	0.6477	0.6369	0.6335	0.6873	0.666	0.6605
4	0.469	0.7862	0.6389	0.6699	0.8119	0.6699	0.6782
5	0.435	0.8044	0.7809	0.7018	0.8138	0.7857	0.7238
6	0.333	0.8291	0.8319	0.8225	0.8377	0.8369	0.8275
7	0.231	0.8746	0.8336	0.8396	0.8808	0.837	0.8394
8	0.202	0.8846	0.8848	0.8501	0.8851	0.8833	0.855
9	0.162	0.9063	0.9041	0.872	0.8851	0.8833	0.855
10	0.149	0.916	0.9046	0.9039	0.9155	0.8911	0.8568
11	0.146	0.9223	0.931	0.9091	0.9156	0.9032	0.8983
12	0.143	0.9379	0.9329	0.9134	0.9156	0.9034	0.9008

5.4.2 Shear Force Distribution

The fundamental period for calculating the base shear force should be determined in consideration of section 6.3.5 (d). After the fundamental period is determined, the base shear can be calculated by response spectrum analysis and equivalent static analysis. As defined in KBC 2016 section 0306.7.3.5., the design base shear force should be designed in consideration of the C_m factor of Eqs. (5-1).

Eqs. (5-1) limits the excessive reduction of the base shear force by the modal analysis method compared to the base shear force obtained using the equivalent static analysis. If the base shear force V_{RS} according to the response spectrum analysis is smaller than 85% of the base shear force V_{ES} calculated by the equivalent static analysis method using the natural period obtained according to 0306.5.3, it is used by multiplying it by the amplication factor C_m. In general, since the modal analysis method can estimate the seismic response more accurately, the base shear force may be somewhat reduced, but it may be wrong to use the excessively reduced base shear force as a result of using a longer period than the equivalent static analysis method. The reason is that the vibration period of the actual building may be smaller than the value predicted using the numerical model due to the influence of non-structural elements.

$$C_m = 0.85\frac{V_{RS}}{V_{ES}} \geq 1.0 \qquad (5\text{-}1)$$

Table 5-12 to Table 5-15 show the period and bottom shear force of the slab model and the diaphragm model that have been analyzed and designed. It can be seen that the shear force applied to the design increases from a minimum of 0% to an ultimate of 20.8% compared to the diaphragm model.

Table 5-12 Base Shear Force and Period of - Shaped Mid-rise Structure

Analysis Model		Diaphragm		Slab Model	
Direction		X	Y	X	Y
Period [sec]	Natural Period	1.13	1.312	0.958	1.237
	Upper Limit Period	1.484	1.484	1.484	1.484
	Approximate Period	1.022	1.022	1.022	1.022
	Fundamental Period	1.13	1.312	1.022	1.237
Base Shear Force [kN]	Equivalent Static	9,511	8,194	10,464	8,647
	Response Spectrum	6,021	5,507	6,734	5,653
	C_m Factor	1.342	1.265	1.235	1.3
	Base Shear Force	8,084	6,964	8,895	7,350
Increased Ratio of Base Shear Force		-	-	10%	5.5%

Table 5-13 Base Shear Force and Period of L Shaped Mid-rise Structure

Analysis Model		Diaphragm		Slab Model	
Direction		X	Y	X	Y
Period [sec]	Natural Period	1.089	1.543	0.917	1.217
	Upper Limit Period	1.474	1.474	1.474	1.474
	Approximate Period	1.014	1.014	1.014	1.014
	Fundamental Period	1.089	1.474	1.014	1.217
Base Shear Force [kN]	Equivalent Static	7,097	5,253	7,607	6,345
	Response Spectrum	4,650	3,782	5,069	4,042
	C_m Factor	1.297	1.181	1.276	1.334
	Base Shear Force	6,032	4,465	6,466	5,394
Increased Ratio of Base Shear Force		-	-	7.2%	20.8%

Table 5-14 Base Shear Force and Period of - Shaped High-rise Structure

Analysis Model		Diaphragm		Slab Model	
Direction		X	Y	X	Y
Period [sec]	Natural Period	1.505	1.859	1.257	1.778
	Upper Limit Period	1.671	1.671	1.671	1.671
	Approximate Period	1.15	1.15	1.15	1.15
	Fundamental Period	1.505	1.671	1.257	1.671
Base Shear Force [kN]	Equivalent Static	10,082	9,091	12,037	9,091
	Response Spectrum	7,333	7,152	8,243	7,312
	C_m Factor	1.169	1.081	1.241	1.057
	Base Shear Force	8,569	7,728	10,232	7,728
Increased Ratio of Base Shear Force		-	-	19.4%	0%

Table 5-15 Base Shear Force and Period of L Shaped High-rise Structure

Analysis Model		Diaphragm		Slab Model	
Direction		X	Y	X	Y
Period [sec]	Natural Period	2.449	2.355	1.631	1.631
	Upper Limit Period	1.723	1.723	1.723	1.723
	Approximate Period	1.186	1.186	1.186	1.186
	Fundamental Period	1.723	1.723	1.631	1.631
Base Shear Force [kN]	Equivalent Static	8,247	8,247	8,279	8,279
	Response Spectrum	5,241	5,263	5,463	5,353
	C_m Factor	1.134	1.332	1.288	1.315
	Base Shear Force	7,010	7,010	7,037	7,037
Increased Ratio of Base Shear Force		-	-	0.4%	0.4%

Figures 5-10 shows the story shear force graph of the analyzed slab model and diaphragm model. Although the tendency of story shear force is similar, it can be seen that the shear force of all stories increased. This is because, in the case of the slab model, the stiffness of the analysis model increased, which decreased the period, and thereby increased the seismic load applied to the structure.

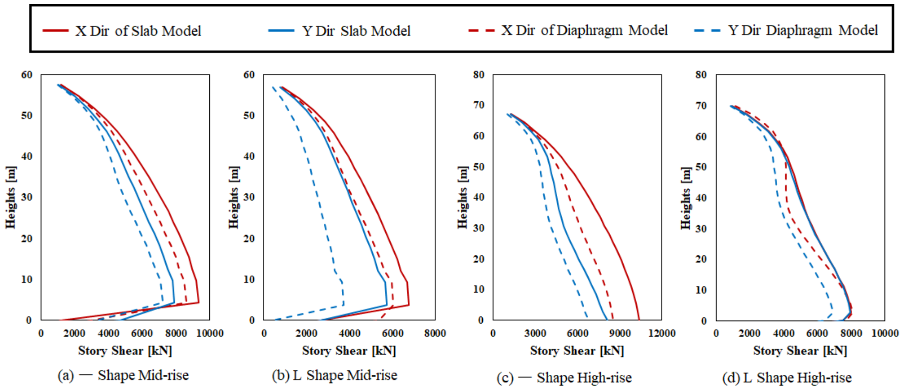

Figure 5-10 Story Shear Force of Prototype Model

5.4.3 Lateral Displacement and Drift Ratio

As can be seen from Figure 5-11, it can be confirmed that the diaphragm model generally has a larger displacement than the slab model. By considering the slab, a load-resisting mechanism such as a moment frame is generated, resulting in increased stiffness and more restrained lateral displacement than the diaphragm model. It can be seen from Table 5-12 through Table 5-15 that the seismic load on the response spectrum is greater in the slab model than in the diaphragm as the stiffness of the structure increases. However, due to the large increase in stiffness due to the slab, the displacement decreased. In the case of high-rise structures, it can be seen that the displacement is significantly reduced except in the x direction of the - shape high-rise structure. As can be seen in Table 5-14 and Table 5-15, the period is limited by the upper limit period, so the seismic load applying on the structure does not increase significantly, so the displacement is greatly reduced. Therefore, the slab effect is expected to occur significantly in high-rise structures.

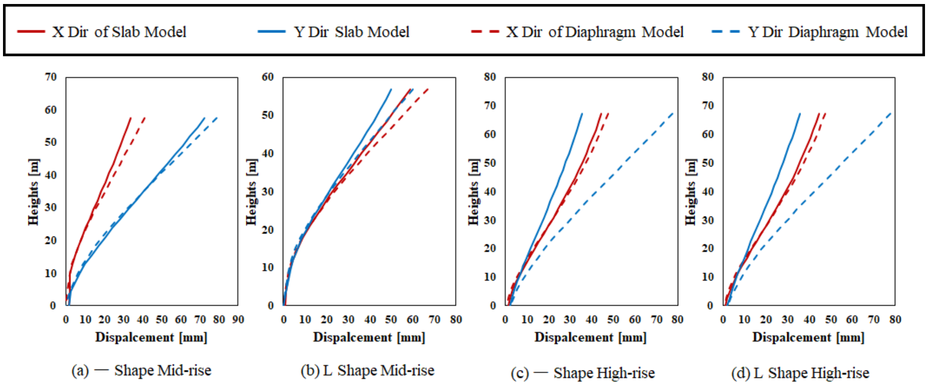

Figure 5-11 Lateral Displacemnt of Prototype Model

5.4.4 Reaction

The gravity load is entered as the slab uniform load (out-of-plane direction of the slab surface). In the ETABS program, due to a small error between the slab model and the diaphragm model, some errors occurred when inputting the load. However, the error was less than 0.5%, so it was judged not to have a significant effect on the analysis study.

Table 5-16 Reaction Force of Analysis Model

Type	Diaphragm			Slab Model			Error [kN]	Error ratio [%]
	D.L. [kN]	L.L. [kN]	Total [kN]	D.L. [kN]	L.L. [kN]	Total [kN]		
- Shaped Mid-rise	147,232	23,640	170,872	146,517	23,633	170,150	722	0.4%
L Shaped Mid-rise	108,143	16,664	124,807	107,919	16,888	124,807	0	0%
- Shaped High-rise	210,092	34,468	244,560	210,041	34,486	244,527	33	0.4%
L Shaped High-rise	196,260	28,953	225,213	197,229	29,230	226,459	-1247	-0.5%

5.4.5 Wall Design

Referring to KBC 2016, ‘0306.8.4.3 Seismic Design Category ‘D'’ determines the design member force of a structure using one of the following two methods.

(1) Add the absolute value of the load effect for 100% of the seismic load in one direction and 30% of the seismic load in the orthogonal direction, and select the greater value from the two combinations.

(2) Combine 100% of the load effects in two orthogonal directions by the root sum square root (SRSS) method.

Therefore, the load combination for wall design is designed through the SRSS load combination, and the load combinations of Eqs. (5-2) to Eqs. (5-5) are used. E in Eqs. (5-4) and Eqs. (5-5) is the SRSS load combination with seismic loads in the X and Y directions.

$$1.4\,D \tag{5-2}$$

$$1.2\,D + 1.6\,L \tag{5-3}$$

$$1.2\,D + 1.0\,L \pm 1.0\,E \tag{5-4}$$

$$0.9\,D \pm 1.0\,E \tag{5-5}$$

The wall was designed by applying the limit state design method through the results obtained based on the elastic analysis. The results obtained through the elastic design must satisfy Eqs. (5-6) to Eqs. (5-8) in all sections.

$$\emptyset P_n \geq P_u \tag{5-6}$$

$$\emptyset V_n \geq V_u \tag{5-7}$$

$$\emptyset M_n \geq M_u \tag{5-8}$$

Frames can have non-sway and sway effects. Therefore, in the case of compression members, it is necessary to determine whether a slenderness effect occurs. Referring to KBC 2016, for '0506.5.1.1 Short Column', the slenderness effect of the compression member is possible to neglected if the following conditions are satisfied.

(1) In the case of compression members of sway frames,

$$\frac{kl_u}{r} \leq 22 \tag{5-9}$$

(2) In the case of compression members of non-sway frames,

$$\frac{kl_u}{r} \leq 34 - 12\left(\frac{M_1}{M_2}\right) \leq 40 \tag{5-10}$$

The value of $(\frac{M_1}{M_2})$ has a positive (+) value when the column has a single curvature, and a negative (-) value when the column has a double curvature. Also, $[34 - 12\left(\frac{M_1}{M_2}\right)]$ cannot exceed 40.

If the wall is slender, the wall will be buckled and be failed. In order to calculate a value at which buckling occurs, it was calculated through Euler load and considered as Eqs. (5-11). If the conditions of Eqs. (5-9) and Eqs. (5-10) are not satisfied, the slenderness effect of the compression member should be considered. When considering the slenderness effect, the non-sway moment magnification factor δ_{ns} by P-δ effect and the sway moment magnification factor δ_s by P-Δ effect should be determined. Since the effect by P-Δ is not considered when designing the wall, δ_s is not calculated. For braced frames, moment frames, and combined frames, the amplified first-order elastic analysis method defined in 0703.3.2 in KBC 2016 can replace the second-order elastic analysis, so the following equations are used.

$$P_c = \frac{\pi^2 EI_{min}}{(kl)^2} \tag{5-11}$$

$$EI = \frac{0.4EI_{E.girder}}{1+\beta_d} \tag{5-12}$$

$$\beta_d = \frac{\text{Factored dead load within a story}}{\text{Total Factored shear in the story}} \tag{5-13}$$

$$\delta_{ns} = \frac{C_m}{(1-\frac{P_u}{0.75P_c})} \tag{5-14}$$

$$C_m = 0.6 + 0.4\frac{M_1}{M_2} \tag{5-15}$$

E : The elastic modulus of column

I_{min} : The minimum moment of inertia of column

$I_{E.girder}$: The effective moment of inertia of girger

The quantity of reinforcing bars in the wall was calculated only for the wall above the ground level. This is excluded because it is judged that there is no significant difference between the slab model and the diaphragm model for the wall below the ground level. The reinforcing bars of the wall were arranged uniformly. In addition, in the case of vertical and shear reinforcing bars, the maximum spacing of D10 rebars is 450mm, and the maximum spacing of D13 and above rebars is 150mm.

The wall design was designed according to the P-M capacity curve. Shear design is designed according to section 0507.10.1 of KBC 2016. This is shown in Eqs. (5-16) to (5-18). For the shear force of concrete, the smaller of V_{c1} and V_{c2} was used.

$$V_{c1} = 0.28\lambda\sqrt{f_{ck}}hd + \frac{N_u d}{4L_w} \tag{5-16}$$

$$V_{c2} = \left[0.05\lambda\sqrt{f_{ck}} + \frac{L_w\left(0.10\lambda\sqrt{f_{ck}} + 0.2\frac{N_u}{L_w h}\right)}{\frac{M_u}{V_u} - \frac{L_w}{2}}\right]hd \tag{5-17}$$

$$V_c = \mathrm{Min}[V_{c1}, V_{c2}] \tag{5-18}$$

In the case of shear reinforcing bars, they were designed differently depending on the value of V_c generated on the wall. This refers to 0507.10.3 in KBC 2016.

(1) When $V_u < \frac{1}{2}\emptyset V_c$, the horizonal shear reinforcement ratio (ρ_h) and the reinforcement ratio for longitudinal reinforcement (ρ_l) shall satisfy the following requirements.

$$\rho_h \geq 0.0025 \tag{5-19}$$

$$s_h \leq \frac{L_w}{5} \ , \ s_h \leq 3h \ , \ s_h \leq 450mm \ , \tag{5-20}$$

$$\rho_l = 0.0025 + 0.5\left(2.5 - \frac{h_w}{L_w}\right)(\rho_h - 0.0025) \geq 0.0025 \tag{5-21}$$

$$s_v \leq \frac{L_w}{3} \ , \ s_h \leq 3h \ , \ s_h \leq 450mm \ , \tag{5-22}$$

(2) When $V_u > \emptyset V_c$, V_s should be calculated by the following Eqs. (5-25).

$$V_s = \frac{A_{vh} f_y d}{s_h} \ , \tag{5-23}$$

A_{vh} : Area of horizontal shear reinforcement within the s_h

Through the above formulas, the nominal shear force of the wall should be calculated as Eqs. (5-24) and Eqs. (5-25)

$$V_n = V_c + V_s \ , \tag{5-24}$$

$$V_u \leq \emptyset V_n \ , \tag{5-25}$$

5.5 Economical Comparison

In the case of the diaphragm model, the natural period is longer than that of the slab model, so the seismic load by the response spectrum is less than slab model. However, in the diaphragm model, since the wall is the main lateral load-resisting system, the demands applied to the wall is greater. On the other hand, the slab model has a short period, which increases the seismic load, but the force acting on the structure is distributed according to the stiffness ratio between the slab and the wall. Also, as mentioned in Chapter 3, when considering the slab, the load resistance mechanism allows the structure to act like a moment frame, thereby reducing the demand of walls. If the quantity of wall reinforcement is compared after designing the walls of prototypes, it will be clearly shown whether the demand on the wall has decreased.

Table 5-17 shows the results of the quantity of reinforcement used when designing the diaphragm model and the slab model (proposed design method). It can be seen that quantity of reinforcing bars in all prototype structures decreased by 10%, 7%, 7%, and 19%, respectively. The design method proposed in Chapter 5 was confirmed to have reasonable stiffness, and this was verified for the prototype.

There is almost no slab effect in the Y-direction composed of long walls in the - shaped plane, but there is a slab effect because the contribution of the moment frame in the X-direction is great. The L-shaped plane with the contribution of moment frame in both directions has a great slab effect regardless of the direction.

Table 5-17 Quantity of Wall Reinforcement

Type	Reinforcement	Diaphragm Model (Wall 100%)	Slab Model (Wall 70% and Slab 35%)
- Shaped Mid-rise	Total Rebar	852 kN	767 kN
	Reduced Rebar	-	85 kN (10%)
L Shaped Mid-rise	Total Rebar	567 kN	527 kN
	Reduced Rebar	-	40 kN (7%)
- Shaped High-rise	Total Rebar	1086 kN	1004 kN
	Reduced Rebar	-	82 kN (7%)
L Shaped High-rise	Total Rebar	1427 kN	1156 kN
	Reduced Rebar	-	271 kN (19%)

5.6 Discussion

When the slab model is used, the natural period is shorter than the diaphragm model, and the seismic load is excessively increased. Therefore, it is necessary to use the effective stiffness of the wall and slab. (wall 70% and slab 35%). Therefore, if 70% of wall stiffness and 15% of slab stiffness is used as a structural design model for a given seismic load (wall 70% and slab 35%), it is shown that the increase in the reinforcement of the slab can be suppressed and the reinforcement of the wall can be effectively reduced.

The amount of vertical reinforcement in the wall decreases by 10%, 7%, 7%, 19% (In order of - shape mid-rise structure, L shape mid-rise structure, - shape high-rise structure, L shape high-rise structure). This corresponds to the rebar reduction amount of 85kN, 40kN, 82kN, and 271kN, respectively. The quantity of horizontal reinforcing bars in the wall is expected to decrease slightly. As a result, the quantity of vertical reinforcement in the wall decreases due to the slab-wall interaction.

There is almost no slab effect in the Y-direction composed of long walls in the - shaped plan structure. However, there is a great slab effect because the contribution of the moment frame in the X-direction. The L-shaped plan structure with the contribution of moment frame in both directions has a great slab effect regardless of the direction. Therefore, the effect of reducing rebar is the greatest in the high-rise L-shape.

Chapter 6. Conclusion

In this study, structural performance tests and structural analysis were performed on the two-story RC frame of slab-coupled wall structure specimens to propose a design method that consider the effect of slab on the structure. For structural analysis, preliminary analysis was carried out first to determine the effect of the slab-wall interaction, and then to identify the typical wall shape in which the slab effect occurs. Structural performance tests were conducted after the specimen was constructed for the wall where the slab effect occurred. After carrying out the structural performance test, numerical analysis was performed on the specimens. The reliability of the test and proposed design method were proved through nonlinear finite element analysis and elastic analysis of the specimen. Through this, it is confirmed that economic benefits have occurred when the proposed design method considering the slab-wall interaction for the prototype is performed. The conclusions of this paper are as follows:

(1) In SWB1, SWB2, SWB3, and SWB4, strength increase of 36%, 53%, 55%, and 61% compared to the diaphragm strength (design strength), respectively, occurred. It can be seen that the slab thickness is the most effective variable for strength improvement, as the strength increase rate by the slab thickness is the greatest. It also proved that the slab thickness had the greatest influence by the load-resisting mechanism.

(2) The failure mode of the specimen includes flexural failure of the wall and punching shear failure of the slab. The load distribution between the

wall and the slab can be predicted through the strain distribution of the reinforcing bar.

(3) Local failure occurred at the slab-wall joint, but the load redistribution to the surrounding slab occurred due to the long width of slab. As a result, the specimen showed great ductility and strength was maintained up to 1.0% of lateral drift ratio.

(4) Among the variables, the thickness of the slab has the greatest influence on the increase in strength due to the slab effect. The ratio of the slab reabar and the local punching shear reinforcing bars do not have a significant effect.

(5) Energy dissipation capacity decreased by -1.3% for SWB1 specimen, 36.2% increase for SWB3 specimen, and 31.6% increase for SWB4 specimen compared to SWB2 specimen.

(6) Test results and nonlinear finite element analysis are similar. This proves the reliability of the test results and FEA. As the element size of the slab is small, the local fracture of the slab and the double curvature of the slab can be simulated. It is analyzed through FEA model that can simulate it.

(7) It is not possible to simulate local fractures of slab in the elastic analysis model. Therefore, in order to simulate the slab effect, the effective stiffness of the slab is applied so that the demands of the slab do not exceed the yield strength of slab.

(8) The elastic analysis result of the 35% of effective stiffness of the slab is close to the initial stiffness of the specimen. Therefore, the reliability of using 35% of effective stiffness of the slab in the model for fundamental period esitimation and model for seismic load calculation is proven.

(9) In the case of setting the effective stiffness of the model for the design in the elastic analysis, it is confirmed that the demand of the wall in the elastic analysis is at the boundary of the wall PM curve. This proves its suitability and reliability as a model for design.

(10) When the slab model is used, the seismic load is excessively increased as the natural period is shorter than that of the diaphragm model. Therefore, it is necessary to control the effective stiffness of the wall and slab (70% for wall and 35% for slab).

(11) When using 70% wall and 15% slab stiffness as a structural design model for a given seismic load, it is possible to control the increase in reinforcing bars in the slab and effectively reduce the rebars in the wall.

(12) The quantity of vertical reinforcing bars in the wall decreases due to the slab-wall interaction. The quantity of vertical reinforcing bars in the wall decreases by 10%, 7%, 7% and 19% (Depending on the wall-type structure floor plan and the story of structure, when 70% of wall and 15% of slab design model used). This corresponds to the rebar reduction value of 85kN, 40kN, 82kN, and 271kN, respectively.

(13) The quantity of horizontal reinforcing bars in the wall is expected to decrease slightly. In addition, since there is not much increase in the quantity of rebar for slab, the decrease in rebar quantity due to the slab effect can be judged as a decrease in the quantity of rebar in the wall.

(14) There is almost no slab effect in the Y-direction composed of long walls in the - shaped plan structure. However, there is a great slab effect because the contribution of the moment frame in the X-direction. The L-shaped plan structure with the contribution of moment frame in both directions has a great slab effect regardless of the direction. Therefore, the effect of reducing rebar is the greatest in the high-rise L-shape.

References

[1] Korean Design Standard (2019) Building Seismic Design Code (KDS 41 17 00), Korean Design Standard

[2] Korena Design Standard (2021) Bending Moment and Compression Design Criteria of Concrete Structure (KDS 41 20 20), Korean Design Standard

[3] Korean Building Code 2016 (2016) Korean Building Code and Commentary (KBC 2016)

[4] ASCE 7-16, "Seismic Design Requirements for Building Structures"

[5] T. Paulay and R.G. Taylor (1981) "Slab Coupling of Earthquake-Resisting Shearwalls", ACI Journal, Title no.78-11

[6] Josheph Schwaighofer and Michael P. Collins (1977) "Experimental Study of the Behavior of Reinforced Concrete Coupling Slabs", ACI Journal, Title no. 74-12

[7] Andri Setiawan, Robert L. Vollum, Lorenzo Macorini and Bassam A. Izzuddin (2020) "Punching Shear Design of RC flat Slabs Supported on Wall Corners", Structural Concrete, 2020;21:859-874

[8] Alexander Coull, F. ASCE and Wong Tang Chee (1983) "Design of Floor Slabs Coupling Shear Walls", Journal of Structural Engineering, Vol. 109 No.1, 1983,109(1): 109-125

[9] Zdeněk P. Bažant and B. H. Oh (1983) "Crack Band Theory for Fracture of Concrete", Matériaux et Construction 16, 155-177

[10] Park. H.G. and Eom. T.S. (2003) "Earthquake Design Method for Structural Walls Based on Energy Dissipation Capacity" Journal of the Earthquake Engineering Society of Korea Volume 7 Issue 6, 25-34

[11] Eom. T.S., Kim. J.Y. and Park. H.G. (2009) "Secant Stiffness for Direct Inelastic Earthquake design of Reinforced Concrete Structures", Journal of the Earthquake Engineering Society of Korea Volume 13 Issue 2, 59-68

[12] Park. H.G. and Eom. T.S. (2004) "Direct Inelastic Earthquake Design Using Secant Stiffness" Journal of the Earthquake Engineering Society of Korea Volume 8 Issue 2, 17-27

[13] Moon. S.K. and Lee. D.G. (1992), "A Study on an Efficient Analytical Model for a Multistory Building Structure with Real In-plane Stiffness of Floor Slab", Architectural Institute of Korea Vol 8, 1992.01, 135-141

[14] Park. Y.M and Han. S.W. (2005) "Stiffness Reduction Factor for Flat Plate Slabs Analysis", Architectural Institute of Korea Structure & Construction 22, 2006.11, 105-114

[15] Mohammad Hossain and Tahsin Hossain (2014) "FEM Approach to Perform Parametric Study on Slender Columns for Flat-Plate Structures", International Journal of Civil and Structural Engineering Research Vol.2 Issue 1, 15-24

초 록

슬래브-벽체 상호작용을 고려한 병렬벽의 구조해석 및 설계

전 명 호

서울대학교 건축학과 대학원

’78년 국내 지진 관측 이래 최대지진인 규모 5.8의 경주지진(’16.09.12) 및 포항지진(’17.11.15)이 발생하였으며 지진 발생 빈도가 지속적으로 증가하고 있어 지진에 대한 구조물의 안전과 관련된 국민적 관심이 증가하고 있다. 이로 인해 1988년 3월 국내 내진설계기준은 1988년 3월 도입 이후 총 4차례의 개정이 이루어 졌으며 이에 따라 설계법과 적용대상이 변경되었다. 설계법과 적용대상이 변경되며 최근 국내에서는 성능기반 내진설계법을 활용하여 벽식구조 공동주택에 대한 비선형해석 및 내진설계가 활발히 수행되고 있으며 일반적으로 내진설계를 위한 국내 벽식공동주택의 구조해석 시 간편한 모델링 및 해석 시간의 단축 등을 위해 층 슬래브의 휨성능을 고려하지 않고 평면을 다이아프램으로 단순화하는 모델링 기법을 사용하고 있다.

그러나 표준바닥구조제도의 도입에 따라 바닥충격음에 대응하기 위하여 구조적인 요구성능과 관계없이 벽식공동주택의 슬래브 두께는 210mm 이상을 만족하여야 한다. 위의 법규로 인해 과거 (120mm ~ 180mm)와 비교하여 크게 증가되었으며 두꺼운 슬래브의 영향에 의해 구조물의 횡 저항능력이 향상될 수 있을 것으로 예상된다.

최근 벽식구조 공동주택의 경우, 벽량이 감소하고 있는 추세다. 또한 벽체형상이 T 형, L 형, H 형 등으로 다양하므로 다이아프램 만으로는 실제 슬래브와 벽체 사이의 상호작용을 모사하기 어려울 것으로 판단된다.

따라서 본 연구에서는 슬래브-벽체 상호작용을 고려한 설계법을 제안하는 것에 초점을 두었다. 슬래브-벽체 상호작용이 일어나는 다양한 형상의 벽체 형상 중 병렬벽 벽체에 대하여 2층 골조 슬래브-벽체 실험체를 제작하여 주기 반복가력 하중을 통해 구조성능실험을 수행하였다. 구조성능실험 결과를 바탕으로 벽식구조 공동주택을 탄성해석시 슬래브-벽체 상호작용을 고려하는 설계방법을 수립하였다. 제안된 설계방법을 검증하기 위해 비선형 유한요소해석과 실험을 통한 슬래브-벽체 구조의 메커니즘을 규명과 탄성해석에서의 슬래브 및 벽체 유효강성 값을 검증하였다.

본 연구는 슬래브-벽체 상호작용을 고려한 설계법을 제안함으로써 실제 구조물의 거동이 모사 가능하고 벽체 철근량을 감소시켜 원가

절감이 가능한 설계법을 제안한다. 본 연구에서는 면내방향 벽체에 대하여 연구를 수행하였으므로 추후 슬래브-벽체 상호작용이 발생하는 다양한 벽체 평면을 고려한 설계법 연구시, 근거로 제공할 수 있을 것으로 기대된다.

주요어 : 슬래브 두께, 다이아프램, 슬래브-벽체 상호작용, 구조성능실험, 비선형 유한요소해석, 탄성설계

학 번 : 2019-26856